

Pilot study and modeling of remineralization of low-temperature desalinated water by calcite filtration



Sara Ghanbari
January 2018

Pilot study and modeling of remineralization of low-temperature desalinated water by calcite filtration

Sara Ghanbari

In partial fulfillment of the requirements for the degree of

Master of Science in Civil Engineering

Date of submission: 15 January 2018
Date of defense: 6 February 2018 at 04:00 PM

Committee:

Prof. dr. ir. L.C. Rietveld

Delft University of Technology
Sanitary Engineering Section

Prof. dr. ir. G.J. Witkamp

Delft University of Technology
Sanitary Engineering Section

Dr. B. M. van Breukelen

Delft University of Technology
Sanitary Engineering Section

Ir. H. van der Laan

Oasen
Research and Development

Sanitary Engineering Section, Department of Water Management
Faculty of Civil Engineering and Geosciences
Delft University of Technology, Delft



Acknowledgements

In truth, I could not have achieved my current level of success without a strong support group. First of all, I would like to thank my supervisors, Professor Luuk Rietveld and Dr. Boris van Breukelen for the advice, time, patience, and guidance that they have given me throughout my research process.

In addition, this study was proudly supported by Oasen, one of the drinking water companies in the Netherlands. The processing path of this study could have faced much more difficulties without the technical and financial support from Oasen. Special thanks go to Harmen van der Laan for the advice and assistance during my project at Oasen. Without his frequent feedback and suggestions, this research would not be what it is today, and might never have been accomplished. Moreover, I would like to thank the staff of Vitens, who provided me with the information necessary for this research project.

Lastly, I would like to thank my dear family and friends for the love, care, and support that they have given me during difficult times.

*S. Ghanbari
Delft, January 2018*

Abstract

The possible increase of organic micropollutants in source water, including traces of medicines, pesticides, and industrial by-products, poses several challenges. It is expected that the conventional treatment of drinking water will not ensure a reliable enough quality in the future. Because of this, Oasen has started to research a new treatment concept in the past few years. Based on 100% reverse osmosis (RO) membrane filtration, it aims to provide an excellent barrier for organic micropollutants. However, the water produced by the RO membranes, called permeate, is corrosive, bitter in taste, and does not comply with the drinking water regulation standards in the Netherlands. To solve these problems and to improve the water quality, a certain degree of remineralization is crucial. A commonly used remineralization process is to filter the desalinated water through a calcite contactor, which adds the right amount of bicarbonate and calcium to the water. In order to properly design and operate the calcite filters as well as to predict the final water quality, it is essential to understand the processes that occur within the filter.

The aim of this study was to find the best kinetic calcite dissolution model to understand the behavior of the calcite grain dissolution inside the filter and subsequently to adequately design and operate a calcite filter. Therefore, an extensive pilot study was conducted to investigate the effects of various parameters on calcite dissolution, such as the calcite grain size, velocity, and carbon dioxide concentration. On top of that, the dissolution was modeled based on a successful empirical expression by Yamauchi et al. (1987). However, it was found that the effect of the flow rate on the diffusion boundary layer encompassing the calcite grains had not been taken into account in the study by Yamauchi et al. (1987). Therefore, the effect of velocity on the calcite dissolution coefficient was investigated at five different velocities: 5, 10, 15, 20, and 30 m/h. A function was then developed to describe the correlation between the flow rate and the dissolution rate coefficient. In order to calculate the equilibrium concentration, the chemical reactions were simulated using PhreeqPython (Phreeqc built in Python).

The main difference of this study compared to previous studies is the lower temperature of the water (12 °C vs. 22-40 °C) and the smaller sizes of the calcite grains (0.5-1.2 mm and 1-2 vs. 2-3 mm) that were tested. Besides this, a broad range of CO₂ dosing (1.45-9.5 mmol/l) was tested. As relevant theories gave reason to expect, the dissolution rates were strongly affected by the various parameters. A conclusion can be drawn: the smaller grain size of 0.5-1.2 mm reduces the required empty bed contact time (EBCT) to 15 minutes, whereas operating the filter with the larger grain size of 1-2 mm requires a minimum EBCT of 25 minutes to reach calcite equilibrium. The CO₂ dosing is recommended to be less than 3 mmol/l, since the CO₂ efficiency will drop below the desired 60% at higher concentrations of CO₂.

Eventually, the optimal design will be introduced for the remineralization process at Oasen treatment plant “De Hooge Boom” located in Kamerik. For this purpose, various operational scenarios were compared on their capital and operational costs. The overall cost, including both Capital Expenditure (CAPEX) and Operational Expenditure (OPEX), was estimated to be between €0.048 and €0.064/m³ for different scenarios. 71% of this amount consists of investment costs. The total treatment cost of this design is €0.057/m³ while the investment cost was found to be €1,351,000 or 32% less than the price estimated by a previous study done by Oasen.

Contents

Acknowledgements	4
Abstract	5
1 Introduction	15
1.1 General background	15
1.2 Problem definition	17
1.3 Research questions	18
1.4 Boundary conditions	18
1.5 Research approach	19
2 Literature review	19
2.1 Introduction	19
2.2 Theory of calcite filtration	19
2.3 Reaction rate of calcite dissolution	20
2.4 Calcite dissolution model	21
2.4.1 Plummer-Wigley-Parkhurst model	21
2.4.2 Yamauchi et al. (1987)	22
2.4.3 Letterman et al. (1987, 1991, and 1995)	25
2.4.4 Conclusion	27
2.5 Parameters affecting the calcite dissolution rate	28
2.5.1 Water composition	28
2.5.2 Calcite characteristics	29
2.5.3 Empty Bed Contact Time (EBCT)	29
2.5.4 Velocity	30
3 Materials and methods	32
3.1 Introduction	32
3.2 Pilot installation	33
3.2.1 Pilot setup	33
3.2.2 Sensors	35
3.2.3 Calcite product	35
3.2.4 Sieving analyses	36
3.2.5 Bed porosity	37
3.2.6 Feed water	37
3.3 Sensor validation	39
3.3.1 Reliability of CO ₂ and pH sensors at pilot plant	39
3.3.2 The relation between electrical conductivity (EC) and calcium/bicarbonate concentrations	41
3.3.3 Tracer test on the calcite filter	43
3.3.4 Ca vs. HCO ₃	45
3.4 Overview of experiments	46
3.4.1 Velocity	46
3.4.2 EBCT	46
3.4.3 Carbon dioxide dosage	46
3.5 Software used	47

4	<i>Results of pilot plant experiments</i>	48
4.1	Velocity tests	48
4.2	EBCT effect	51
4.3	Carbon dioxide concentration effect	51
5	<i>Mathematical model</i>	54
5.1	Simulation of chemical reactions	54
5.2	Reaction rate based on Yamauchi model	54
5.3	Calibration of Yamauchi model	57
5.3.1	Result from modified model	57
5.3.2	Testing the Yamauchi assumptions	59
5.3.3	Model application regarding operational variable	62
6	<i>Application and optimal design</i>	63
6.1	Introduction	63
6.2	General process scheme	63
6.3	Assumptions and boundary conditions	65
6.4	Model application	67
6.5	Design scenarios	69
6.5.1	CO ₂ dosing for DWTP with higher capacity	72
7	<i>Conclusions and recommendations</i>	73
7.1	Conclusions	73
7.1.1	Pilot study and modeling	73
7.1.2	Practical application	74
7.2	Recommendations	75
8	<i>Bibliography</i>	77
	<i>Appendices</i>	80
	Appendix I : CO₂ Calculations methods	80
	Appendix II : EC vs. TDS relation	81
	Appendix III: EC and Ph relation	83
	Appendix IV: Phreeqc simulation of EC and Ca/HCO₃ relationship	85
	Appendix V: Pilot Components	87
	Appendix V-A : Measurement sensors information	87
	Appendix V-B : Calcite characteristics	88
	Appendix V-C : Pilot Drawing	89
	Appendix VI: The CO₂ experiment simulations	90
	Appendix VII: PhreeqPython codes	90
	Appendix VII –A PhreeqPython code-velocity test- grain size 0.5-1.2 mm	90
	Appendix VII –B PhreeqPython code-velocity test- grain size 0.5-1.2 mm	94
	Appendix VII –C PhreeqPython code-velocity test- grain size 1-2 mm	96
	Appendix VII –D PhreeqPython code-CO ₂ test- grain size 0.5-1.2 mm	99
	Appendix VII –E PhreeqPython code-translate-full-scale	104

List of Figures

Figure 1. Schematics of the new treatment concept (Van Der Laan et al., 2016)	16
Figure 2. Diagram of the remineralization process in a limestone dissolution (Yamauchi et al., 1987)	23
Figure 3. Average [Ca ²⁺] in the calcite reactor as a function of retention time for the six case studies: 10, 20, and 30 m/h flow rates (□, Δ, and X, respectively) and gray and black signs for the 2 different acid dosages of 490 and 721 mgH ₂ SO ₄ /L. (Lehmann et al., 2013)	30
Figure 4. The relation between the velocity and the Reynolds number with a porosity of 49% and mean diameters of 0.81 and 1.5 mm, with kinematic viscosity at 12 °C.	31
Figure 5. The main water flow scheme of the pilot installation located at the production site “De Hooge Boom” in Kamerik	33
Figure 6. Photo of pilot calcite filter at Kamerik, both from the front and the back	34
Figure 7. Filter bed material: Juraperle 0.5-1.2 mm and Juraperle 1.0-2.0 mm	36
Figure 8. The microscope photo of Juraperle 0.5-1.2 mm on the right and Juraperle 1-2 mm on the left, with a magnification of 4	36
Figure 9. The cumulative distribution curve for grain sizes ranging between 0.5-1.2 mm on the left and 1-2 mm on the right, derived from sieving analyses of 2 samples per grain size	37
Figure 10. The EC of permeate water between 10-30 July	39
Figure 11. CO ₂ consumption measured by a CO ₂ sensor in the pilot plant for 4 consecutive days from 17 to 20 July	40
Figure 12. Distribution of CO ₂ species at different pH levels simulated in PhreeqPython (Appendix VIII-F)	40
Figure 13. Comparing calculated CO ₂ concentrations based on p and m alkalinity (reference value) with CO ₂ measured or calculated from pH	41
Figure 14. Plotting EC vs. calcium on the left and plotting EC vs. bicarbonate on the right with R ² = 0.9991	42
Figure 15. Predicted calcium and bicarbonate based on EC are shown in red lines, while the blue points are the measured data in the filter with grain size 0.5-1.2 mm and a velocity of 5 m/h. The error bars mark a deviance of 5% from the actual data	42
Figure 16. Predicted calcium and bicarbonate based on pilot-EC meter and measured data in the filter with grain size 1-2 mm and a velocity of 5 m/h. The error bars mark a deviance of 5% from the actual data	43
Figure 17. The filter filled with calcite where the sample point EC was measured	44
Figure 18. The figure on the left shows the original values of EC measured for filter 1 with grain size 1-2 mm while the figure on the right shows the same but the extra EC from calcite dissolution is excluded and the time phase between the two samples is removed	45
Figure 19. The figure on the left shows the original values of EC measured for filter 1 with grain size 0.5-1.2 mm while the figure on the right shows the same but the extra EC from calcite dissolution is excluded and the time phase between the two samples is removed	45
Figure 20. The measured and calculated bicarbonate concentration at various heights over the filter with grain size 0.5-1.2 mm. The error bars mark a deviance of 2% from the measured data	45
Figure 21. Measured [Ca ²⁺] concentration divided by the equilibrium concentration of calcium calculated by PhreeqPython as a function of bed height for the five tested velocities of 5, 10, 15, 20, and 30 m/h flow rates and a CO ₂ concentration of less than 1.5mmol/l	48
Figure 22. Measured [Ca ²⁺] concentration divided by the equilibrium concentration of calcium calculated by PhreeqPython as a function of retention time for the five tested velocities of 5, 10, 15, 20, and 30 m/h flow rates and a CO ₂ concentration of less than 1.5mmol/l	49
Figure 23. Measured [Ca ²⁺] concentration divided by the equilibrium concentration of calcium calculated by PhreeqPython as a function of retention time for the five tested velocities of 5, 10, 15, 20, and 30 m/h flow rates and a CO ₂ concentration of less than 1.5mmol/l	49
Figure 24. Effluent EC converted to the reference temperature of 250 °C measured at the pilot plant for 7 consecutive days. Filter 1 and 2 contain grain size 1-2 mm and 0.5-1.2 mm respectively	50
Figure 25. The calcium concentration at various EBCT at the beginning of the running period with CO ₂ concentrations of 2 and 1.45 mmol/l and after 3 weeks with CO ₂ concentrations of 1.3 and 1.7 mmol/l	51
Figure 26. The effect of the initial CO ₂ concentration on the calcite dissolution rate	52

Figure 27. The CO ₂ efficiency for calcite grain sizes at various carbon dioxide concentrations at constant EBCT of 30-33 minutes	52
Figure 28. The CO ₂ efficiency versus the EBCT where the EBCT changes by adjusting the bed height for grain size 0.5-1.2 mm and constant velocity	53
Figure 29. The linear plot of $\ln C_{ae} - \text{Cal}(C_{ae} - C_{ao})$ vs. EBCT for grain size 0.5-1.2 mm on the left and 1-2 mm on the right, where $R^2 > 0.99$ for grain size 0.5-1.2 mm and $R^2 > 0.98$ for grain size 1-2 mm.	55
Figure 30. The linear plot of $\ln C_{ae} - \text{Cal}(C_{ae} - C_{ao})$ vs. EBCT for various grain sizes at the velocity of 5 m/h and 13 °C	55
Figure 31. Recap from previous studies on calcite dissolution rates using the Yamauchi model	56
Figure 32. Reaction rate constant plotted as a function of velocity. Points were obtained from a velocity test and the Yamauchi model, and the line was fitted to data by method of least squares	57
Figure 33. Modeling data using the modified Yamauchi model for grain size 0.5-1.2 mm. The error bars mark a deviance of 5% from the measured data	58
Figure 34. Modeling data using the modified Yamauchi model for grain size 1-2 mm. The error bars mark a deviance of 5% from the measured data	58
Figure 35. Modeling data using PhreeqPython, grain size 0.5-1.2mm, CO ₂ test, and filter 1 at constant flow of 3.8 m/h	58
Figure 36. Calcite dissolution simulation at constant water quality and grain size using the modified Yamauchi model	59
Figure 37. Calcite dissolution simulation at constant water quality and grain size reduction using PhreeqPython	60
Figure 38. The simulation result from the multilayer model by G. Zweere (2017) on the left and the modified Yamauchi model from this study on the right where the velocity, water quality, and grain size are the same	62
Figure 39. Sensitivity analyses based on the Yamauchi model (Yamauchi et al., 1987) with various levels of porosity, diameter, and velocity created using Python and Plot.ly (https://plot.ly/create/?fid=sara.ghanbari)	62
Figure 40. General treatment process scheme for the new to build DWTP "De Hooge Boom"	63
Figure 41. Predicted and actual EC values at 2.1 m (tracer test Zweere & Teunissen, 2015)	67
Figure 42. Predicted and actual EC values at 0.6 m (tracer test Zweere & Teunissen, 2015)	67
Figure 43. The result from the Yamauchi model at the minimum required concentration and average concentration of CO ₂	68
Figure 44. Cost comparison in € per year for different scenarios	71
Figure 45. Cost difference in percentage related to the reference scenario where gray error bars indicate the general uncertainty in the cost model of +/- 20%	71
Figure 46. Cost comparison in € per year determined for both with and without additional CO ₂ dosage at a high design capacity of 5000 m ³ /h	73
Figure 47. Measured data of EC against TDS fitted in Python. The linear equation is equal to: $TDS = 0.8801 EC + 5.227$	81
Figure 48. pH vs. EC relation where the water composition is kept constant and pH levels vary between 4 and 8	83
Figure 49. Calcium/alkalinity vs. various EC plotted using Phreeqc (Tony Appelo's Phreeqc version with notepad++ done by Boris van Breukelen)	85
Figure 50. The relation between the calcium/bicarbonate concentration and EC from measured data as well as from theoretical data from the Phreeqc simulation	85
Figure 51. Filter draw above and A-A section of bottom	89
Figure 52. Filter draw with sampling points position	89

List of Tables

Table 1. Results of the pilot study conducted by Oasen Water Company on remineralization techniques (Van Der Laan et al., 2016)	16
Table 2. Drinking water quality targets	19
Table 3. Shape factor for various shapes and their ratio compared to the standard spherical shape (calculated using the volume and surface formula of each shape where volume was the same in all shapes)	29
Table 4. List of experiments and aims of experiments	32
Table 5. Design and operational characteristics of the pilot calcite filter at Kamerik	35
Table 6. The well configuration corresponding to each experiment day and the number of wells in operation during each experiment	38
Table 7. The average water quality characteristics from 4 samples taken between 17-20 July	38
Table 8. The calcite dissolution rates (Ya coefficient) from previous studies regarding their operational conditions and our experimental data	56
Table 9. Oasen water quality regulations	63
Table 10. Design parameters for the full-scale treatment plant “De Hooge Boom” in Kamerik	64
Table 11. Factors used for interest and depreciation, operation, and maintenance (Van Der Laan et al., 2016)	64
Table 12. Cost for chemicals, energy, and other operational parameters (Van Der Laan et al., 2016)	65
Table 13. Various operational scenarios	69
Table 14. Comparison of various calcite filter scenarios	70
Table 15. Major components of calcite filtration	72
Table 16. Comparison of the system with and without the CO ₂ dosing system at a treatment capacity of 5000 m ³ /h	72
Table 17. Calculation of carbonate, bicarbonate, and hydroxyl based on p and m alkalinity	80
Table 18. pH sensor characteristics	87
Table 19. Electric conductivity characteristics	87
Table 20. Turbidity sensor characteristics	87
Table 21. CO ₂ meter characteristics	88
Table 22. Calcite product characteristics	88

List of abbreviations

CAPEX	Capital Expenses
EBCT	Empty Bed Contact Time
EC	Electric Conductivity
MFC	Mass Flow Controller
MSFE	Multi-Stage Flash Evaporator
OMP	Organic Micropollutants
OPEX	Operating Expenses
PWP	Plummer-Wigley-Parkhurst
RO	Reverse Osmosis
TDS	Total Dissolved Solids

Nomenclature

k_1, k_2, k_a, k_s	reaction constant
K	(calcite) dissolution rate constant
D_m	mass transfer
dC	concentration change
A/V	surface-to-volume ratio
d	particle diameter
ε	porosity
ϕ	form factor
R	overall dissolution rate (moles/cm ² .s)
r_I, r_{II}, r_{III}	reaction rate of equation I, II, and III
K_1, K_2, K_3	rate constant for reaction 1, 2 and 3
K_4	rate constant for the backward reaction
$\alpha_1, \alpha_2, \alpha_3$	ion activities
C_e	concentration at equilibrium (mmol/l)
C_L	concentration at each bed height (mmol/l)
C_0	concentration at start (mmol/l)
Z_L	bed height (mm)
U_L	superficial velocity (mm/s)
$\frac{6k}{\phi}$	Ya coefficient (dissolution rate constant including the form factor)
Ca_0	initial calcium concentration (molar)
S	the concentration of dissolved calcium carbonate
S'	the concentration of dissolved calcium carbonate at equilibrium
K_w	the activity-coefficient-corrected ion product for water
DIC_0	the initial dissolved inorganic-carbon concentration (molar)
C_c	the influent concentrations of cations excluding calcium and hydrogen
C_a	the influent concentrations of anions excluding DIC species and hydroxide
α_1 & α_2	the ionization fractions for the deprotonation of carbonic acid
N_d	axial dispersion number, dimensionless ($N_d = \frac{F \cdot \varepsilon}{(U_L \cdot L)}$)
F	dispersion coefficient
Z	dimensionless axial distance ($z=z/L$)
r	reaction rate expression
a	$\frac{6(1-\varepsilon_L)}{D_p \phi}$
k_L	liquid film mass transfer
k_c	surface reaction
k_f	residual layer mass transfer
MR	modified Reynolds
SC	Schmidt number
ν	kinematic viscosity
D	calcium ion diffusivity

1 Introduction

1.1 General background

Oasen is a drinking water company located in the province of South Holland in the Netherlands. It provides reliable and fresh drinking water for 750,000 people and 7,200 companies in this region, using riverbank infiltration as its main water source. As the wells are recharged by bank filtration from the Lek River, the water quality is susceptible to pollution. Pollutants include, but are not limited to, organic micropollutants (OMP) such as trace amounts of pharmaceuticals and pesticides, which could pose a serious threat to the successful treatment of drinking water in the future. Furthermore, it is expected that source water will increase in salinity in the long term due to the effects of climate change. The current conventional treatment method consists of tower aeration, rapid sand filtration, pellet softening, and adsorption by granular activated carbon, followed by UV disinfection. This method has its limitations with regards to removing OMP and chloride and is therefore not seen as a robust and durable solution (Van Der Laan et al., 2016). Consequently, Oasen has started to research a new treatment concept based on 100% reverse osmosis (RO) membrane filtration in recent years. With this technique, they aim to be prepared for possible increases in the concentrations of OMP and chloride in the source water in the future.

The product water derived by RO, called permeate, is aggressive, has a low pH, is bitter in taste, and does not comply with the drinking water regulation standards in the Netherlands. Moreover, transporting such corrosive water through water supply systems lacking the appropriate treatment could cause a deterioration of the piping system (Yamauchi et al., 1987; Letterman et al., 1987). In order to prevent corrosion in the transport system and to provide healthy water to consumers, it is essential to take the step of remineralization.

For this purpose, various types of remineralization techniques have been proposed. Table 1 gives an overview of the results from the pilot study done by Oasen during 2014-2016. The aim was to find the optimal remineralization technology to use as post-treatment of RO permeate water at the treatment plant “De Hooge Boom” in Kamerik. Based on several studies, calcite filtration was found to be the best remineralization technique, since it is inexpensive, easy and safe to operate and maintain, and does not require the continuous feed of chemicals that other techniques do (Benjamin et.al 1992; Letterman, 1995; Shemer et al., 2015; Van Der Laan et al., 2016).

Table 1. Results of the pilot study conducted by Oasen Water Company on remineralization techniques (Van Der Laan et al., 2016)

Source		Calcium carbonate			Calcium Chloride	
Form		Granular	Micronised			
Grain size		0.5 - 1.2mm	3 µm			
Technology		Filter	Dosing	MCR	Dosing	Dosing
Partial/Full treatment		100%	25%	25%	100%	100%
Required additives (CIP = Cleaning In Place; CEB = Chemically Enhanced Backwash)		-	CO ₂ CIP	CO ₂ CEB	NaOH CO ₂	NaHCO ₃
Water quality						
Turbidity, SI, pH		✓	✓	✓	✓	✓
CCPP _{test}		<0.4mmol	✓ 0.2	✓ 0.2	-	-
Growth potential		% current	11%	8%	-	-
Operational performance						
Contact time		min	15-20	30	<10	<1
CO ₂ efficiency		%	85%	35%	40%	>98%
CO ₂ use		mmol/L	-	10	8.5	0.2
Energy use		kWh/m ³	0.06	0.07	0.05	0.00
Failure Mode, Effects and Criticality Analysis						
Risks Objectives		#	6	21	22	6
Environmental sustainability						
Impact/2.6Mm ³		kg CO ₂ eq/yr	11·10 ⁴	19·10 ⁴	17·10 ⁴	110·10 ⁴
Costs						
Total costs		€/m ³	0.08	0.14	0.09	0.12

Figure 1 gives an overview of the complete treatment plant: the permeate water created by RO first goes through an ion exchanger to remove the remaining ammonium from the permeate water. This process is followed by remineralization using the calcite filter. As a last step, the remaining CO₂ and CH₄ are removed and O₂ is added to the water by aeration/degasification.



Figure 1. Schematics of the new treatment concept (Van Der Laan et al., 2016)

In the stage of calcite filtration, the desalinated water, additionally acidified with CO₂ if required, is channeled through a filter containing calcite particles. This results in an increase in the concentration of calcium and bicarbonate in the water due to the following reaction (Yamauchi et al., 1987):



The effectiveness and costs of this process are strongly dependent on parameters such as bed height, temperature, contact time, and inlet CO₂ concentration, which all affect the dissolution of calcium carbonate (Shemer et al., 2012). In order to understand and predict the calcite dissolution rate as a function of these design parameters, knowledge of the kinetics and equilibrium of these processes is required. For this purpose, Oasen aims to

develop a model for the design and optimization of calcite filtration, to incorporate it as one of the main steps in its treatment processes.

Several theoretical and practical models (e.g. Erga & Terjesen 1956; Plummer et al., 1979; Yamauchi et al., 1987; and Letterman et al., 1991) have been developed to describe the kinetics of calcite dissolution. Hasson et al. (2006) evaluated various kinetics expressions published in scientific literature to determine the most reliable dissolution kinetics model. He concluded that the model provided by Yamauchi et al. (1987) was the most accurate model to describe the kinetics of calcite dissolution, which was further confirmed by extensive experimental data obtained from a study conducted by Shemer et al. (2012) on this subject. Besides these published models, there are also more complex computer models based on multilayer concepts, such as the one proposed in the MSc study conducted by Bang (2012) and a more recent one by Zweere (2016).

1.2 Problem definition

Although an extensive amount of literature has been published on the subject of calcite dissolution kinetics, the study conducted by Hasson & Bendrihem (2006) has shown that theoretical models, such as the one by Plummer et al. (1978, 1979), are not suitable for simulating the calcite dissolution rate in practice as they overestimate the dissolution rate. This is because Plummer et al. (1979) determined the calcite dissolution rate under turbulent flow conditions. Using a large specific surface area affects the dissolution rate and limits the effects that both mass transport and surface reactions have on the rate of calcite dissolution (Bang, 2012).

On the other hand, current available empirical models were generally tested with high-temperature water and larger calcite grain sizes. The higher temperature is due to the fact that previous studies were mainly carried out in Middle Eastern countries, where the temperature is higher than in the Netherlands. It could also be accounted for by the use of heat-generating techniques such as a multi-stage flash evaporator (MSFE) to desalinate the water, which further increases the water temperature. As Oasen works with a relatively low groundwater temperature of 12 to 14 °C, the empirical models that are currently available are not applicable.

In addition, it is questionable whether the accuracy of complex multilayer models, such as the ones provided by Bang (2012) or Zweere (2016), is significantly higher than the accuracy of simpler one-layer models in describing the kinetics of the dissolution of calcium carbonate. Furthermore, calcite dissolution kinetics play a key role in the efficient design, operation, and maintenance of a calcite filter. The lack of a reliable kinetics model may not only result in incorrectly designed calcite filters, but also in the improper maintenance of the filter.

In conclusion, despite all previous work done by various authors on the kinetics and equilibrium of calcite dissolution, the accuracy of the available models still leaves room for improvement. To apply the technique at Oasen, the low temperature of the present water needs to be accounted for specifically. To do this, a simpler model would be preferred over a complex multilayer model, as it is possible that an increase in complexity results in a higher degree of uncertainty. A proper model is crucial, as the effectiveness and costs of the process are dependent on the design parameters of the calcite filter, such as flow rate, acid type and concentration, bed height, bed porosity, temperature, and grain size.

1.3 Research questions

The objective of this research is to develop a kinetics model as a function of the design parameters to simulate the dissolution kinetics of calcite in practice. The model could be used to optimize the design and operating conditions of a calcite filter, as well as to predict the quality of the product water with regards to the concentration of calcium and bicarbonate.

For this purpose, two main research questions are defined:

1. What is the most reliable calcite dissolution kinetics model among the available models?

To answer this question, the following sub-questions should be answered first:

- What are the design parameters that have an influence on this model?
 - How might the calcium and bicarbonate concentration be affected by these parameters?
 - How can the model be validated and calibrated using pilot studies?
 - Is the one-layer model accurate enough compared to the multilayer model in which filters are divided into several layers and the effluent water quality of each layer is used as the influent water quality of the subsiding layer?
2. How can the design and operational conditions be optimized using the dissolution model?

To answer this question, the following sub-questions should be answered first:

- What is the effect of the calcite dissolution rate on the bed height?
- What are the optimal design parameters, such as empty bed contact time (EBCT), filtrate velocity, and required bed height?
- What is the refilling frequency of the filter to keep the design EBCT and consequently the effluent water quality of the filter constant?

1.4 Boundary conditions

Table 2 illustrates the targets for the quality of the water that should be achieved based on the Dutch drinking water regulations and internal standards of Oasen. It should be noted that there are several other parameters that determine the final water quality that are beyond the scope of this research. These include the saturation index (SI) and pH values, which are further adjusted by the final step of aeration/degasification. The turbidity and the presence of particles in the effluent water that could be affected by the filtration velocity and backwash regimes are not taken into account here either, because a model to predict the occurrence of particles in the final water quality is beyond the scope of this research.

Table 2. Drinking water quality targets

Parameter	Oasen standard	Dutch legal standard
Total Hardness	1 mmol/L	> 1 mmol/L
HCO ₃ ⁻	2 mmol/L	> 0.99 mmol/L
pH	7.8 < pH < 8.3	7.5 < pH < 9.5
SI (Calcite)	-0.2 < SI < 0.4	SI > -0.2
Turbidity	≤ 0.15 NTU	≤ 1 NTU
Calcium	0.625 mmol/l	?
Magnesium	0.375 mmol/l	?
O ₂	> 2 mg/L	> 2 mg/L

1.5 Research approach

To answer the above research questions, various experiments have been carried out in the period from May to August 2017. The pilot study aimed to examine calcite dissolution at low temperatures using two different calcite grain sizes and to research several variants in the operational conditions, such as filtration velocity and inlet CO₂ concentration. Based on the data measured by the pilot study, the empirical model by Yamauchi (1987) has been modified in order to better capture the calcite dissolution kinetics at low temperatures for various calcite grain sizes.

Subsequently, the developed kinetics model could be applied to translate the results of the pilot study into a full-scale application based on a kinetics model and cost-efficiency analyses. Finally, the model will be used to optimize the design of the calcite filter at “De Hooge Boom” and to analyze the various operational scenarios.

2 Literature review

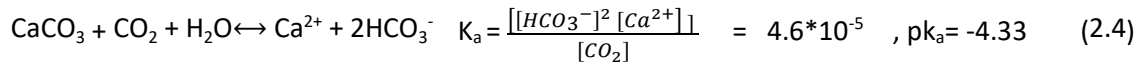
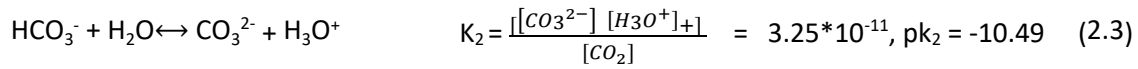
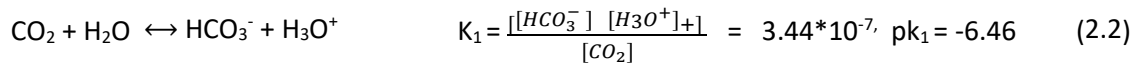
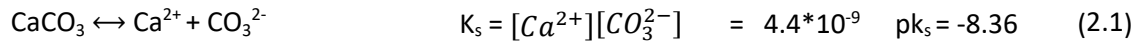
2.1 Introduction

Since the permeate water from the RO process is free from minerals and has a low buffering capacity and a low pH, a certain degree of remineralization is essential to prevent corrosion in the transport system. Remineralization is also necessary to mitigate corrosion by-products, such as copper, and consequently to provide consumers with healthy drinking water (Shemer, Hasson, Semiat, et al., 2013). There are several possible remineralization processes, but calcite filtration is the most cost-efficient and most widespread method for remineralization (Hasson & Bendrihem, 2006; Ruggieri et al., 2008; Shemer et al., 2013; Van Der Laan et al., 2016).

2.2 Theory of calcite filtration

In the remineralization process, the permeate water, additionally acidified by carbon dioxide if necessary, flows through a packed bed of calcite when the system is closed to the atmosphere. The chemical reactions that occur when the permeate passes through the column are described below (Lehmann et al., 2013).

Calcium carbonate acid equilibrium at 10 °C:



$$[\text{Ca}^{2+}] = \frac{1}{2} [\text{HCO}_3^-] \quad (2.5)$$

Where:

K = reaction constant, with given temperature and ionic strength (mole/m²/s)

PK = - log(k)

[] = stoichiometric molar concentration (mol/l).

2.3 Reaction rate of calcite dissolution

In general, the dissolution of solids in water can be expressed based either on the mass balance or on the kinetics of dissolution. Based on the mass balance, the mass change in the solid phase is equal to the mass change in the liquid phase (Bang, 2012):

$$dM = dC * V \quad (2.6)$$

Where:

dM = mass change (mol)

dC = mole change per volume of the same substance (mole/m³)

V = volume (m³)

On the other hand, the kinetics of dissolution can be calculated as follows:

$$\frac{Dm}{dt} = K * A \quad (2.7)$$

Where:

dt = retention time (s)

K = calcite dissolution rate constant (mole/m²/s)

A = surface area of calcite grains (m²)

Therefore, the general dissolution rate of CaCO₃ as a solid is:

$$dM = K * A * dt = dC * V \quad (2.8)$$

$$\frac{dC}{dt} = K * \left(\frac{A}{V}\right)$$

K is the calcite dissolution rate constant, which involves complex mechanisms controlled by mass transport at a low pH, by surface reactions at a high pH, and by a combination of the two at intermediate pH levels (Shemer et al., 2013). Furthermore, as can be seen in equation (2.8, the surface-to-volume ratio (A/V) of the calcite particles also plays an important role in the calcite dissolution rate. This parameter can be calculated for spherical or irregular grains by equation 2.9. The porosity also influences the surface area of the calcite grains in the filter bed, which should be taken into account when calculating A/V.

$$A_{\text{sphere}} = \pi d^2 \epsilon n \quad V_{\text{sphere}} = \frac{\pi d^3}{6} \rightarrow \frac{A_{\text{sphere}}}{V_{\text{sphere}}} = \frac{6}{d} \quad (2.9)$$

$$\text{For irregular particles: } \varphi = \frac{\frac{A_{\text{sphere}}}{V}}{\frac{A_{\text{Irregular}}}{V}} \rightarrow \frac{A}{V} = \frac{6}{d \cdot \varphi}, \quad \frac{A}{V} = \frac{6 \cdot (1 - \epsilon)}{d}$$

Where:

- d = particle diameter (m)
- ϵ = porosity of the filter bed (-)
- φ = form factor

2.4 Calcite dissolution model

In general, there are two perspectives when describing the calcite dissolution. One assumes that the dissolution process is controlled by surface reactions and neglects the diffusional mass transport processes (Erga & Terjesen, 1956; Plummer et al., 1979; and Yamauchi et al., 1987). The other perspective defines the calcite dissolution rate by assuming a mass transfer as the main controlling process (Letterman et al., 1987). The purpose of this paragraph is to discuss previous studies on calcite dissolution rates and to summarize the central features of three main studies on dissolution kinetics in water where metal impurities were absent.

2.4.1 Plummer-Wigley-Parkhurst model

The most extensive studies describing the dissolution of calcite are by Plummer et al. (1979) and Plummer (1978). Nowadays, the model from these studies is used as the standard model in modeling environments such as a PHREEQC (Parkhurst & Appelo, 1999).

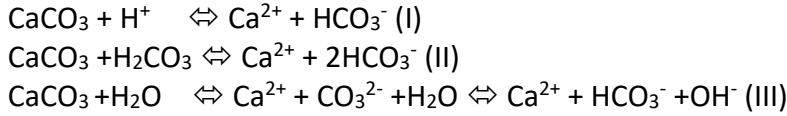
Experimental setup: Dissolution of calcite in a stirred system with the following characteristics:

- 0.3-0.6 mm CaCO₃ powder
- Temperatures of 5-60 °C
- Open-to-atmospheric-carbon-dioxide, in contact with constant pressure CO₂

Method to determine the dissolution rate: pH-stat far from equilibrium and drift-free near equilibrium

Assumptions: (1) The diffusional mass transfer is neglected due to the turbulent flow; (2) The dissolution rate on the heterogeneous surface is described as a function of the surface activities of the species Ca²⁺, H⁺, HCO₃⁻, and H₂CO₃, where the A/V ratio is too large; (3) The

dissolution is governed by the three following chemical reactions as the main processes behind dissolution and the precipitation of calcite:



In this model, the dissolution rate is defined as follows:

$$\begin{aligned} R_{\text{pwp}} &= r_{\text{I}} + r_{\text{II}} + r_{\text{III}} \\ R_{\text{pwp}} &= K_1 \alpha_{\text{H}^+} + K_2 \alpha_{\text{H}_2\text{CO}_3} - K_3 \alpha_{\text{H}_2\text{O}} - K_4 \alpha_{\text{Ca}^{2+}} - \alpha_{\text{HCO}_3^-} \end{aligned} \quad (2.10)$$

Where:

R = overall dissolution rate (moles/cm².s)
 r_{I} , r_{II} , r_{III} are the reaction rates of equations I, II, and III
 K_1 , K_2 , K_3 are the forward reaction constants and are equal to (mmol/cm²/s)
 $K_1 = 10^{(0.198 - 444/T)}$
 $K_2 = 10^{(2.84 - 2177/T)}$
 $K_3 = 10^{(-5.86 - 317/T)}$ ($T \leq 298$ kelvin)
 $K_3 = 10^{(-1.1 - 1737/T)}$ ($T > 298$ kelvin)
 K_4 describes the rate of the backward reaction of I (precipitation) and is a function of both temperature and P_{CO_2}
 α 's = the ion activities (-)

2.4.2 Yamauchi et al. (1987)

According to the Yamauchi et al. (1987), the calcite dissolution rate is controlled by the excess concentration of CO₂, i.e., the concentration of CO₂ above equilibrium. This is also called aggressive CO₂.

Experimental setup: Dissolution by flow of CO₂ acidified distilled water at 40 °C in a column with a diameter of 100 mm packed with CaCO₃ particles with the following characteristics:

Packing length = 0.5-2.4 m
 Particle sizes = 1.4-10 mm
 $[\text{CO}_2]_0 = 2.4\text{-}5$ mM
 Superficial velocity = 2.5-9 mm/s
 Retention time = 55-270 s
 Closed-to-atmospheric-carbon-dioxide

Method to determine dissolution rate: Describe the dissolution rate of CaCO₃ using Tillman's curve (Figure 2).

Assumptions: (1) The surface chemical reaction controls the dissolution reaction; (2) Diffusional mass transfer can be neglected as the processes are fast; (3) Steady state condition; (4) The concentration of aggressive CO₂ is used as the driving force; (5) The calcite dissolution has no effect on the size of the calcite particles as they are replaced by fresh calcite frequently.

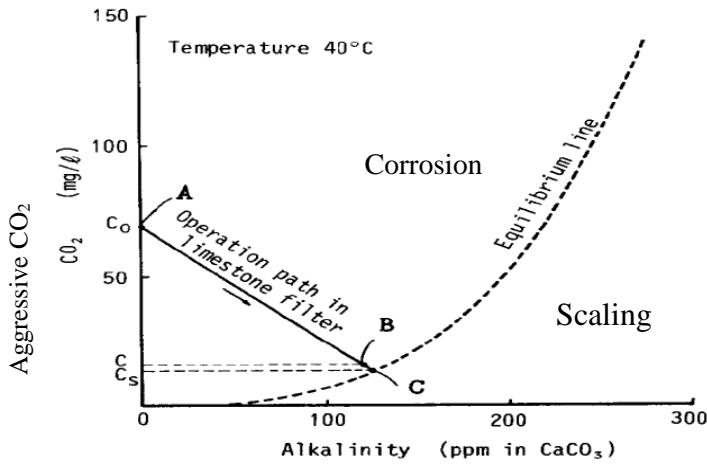


Figure 2. Diagram of the remineralization process in a limestone dissolution (Yamauchi et al., 1987)

C_0 is the initial CO_2 concentration at the filter inlet, C is the final CO_2 concentration at the filter outlet, and C_e is the equilibrium CO_2 concentration. The equilibrium line can be calculated using the constant values derived from equations 2.1, 2.2, and 2.3:

$$[CO_2] = (K_2/K_1 * K_s) [Ca^{2+}][HCO_3^-]^2 = C_e \quad (2.10)$$

Furthermore, the operation path in the calcite filter starts from the inlet to the outlet as it moves further towards the point of equilibrium. It can be represented as follows:

$$(C_0 - [CO_2]) / [HCO_3^-] = \frac{1}{2} \quad (2.11)$$

Yamauchi et al. (1987) reported that in reality equilibrium cannot be reached in a finite time, as was also shown in Figure 2. This means that the calcite dissolution stops before the equilibrium is reached ($c > c_s$). The difference between the initial CO_2 (C_s) and the final CO_2 concentration was defined by an aggressive CO_2 as the driving force behind the dissolution rate. As a result, the relation between the reaction rate and the concentration of aggressive CO_2 can be defined as follows:

$$-\frac{dc}{dt} = k(C - C_e) \quad (2.12)$$

By integrating equation (2.12) from t_0 to $t=t$, equation (2.13) can be derived:

$$\frac{\ln(C - C_e)}{(C_0 - C_e)} = -kt \quad (2.13)$$

Subsequently, the reaction can be expressed with equation (2.14):

$$\frac{C - C_s}{(C_0 - C_e)} = e^{-kt} \quad (2.14)$$

Moreover, the conversion ratio of carbon dioxide can be calculated as follows:

$$\eta = \frac{(C_0 - C)}{(C_0 - C_e)} \quad (2.15)$$

From equations (2.14 and (2.15, it can be concluded that:

$$1 - \eta = \frac{C - C_s}{(C_0 - C_s)} = e^{-kt} \quad (2.16)$$

The EBCT is represented by t and can be calculated. It represents the ratio of the empty column volume to the volumetric water flow rate and can be defined as follows:

$$t = \frac{z_L}{U_L} \quad (2.17)$$

Where:

- z_L = height of the calcite filter (m)
- U_L = superficial liquid velocity (m/s)
- t = residence time of the water inside the filter (s)

The reaction rate also depends on the specific surface area A/V , which can be derived from equation 2.9.

$$R \propto \frac{\text{particle surface}}{\text{bed volume}} = \frac{A_p}{V_p} = \frac{(1-\varepsilon)}{D} = \frac{6 \cdot (1-\varepsilon)}{d \cdot \varphi} \quad (2.18)$$

By replacing equations (2.17 and (2.18 in equation (2.13 and multiplying it with the calcite dissolution rate constant, the final Yamauchi reaction can be rewritten as:

$$\ln \frac{C - C_s}{C_0 - C_s} = - \frac{6k(1-\varepsilon)}{D_p \varphi} * \frac{z_L}{U_L} \quad (2.19)$$

From now on, the $\frac{6k}{\varphi}$ equation will be referred to as the Ya coefficient, which is the calcite dissolution rate including the form factor and can be found experimentally.

2.4.3 Letterman et al. (1987, 1991, and 1995)

Letterman et al. (1987) developed a model of the CaCO_3 dissolution rate sensitive to variables such as particle size, bed depth, flow velocity, and pressure drop. These parameters affect the dissolution rate and refilling frequency.

Experimental setup: Dissolution by flow of HCl acidified soft water between 9 °C and 22 °C in four 150-380 mm diameter columns packed with CaCO_3 particles with the following characteristics:

- Packing length = 2.1-3.5 m
- Particle sizes = 9.6-32 mm
- $[\text{CO}_2]$ and HCl acidity = 0.002-0.4 mM
- Superficial velocity = 0.15-12 mm/s
- Retention time = 230-3800 s
- Closed-to-atmospheric-carbon-dioxide

Method to determine dissolution rate: Describe the dissolution rate of CaCO_3 using mass balance and model the process based on studies done by Sjöberg & Rickard (1983) and Sjöberg & Rickard (1984), in which the kinetics of the reaction are modeled by the use of three resistances in series: (1) Liquid film transfer; (2) Surface reaction; and (3) Residual layer mass transfer.

Assumptions: (1) The mass transfer and the first order surface reaction control the dissolution reaction; (2) Steady state condition; (3) The calcium difference is used as the driving force; (4) The calcite dissolution has no effect on calcite particle size.

Letterman et al. (1987) described the calcite dissolution model based on a calcium ions transport rate from the calcite surface to bulk solution, where the dissolution rate is a function of the calcium concentration at equilibrium. This is based on a charge-balance relationship under closed-to-atmospheric-carbon-dioxide conditions:

$$2(C_0 + C) + C_c + [\text{H}^+] = (\text{DIC}_0 + S)(\alpha_1 + 2\alpha_2) + C_a + \frac{k_w}{[\text{H}^+]} \quad (2.20)$$

Where:

- S = the concentration of dissolved calcium carbonate
- K_w = the activity-coefficient-corrected ion product for water
- DIC_0 = the initial dissolved inorganic-carbon concentration (molar)
- C_c = the influent concentrations of cations excluding calcium and hydrogen
- C_a = the influent concentrations of anions excluding DIC species and hydroxide
- α_1 & α_2 = the ionization fractions for the deprotonation of carbonic acid, calculated using the pH, activity-coefficient-corrected ionization constants, and standard relationships used in aquatic chemistry (Colombani, 2008)

Subsequently, the solubility product (k_{sp}) can be calculated as follows:

$$(C_0 + S)(\alpha_2)(\text{DIC}_0 + S) = k_{sp} \quad (2.21)$$

Where:

S' = the concentration of dissolved calcium carbonate at equilibrium

The calcium concentration at any point of the calcite filtration (C_L) can be calculated by:

$$C_L = C_0 + S' ; (S \leq S') \quad (2.22)$$

The calcium concentration at equilibrium conditions can be calculated by:

$$C_e = C_0 + S' ; (S \geq S') \quad (2.23)$$

Where the S' can be calculated by solving the equation (2.20 and (2.21).

Based on a dispersion model for packed beds by Levenspiel et al. (1972) and the reaction rate expression by Letterman et al. (1987), the provided calcite dissolution rate model is presented in equation (2.22).

Levenspiel et al. (1972) developed the dispersed plug flow model with the rate equation shown in (2.24). In this model, it is assumed that there are no stagnant pockets and that there is no gross bypassing or short-circuiting of fluid in the vessel. However, the dispersion number includes back mixing to some extent.

$$N_d \frac{d^2 Ca}{dZ^2} - \varepsilon \frac{dCa}{dZ} + rt = 0 \quad (2.24)$$

Where:

- N_d = axial dispersion number, dimensionless ($N_d = \frac{F * \varepsilon}{(U_L * L)}$) and
- F = dispersion coefficient
- Z = dimensionless axial distance ($z=z/L$)
- r = reaction rate expression

The calcium carbonate dissolution rate is defined as follows:

$$R = k a (C_{eq} - C) \quad (2.25)$$

Where:

$$a = \frac{6(1-\varepsilon_L)}{D_p \varphi} \text{ and is an area of CaCO}_3 \text{ per unit volume of fluid, cm}^{-1}$$

Based on Letterman, Hadad, & Driscoll (1991), the overall dissolution rate coefficient depends on the following three constants: (1) Liquid film mass transfer (k_f); (2) Surface reaction (k_c); and (3) Residual layer mass transfer (k_r). It can be expressed as:

$$k = \left(\frac{1}{k_f} + \frac{1}{k_c} + \frac{1}{k_r} \right)^{-1} \quad (2.26)$$

Liquid film mass transfer (k_L):

A set of expressions by Chu et al. (1953) can be used to calculate the liquid film mass transfer (k_L) in these equations:

$$\begin{aligned} k_L &= 5.7 U_s (MR)^{-0.87} (Sc)^{2/3} & 1 \leq MR \leq 30 \\ k_L &= 1.8 U_s (MR)^{-0.44} (Sc)^{2/3} & 30 \leq MR \leq 10000 \end{aligned} \quad (2.27)$$

MR and SC are the modified Reynolds and Schmidt numbers respectively and are defined as follows:

$$MR = \frac{dU_s}{[\nu(1-\varepsilon)]} \quad , \quad Sc = \frac{\nu}{D} \quad (2.28)$$

Where:

ν = kinematic viscosity
 D = calcium ion diffusivity

The surface reaction (k_c):

The surface reaction controlled by the surface protonation and the equation derived empirically using experiments conducted by Sjoberg & Rickard (1984) are:

$$\log k_c = 14.2 - 1.7 pH_{eq} \quad (2.29)$$

Residual layer mass transfer (k_f):

As the calcite used in this study has high purity, more than 99%, and the filter is frequently refilled with fresh calcite, it is assumed that the layer of impurities does not exist. Consequently, k_f can be neglected.

Replacing equation (2.25) in equation (2.24) and solving it, the following equation is represented by Letterman et al. (1987):

$$\frac{[Ca]_e - [Ca]_l}{[Ca]_e - [Ca]_o} = \exp\left[-\frac{6k(1-\varepsilon_L)}{D_p \varphi} * \frac{z_L}{U_L} + \left(\frac{6k(1-\varepsilon_L)}{D_p \varphi} * \frac{z_L}{U_L}\right)^2 N_d\right] \quad (2.30)$$

Where N_d is calculated using the expression by Levenspiel et al. (1972) for $N_D < 0.01$:

$$N_d = 2\left(\frac{d}{L}\right) \quad (2.31)$$

However, since the dispersion term N_D is so small that it can be considered negligible (<0.01), equation (2.30) can be simplified to the Yamauchi equation in (2.19). This is because in equation (2.30), the term $\frac{6k(1-\varepsilon_L)}{D_p \varphi} * \frac{z_L}{U_L}$ is often around 10 to 20, meaning that the second term is about 1 to 4 and can be neglected. This makes the Letterman equation identical to Yamauchi equation, which also neglects dispersion (Shemer et al., 2015).

2.4.4 Conclusion

As demonstrated above, there are disparities in the experimental setups, the methods utilized to measure the dissolution rate, and the models applied to correlate the dissolution

rate data. A critical study carried out by Hasson & Bendrihem (2006) showed that the calcite kinetics expression by Plummer et al. (1979) and Plummer (1978) overestimates the dissolution rate by a factor of 3 to 4 at high CO₂ concentrations and a factor of 1.5 to 2 at low CO₂ levels. This was further confirmed by a recent study done by Bang (2012). Yamauchi et al. (1987) and Letterman et al. (1991) are both empirical models suitable for improvement in this study, since both of them investigate the kinetics of calcite dissolution throughout the packed bed of calcite.

The main difference between the Letterman model and the Yamauchi model is the driving force that controls the dissolution process. Letterman (1991) defines mass transfer as the process controller, while Yamauchi (1987) considers surface chemical reactions as the process controller and uses CO₂ as the driving force in deriving the same equation. However, Letterman (1991) considers the dispersion effect on calcite dissolution, while Yamauchi (1987) assumes an ideal plug flow inside the filter.

Later on, Shemer (2015) shows that the magnitude of the dispersion coefficient is insignificant and rewrites the Yamauchi equation based on a material balance as shown in equation (2.32). This makes the Yamauchi expression identical to the Letterman (1987) equation without the dispersion modification.

$$\ln \frac{[Ca]_e - [Ca]_i}{[Ca]_e - [Ca]_o} = \ln \frac{[HCO_3]_e - [HCO_3]_i}{[HCO_3]_e - [HCO_3]_o} = \ln \frac{[CO_2]_i - [CO_2]_e}{[CO_2]_o - [CO_2]_e} = -k \frac{6(1 - \varepsilon)}{d \cdot \varphi} * \frac{z_L}{U_L} \quad (2.32)$$

Because of this, Yamauchi's equation was chosen to be used as a starting point to consolidate the reliability of the Yamauchi model. Subsequently, it is used to further investigate the effects of operational characteristics such as velocity, CO₂ concentrations, and specific calcite grain sizes on the calcite dissolution rate.

2.5 Parameters affecting the calcite dissolution rate

Several studies have investigated the effects of various chemical and physical parameters on calcite dissolution. In the following paragraph, the effects of each parameter on the kinetics of calcite dissolution are investigated by a review of available literature.

2.5.1 Water composition

Several studies have confirmed the influence of substances such as magnesium, organic matter (Morse 1974a, 1974b; Berner and Morse, 1974), and copper (Erga & Terjesen, 1956) on the calcite dissolution rate in influent water. However, the focus of this study is on the remineralization of high quality water from a RO membrane. Therefore, the influence of inhibitors, such as metallic impurities, on the dissolution of calcium carbonate, is beyond the scope of this study.

The initial water carbon dioxide concentration is an important parameter to determine calcite dissolution. The degree of additional CO₂ dosage is associated with the initial pH value. However, as shown in the Tillman curve in Figure 2, increasing the buffer capacity decreases the amount of aggressive CO₂, resulting in a decrease in the calcite dissolution rate.

2.5.2 Calcite characteristics

A study conducted by Ruggieri et al. (2008) showed that the calcite dissolution rate is influenced by the reaction surface area of calcite grains as well as by the impurities that they contain. This can be explained by the general rate formula for CaCO_3 dissolution in equation (2.8). As can be seen from this equation, a higher specific surface area (A/V) accelerates the calcite dissolution rate. In general, A/V is affected both by the size and the sphericity of a calcite particle. Several articles have shown that larger calcite particles have a slower dissolution rate due to their smaller specific surface area (Yamauchi et al., 1987; Letterman et al., 1991; Shemer et al., 2013). Moreover, the sphericity of a particle is equal to the specific surface area of a sphere divided by the surface area of the particle as long as their respective volumes are kept the same. The shape factor can be estimated using the known factors for various shapes as shown in Table 3. As can be seen, an irregularly shaped grain provides a larger surface area than the spherically shaped ones.

Table 3. Shape factor for various shapes and their ratio compared to the standard spherical shape (calculated using the volume and surface formula of each shape where volume was the same in all shapes)

Unites	Form	V(mm ³)	a(mm)	A(mm ²)	A/V(mm)	Compare to spherical (A/V / A _p /V _p)
a	Spherical	0,52	1,0	3,14	6	1,00
a, b = a/3 h = 2a	Rectangle	0,52	0,9	5,11	10	0,62
a	Square	0,52	0,8	3,90	7	0,81
a	Tetrahedron	0,52	1,6	4,68	9	0,67
a, h = 2a	Cylinder	0,52	0,7	3,78	7	0,83
a, a=h	Cone	0,52	1,3	5,17	10	0,61
					Average	0,76

Calcite impurities also have an effect on the kinetics of calcite dissolution, as impurities in the calcite provide a coating of thin residue that leaches from the surface matrix of calcite (Letterman et al., 1991). Dutch drinking water regulations define that calcium carbonate should comply with NEN-EN 1018:2006. Based on this regulation, the purity of calcite used for calcite filters should be higher than 98%. At such high purities, the effects of the porous layer, formed by insoluble impurities in the calcite matrix on mass transfer to and from the calcite surface, are considered to be negligible.

2.5.3 Empty Bed Contact Time (EBCT)

The empty bed contact time (EBCT) represents the ratio of the filter volume to the flow rate. It can be calculated by equation (2.33):

$$\text{EBCT} = \frac{(\text{Volume of the filter})}{(\text{Flow rate})} = \frac{\frac{\pi D^2}{4} \times Z_L}{\frac{\pi D^2}{4} \times U_L} = \frac{Z_L}{U_L} \quad (2.33)$$

The EBCT can be adjusted by either augmenting the flow over the filter or by taking a sample from the calcite height. From a process control point of view, it is advantageous that the reaction approaches the equilibrium before water leaves the filter. This is due to the fact

that, should production variation or maintenance slightly shift the EBCT, the effect on the effluent quality would remain minimal (Van Der Laan et al., 2016). In general, according to Voutchkov (2013), the EBCT should range from anywhere between 10 to 30 minutes. This assessment was also confirmed by a recent study by the drinking water company Evides (Van Opijnen et al, 2017).

2.5.4 Velocity

The hydrodynamic condition is another variable that affects the calcite dissolution process. Increasing the flow rate tends to minimize the thickness of the boundary layer encompassing the grain. This influences film diffusion due to elevating Reynolds numbers, which in turn enhance the flux of mass between the solid surface and bulk solution, i.e., an increasing reaction rate (Lehmann et al., 2013). Figure 3 shows that elevating the flow velocity from 10m/h to 20 m/h increases the dissolution rate, as is illustrated by the slope of the line in the figure (Lehmann et al., 2013).

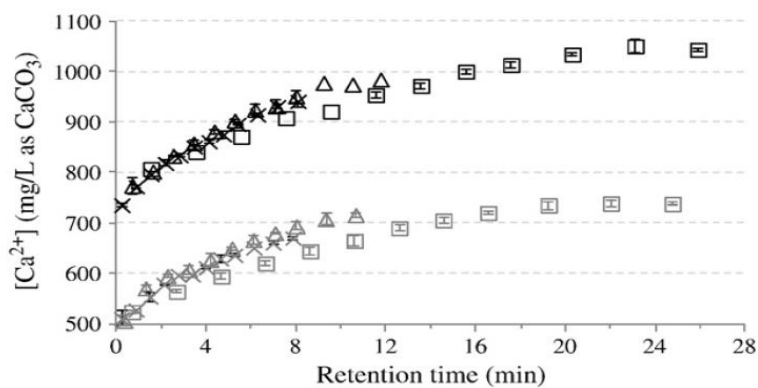


Figure 3. Average $[Ca^{2+}]$ in the calcite reactor as a function of retention time for the six case studies: 10, 20, and 30 m/h flow rates (\square , Δ , and X , respectively) and gray and black signs for the 2 different acid dosages of 490 and 721 mgH₂SO₄/L. (Lehmann et al., 2013)

The modified Reynolds number is inversely proportional to the kinematic viscosity and porosity of the filter bed and proportional to the filtration rate and grain diameter (Letterman et al., 1991):

$$Mre = \frac{d * U_L}{\vartheta(1 - \varepsilon)} \quad (2.34)$$

Where:

Re = Reynolds number [-]

Calculating the Reynolds number for both grain sizes shows that the velocity effect is more pronounced for grain sized between 1-2 mm as it has a larger diameter.

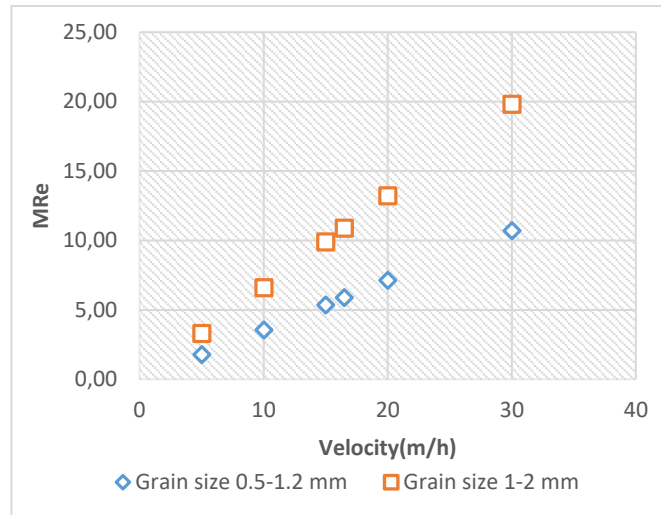


Figure 4. The relation between the velocity and the Reynolds number with a porosity of 49% and mean diameters of 0.81 and 1.5 mm, with kinematic viscosity at 12 °C.

However, it should be noted that the design EBCT, which is the EBCT that is required to reach equilibrium, is inversely related to the filtration rate. Therefore, a higher filtration velocity requires a higher calcite bed height in order to maintain the design EBCT constant.

In conclusion, the reaction rate will be increased by:

- Decreasing the influent pH by increasing the CO₂ concentration
- Decreasing the particle size
- Decreasing the particle sphericity
- Increasing the velocity
- Increasing the EBCT

3 Materials and methods

3.1 Introduction

A pilot study was conducted to investigate the kinetics of calcite dissolution. In general, the research period of this study can be divided into the following three periods:

- In the period from 8 May to 25 June, both columns were filled with grain size 0.5-1.2 mm. This period will from now on be referred to as run 1.
- In the period from 29 June to 24 July, both columns were filled with grain size 1-2 mm. This period will from now on be referred to as run 2.
- In the period from 24 July to 20 August, one column was filled with grain size 0.5-1.2 mm while the other column was refilled with fresh calcite grain size 1-2 mm. This period will from now on be referred to as run 3.

Table 4 lists an overview of the experiments that were conducted as well as their respective objectives. The details of each experiment will be explained in Part 3.4.

Table 4. List of experiments and aims of experiments

Experiments	Aim of experiment
Grain size test	Investigate the effect of the calcite grain size on the dissolution rate and the subsequently required EBCT
Velocity test	Investigate the effect of velocity on the calcite dissolution rate
CO ₂ test	Investigate the effect of extra CO ₂ on the calcite dissolution rate, the required EBCT, and the ratio of the bypass
EBCT test	Find the required EBCT to reach equilibrium
Runtime test	Investigate the effect of filter runtime on calcite dissolution rate and the required EBCT

The pilot installation was used to investigate the influence of various parameters on the calcite dissolution rate, as well as to verify the reliability of the Yamauchi model (Yamauchi et al., 1987) and possibly to improve the model. Finally, the model was used as a tool to answer research questions regarding water quality and calcite filter operation. In order to limit manual calculations and to increase the accuracy of the calculations, the modeling environment PhreeqPython¹ was used to simulate the chemical reactions and to calculate the equilibrium values. PhreeqPython made it possible to perform all necessary steps in one and the same simulating environment.

¹ [PhreeqPython](#) is an extension of the Phreeqc chemical calculation engine (Parkhurst & Appelo, 1999) written in Python and is partly derived from the PhreeqPy extension for IPHreeqc (Mike Müller).

3.2 Pilot installation

To answer the research questions, a pilot study was carried out in which the results in terms of water quality could be extrapolated to a practical scale. This pilot installation was placed at the production site “De Hooge Boom” in Kamerik and used groundwater extracted by an existing water treatment plant. The calcite filter was preceded by the RO filters and an ion exchanger.

3.2.1 Pilot setup

Figure 5 shows the process scheme of the pilot setup. A storage tank was used as an intermediate buffer in front of the calcite filters. Subsequently, the feed water was pumped into the top of the column, from where it found its way through each set of filters. The pilot line consisted of closed columns filled with granular calcium carbonate (CaCO_3) in two different sizes, followed by a degasification tower with an integrated backwash buffer for the contactors. Furthermore, the column itself was supplied with a CO_2 injection line controlled by a mass flow controller (MFC). The water quality was continuously measured at various places. Figure 6 shows the pilot plant.

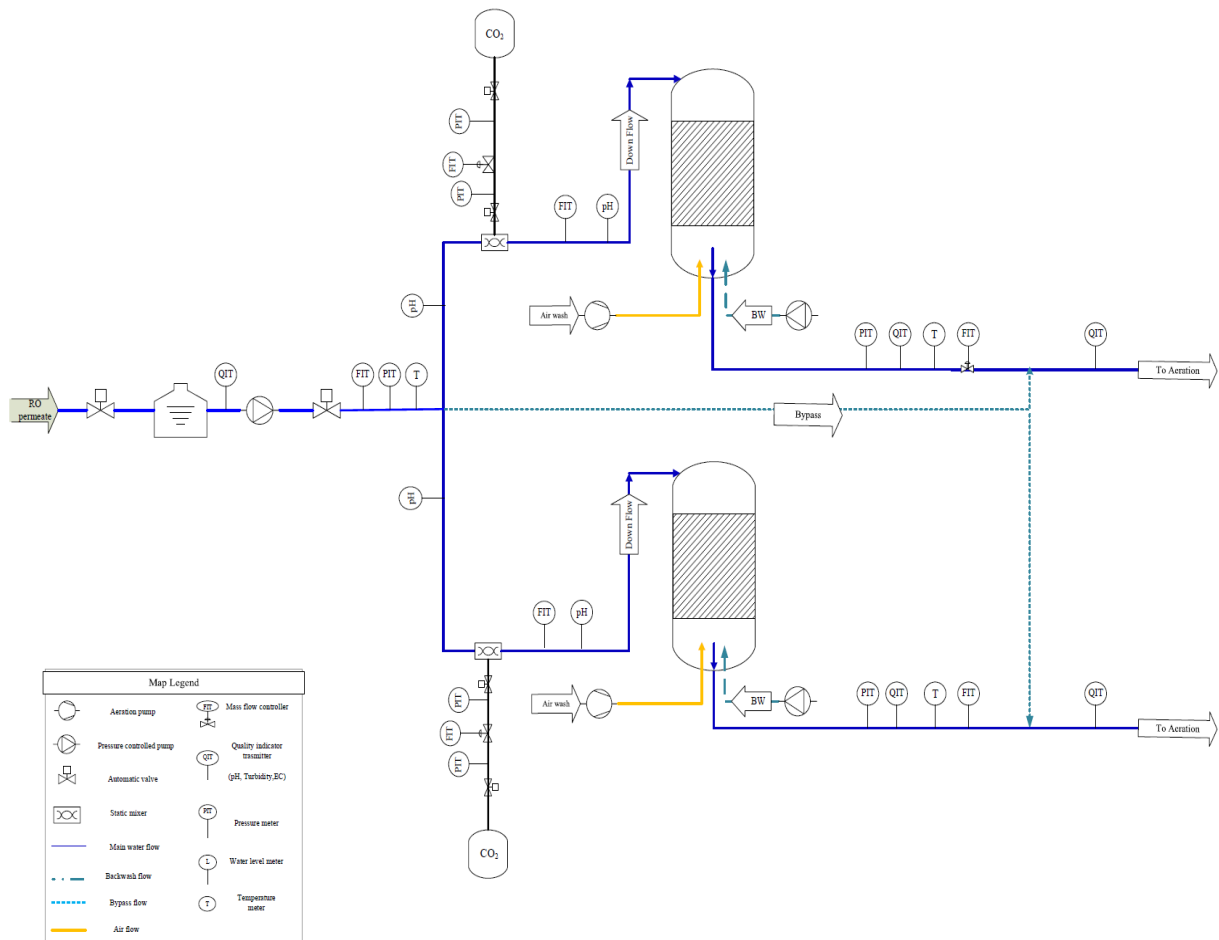


Figure 5. The main water flow scheme of the pilot installation located at the production site “De Hooge Boom” in Kamerik



Figure 6. Photo of pilot calcite filter at Kamerik, both from the front and the back

The two pilot lines shared an influent pump, but the flow rate could be adjusted individually for each contactor and was controlled by automatic control valves. Because of this, the contact time was adjustable in each contactor regardless of the calcite bed height. The air supply for the degasification tower and the CO₂ dosing were both also adjustable by the use of a so-called Automatic Settings Program (ASP), in which up to 20 different settings could be programmed.

Other relevant aspects of the contactors were:

- To inspect the contents of the contactors, the columns were fitted with sight glasses distributed along the height of the contactor.
- The bed height was monitored continuously during the second run using an ultrasonic interface sensor, while it was measured with measuring tape through the sight glasses during the first run.
- Both columns were filled through the sight glass on top.
- To prevent CO₂ accumulation, a sensor and a vent valve were mounted on top of the contactors. When a certain amount of CO₂ had accumulated, the vent valve opened automatically.
- 20 sampling points were embedded in the column: one was placed right behind the CO₂ dosage unit in the influent line and the other 19 were distributed along the height of the column.
- There were six sampling points from where the calcite along the filter could be removed.

Table 5 lists some of the design and operational characteristics of the pilot installation. Further details about the pilot installation can be found in Appendix V.

Table 5. Design and operational characteristics of the pilot calcite filter at Kamerik

Filtration rate	2.6-28.7 m/h*
Flow orientation	Downward
Sampling point	Started from 250 cm above the filter with distance of 12.5 cm between each sampling point

*The maximum velocity can only be reached when one column is used.

3.2.2 Sensors

As depicted in Figure 5, different kinds of sensors were installed to continuously measure the water quality parameters both before and after the remineralization as well as after the degasification. There were two sets of analyzers, consisting of similar sensors for each column, that measured turbidity, electrical conductivity, and pH levels. There were also two online CO₂ sensors: the first one was placed just behind filter 1, while the second one measured the CO₂ concentration in the permeate flow at the beginning of the experiments. Afterwards, filter 2 was removed and attached to the flow of filter 1. Furthermore, the process was monitored and controlled by several online sensors that measured operational parameters such as flow, pressure, and temperature. The details of these sensors, such as their accuracy and detection limits, are provided in appendix V-A.

In addition, the following details are provided:

- The reliability of the data from the water quality sensors were verified a number of times by handheld meters and laboratory measurements;
- Starting with the second run of the experiment, an automatic bed height meter was installed to record the bed height each minute. During the first run, the bed height was estimated by optical observations through the sight glasses.
- Online pH and turbidity meters were calibrated prior to each experiment;
- Data from the various online sensors was collected every second and recorded in an online PI database;
- The calcite dissolution path along the packed bed was tracked by testing the composition of water extracted from 20 sampling points located along the length of the two columns. Each sample was analyzed to determine its pH, carbon dioxide, bicarbonate, and calcium contents.

3.2.3 Calcite product

Two different sizes of calcium carbonate were used to investigate the effects of the grain size on calcite dissolution. In our experiments, Aqua-TECHNIEK's Juraperle calcium carbonate grains with a purity of 99.1% were used. Two different grain size classes were studied: 0.5-1.2 mm and 1-2 mm. The characteristics of these kinds of grains are shown in appendix V-B.



Figure 7. Filter bed material: Juraperle 0.5-1.2 mm and Juraperle 1.0-2.0 mm

Figure 8 depicts the irregular shape of calcite grain, as well as the size variation between two tested grains.

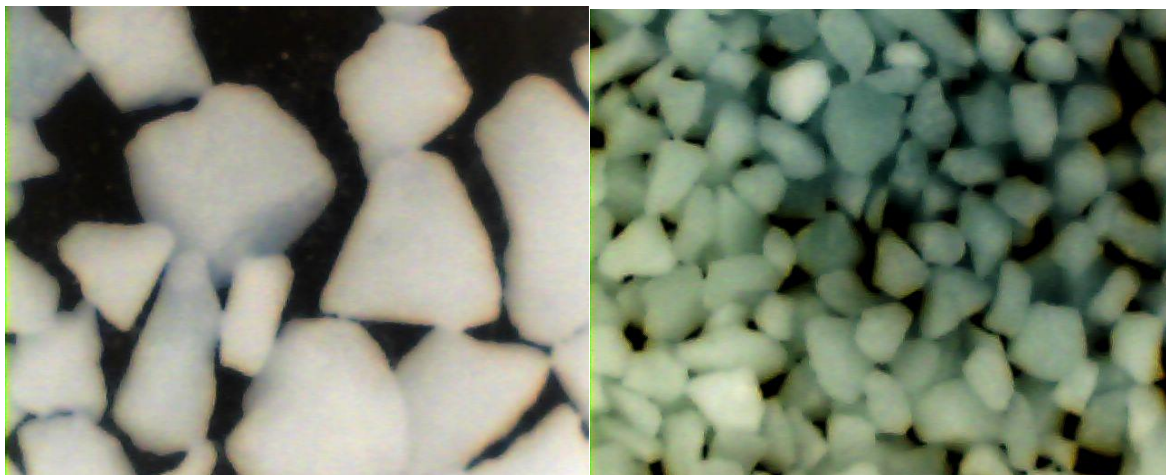


Figure 8. The microscope photo of Juraperle 0.5-1.2 mm on the right and Juraperle 1-2 mm on the left, with a magnification of 4

3.2.4 Sieving analyses

In order to determine the particle size distribution and subsequently the representative calcite diameter size, calcite samples of both grain size classes were analyzed using sieve analyses executed by the Vitens laboratory. Subsequently, the median diameter (D50) was chosen as the representative diameter for future calculations (Bear, 1988).

Particle size affects the calcite dissolution rate. The results from the sieving analyses are depicted in Figure 9 as a cumulative distribution curve. Based on these results, median diameters (D50) of 0.81 mm and 1.5 mm were chosen as the representative diameters for particles ranging between 0.5-1.2 mm and 1-2 mm respectively.

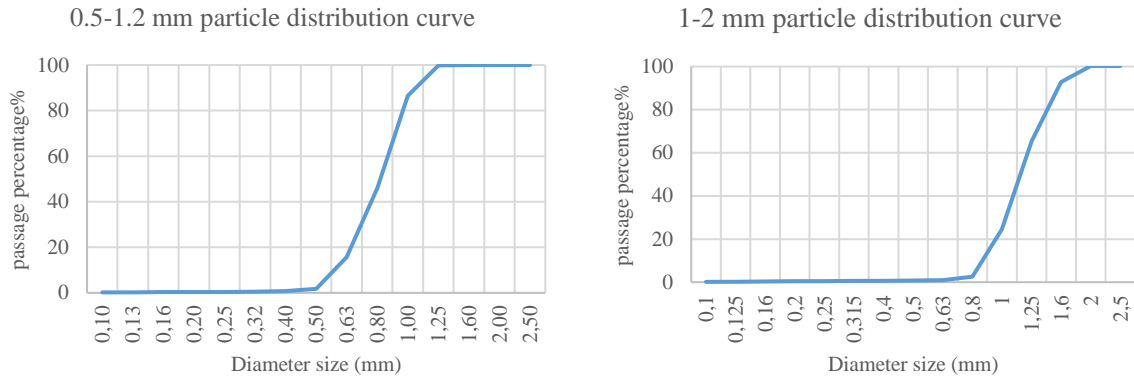


Figure 9. The cumulative distribution curve for grain sizes ranging between 0.5-1.2 mm on the left and 1-2 mm on the right, derived from sieving analyses of 2 samples per grain size

3.2.5 Bed porosity

By definition, the bed porosity is equal to the ratio of the void space (v_p) to the total enclosed volume of the bed (v_t). The following steps were taken to calculate each volume and subsequently to obtain the porosity:

- The calcite filters were filled with nine bags of calcite weighing 25 kg each. Given that the known calcite density as provided by the supplier was 2.7 g/cm^3 , the calcite volume was calculated with equation (3.1):

$$v_s = \frac{\text{No. of bags to fill the filter} * \text{weight of each bag}}{\text{Calcite density}} \quad (3.1)$$

- Using the calcite height in the column and the area of the column, the total volume of the beds was calculated:

$$V_t = H_{\text{calcite}} * A_{\text{column}} \quad (3.2)$$

- Since v_t is the sum of the pores and the solid volumes, knowing v_t and v_s , the pore volume (v_p) was calculated.
- Finally, by replacing v_t and v_p into the porosity equation, $\epsilon = v_p / v_t$, the porosity was calculated separately for each grain size range.

The measured porosity for the column that contained the calcite particles ranging between 0.5-1.2 mm was 0.5, whereas the porosity of the calcite particles ranging between 1-2 mm was 0.49. Although several studies have illustrated that the porosity of a packed bed is higher closer to the wall (Vortmeyer & Schuster, 1983), this wall effect was negligible, as the column-to-particle diameter ratio was higher than 10 (Delgado, 2006; Letterman et al., 1991).

3.2.6 Feed water

During the experimental period, the feed water was of the treatment plant “De Hooge Boom” was extracted from 15 different wells. This water was also used as feed water in the

pilot plant. However, due to changes in the water demand throughout the day, the number of wells in use was susceptible to changes. The various combinations of these wells formed four different well configurations. Table 6 shows these well configurations and the number of wells that were in operation for each day of experiments. It should be noted that an increase in the number of wells could either reduce or increase the CO₂ concentration, since the extra wells could have either had lower or higher concentrations of CO₂. To determine the water quality of each well configuration, the water quality was measured for 4 consecutive days and analyzed by the Vitens laboratory. It was also continuously monitored by quality sensors at the pilot plant.

Table 6. The well configuration corresponding to each experiment day and the number of wells in operation during each experiment

Configuration	Date	NO. of in use wells
1	10-5-2017	6-8
	15-5-2017	7-9
	23-5-2017	7-9
	29-5-2017	8-10
2	3-7-2017	9-11
	4-7-2017	9-11
	10-7-2017	7-9
3	12-7-2017	4-6
	17-7-2017	7-8
	18-7-2017	7-9
4	19-7-2017	8-10
	20-7-2017	7-9

As shown in Figure 5, the feed water of the pilot calcite filters is the permeate water produced by the RO membrane installation. This water has had a post-treatment of ion exchange to remove the remaining ammonium. Several water analyses were carried out to identify the quality of the permeate water. For this purpose, one water sample was taken for 4 consecutive days from 17-20 July. The water composition was analyzed at the laboratory. Table 7 lists the average cation and anion composition of the water analyses that were carried out in this period. As expected, the permeate water contained only a low concentration of sodium and chloride. However, due to the low EC and alkalinity capacity as well as fluctuations in the CO₂ concentration, it was challenging to measure the pH and carbon dioxide in the permeate water. Therefore, the reliability of the pH and carbon dioxide measurements were further investigated through various experiments as described in Chapter 4.

Table 7. The average water quality characteristics from 4 samples taken between 17-20 July

Feed water characteristic		
Parameter	Unit	Value
Ammonium	mg/L NH ₄	0.0
Aluminium	Mg/l	0.0
Calcium	mg/L Ca	0.0
Chloride	mg/L Cl	1.3-2
Iron	mg/L Fe	0.0

Magnesium	mg/L Mg	0.0
Manganese	mg/L Mn	0.0
Potassium	mg/L K	0.0
Nitrate	mg/L NO ₃	0.0
Sodium	mg/L Na	3.5-4
Sulphate	mg/L SO ₄	0.15
Bicarbonate	mg/L HCO ₃	7.9-12
pH	-	> 5.5
CO ₂	mg/L CO ₂	?
Methane	mg/L CH ₄	1.3-2.5
O ₂	mg/L O ₂	0.0
CO ₃	mg/L CO ₃	0.0
Temperature	°C	12±2

A change in the concentration of ions will alter the conductivity value. As a result, confirming the stability of the permeate water quality with regards to the ion content required the electrical conductivity (EC) of permeate water to be continuously monitored for a longer period of time than the laboratory analyses. This was done using the EC sensor at the pilot plant. Figure 10 shows the constant value of EC, which confirmed the stability of the ion content of the permeate water.

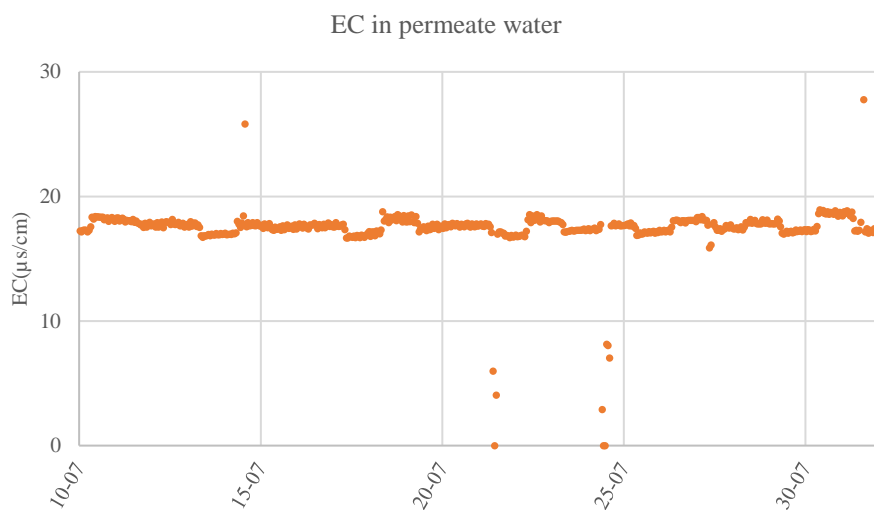


Figure 10. The EC of permeate water between 10-30 July

3.3 Sensor validation

3.3.1 Reliability of CO₂ and pH sensors at pilot plant

As described in Chapter 0, the calcite dissolution rate is strongly affected by the CO₂ concentration in the feed water. Therefore, it is crucial to measure the CO₂ concentration in the feed water with a high accuracy. However, as is illustrated in Figure 11, the permeate water contained a certain amount of carbon dioxide that fluctuated from day to day. It also fluctuated within each day due to the various well configurations. These fluctuations made it difficult to measure the exact concentration of carbon dioxide in the feed water of the filter.

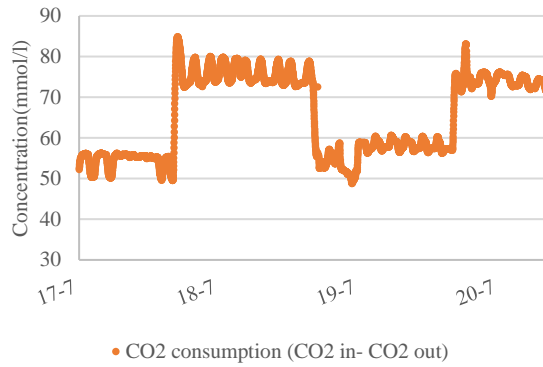


Figure 11. CO2 consumption measured by a CO2 sensor in the pilot plant for 4 consecutive days from 17 to 20 July

To measure the levels of carbon dioxide in a reliable way, CO₂ was captured in the form of carbonate, as this makes it impossible for the CO₂ to escape. Figure 12 shows the distribution of CO₂ species at different pH levels. Based on this relation between pH and CO₂, the pH of a solution should be increased to 12 or higher in order to convert all of the carbon dioxide to its carbonate form. For this purpose, sodium hydroxide was applied to the sample bottle before sampling. Subsequently, the CO₂ concentration was calculated using p and m alkalinity measured by the laboratory. This concentration was used as a reference point for CO₂ concentration to determine the accuracy percentages of other methods. A more detailed description of this method is provided in appendix I. Moreover, the levels of CO₂ were either measured directly using a CO₂ meter at the pilot plant or calculated based on the pH, alkalinity, EC, and temperature of each sample using the NPR 6538 and NEN 6533 methods.

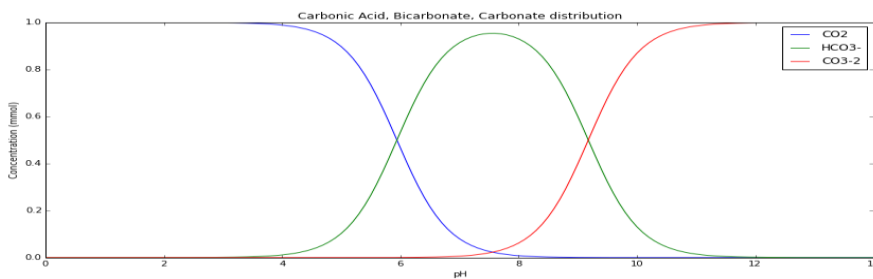


Figure 12. Distribution of CO₂ species at different pH levels simulated in PhreeqPython (Appendix VIII-F)

Figure 13 depicts the error percentage of each method based on the reference CO₂ concentration described above. This error was calculated based on equation (3.3):

$$\text{Error CO}_2 \text{ method} = \frac{\text{CO}_2 \text{ measured or calculated}}{\text{CO}_2 \text{ measured based on p and m alkalinity}} - 1 \quad (3.3)$$

The result confirmed the reliability of the CO₂ meters at the pilot plant, while the CO₂ concentrations that were calculated based on the pH measured at the pilot plant showed a considerable overestimation of the concentration of CO₂. Moreover, while the CO₂ that was calculated based on the pH determined by the laboratory seemed to be more accurate at low pH values, it also overestimated the CO₂ at lower concentrations. These overestimations can be explained by an error in the pH measurement.

There are several causes that can account for an error in pH measurement (McDermid, 2017):

- A low electrical conductivity and buffering capacity of the RO permeate, which makes the pH value unstable;
- An inappropriate and/or irregular calibration of the pH meter;
- The CO₂ release during sampling or analyses;
- The CO₂ absorption from the air into the sample;
- The temperature variation affecting the hydrogen mobility;
- The CO₂ absorption in the water, which creates carbonic acid and causes the pH to drop in the time between sampling and analysis;
- The fluctuations in CO₂ concentrations reduce the accuracy of the pH meter and increase the calibration interval.

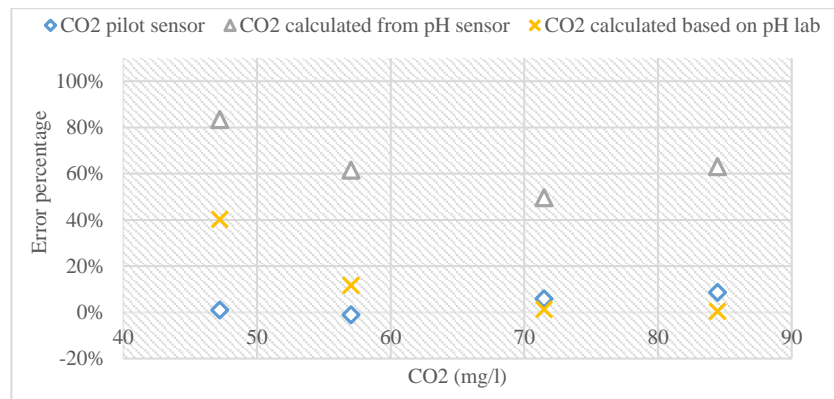


Figure 13. Comparing calculated CO₂ concentrations based on p and m alkalinity (reference value) with CO₂ measured or calculated from pH

Having drawn these conclusions, the CO₂ meter was used to estimate the CO₂ concentration in further calculations, as it proved to have the lowest error percentage. The error percentage of this method was found to be 9% at high levels of CO₂. This is slightly higher than the device accuracy provided by the sensor characteristics (appendix V-A). However, as there were no CO₂ measurements at the pilot plant during the first run, the CO₂ concentrations calculated by the laboratory based on the pH, bicarbonate, and EC from the laboratory were used as starting points in this run.

3.3.2 The relation between electrical conductivity (EC) and calcium/bicarbonate concentrations

As the permeate water has a constant EC value, increases in EC values can be explained by changes in the calcium and bicarbonate concentrations. To find the relation between EC and these two ions, the results from the EC measured at the pilot plant were plotted against the levels of calcium and bicarbonate that were measured at the laboratory. Figure 14 illustrates a linear correlation between EC and calcium as well as EC and bicarbonate respectively. Fitting this data using Python resulted in the following equations:

$$\begin{aligned} \text{Ca (mmol/l)} &= 0.005506 * \text{EC } (\mu\text{s/cm}) - 0.1357 \\ \text{HCO}_3 \text{ (mmol/l)} &= 0.01081 * \text{EC } (\mu\text{s/cm}) - 0.1127 \end{aligned} \quad (3.4)$$

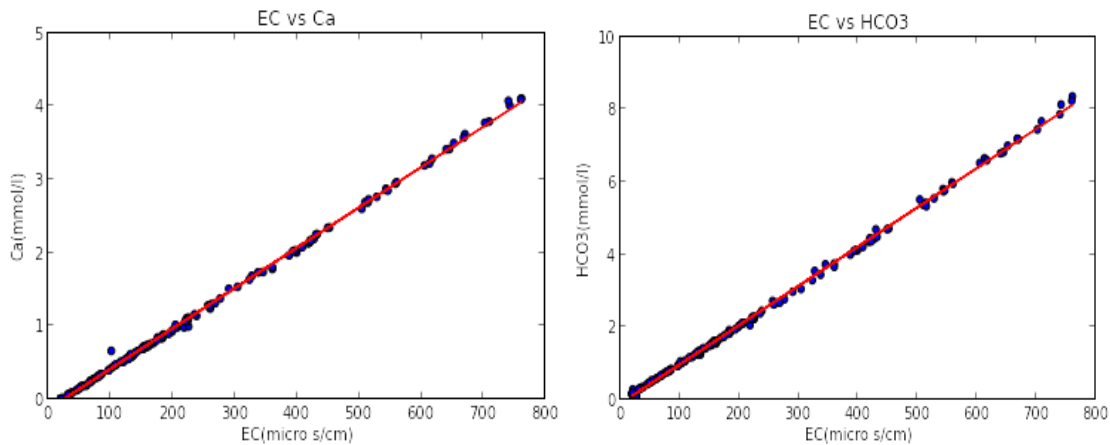


Figure 14. Plotting EC vs. calcium on the left and plotting EC vs. bicarbonate on the right with $R^2 = 0.9991$

To check the reliability of the relation derived above, several samples from both filters, one with grain size 0.5-1.2 mm and one with grain size 1-2mm, were taken on a random day. Figure 15 and Figure 16 illustrate the data from both filters vs. the data that was predicted using the EC relation. As can be seen from these two graphs, the predicted data closely matches the measured data for both filters. Moreover, the error percentage calculated for both filters, except for the sample with a calcium concentration below 0.4 mmol/l, is around 1%.

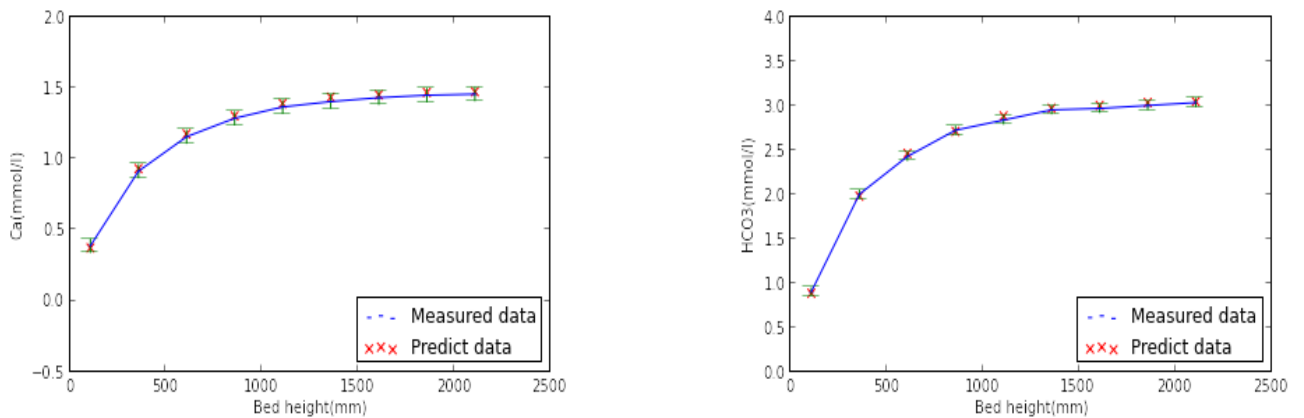


Figure 15. Predicted calcium and bicarbonate based on EC are shown in red lines, while the blue points are the measured data in the filter with grain size 0.5-1.2 mm and a velocity of 5 m/h. The error bars mark a deviance of 5% from the actual data

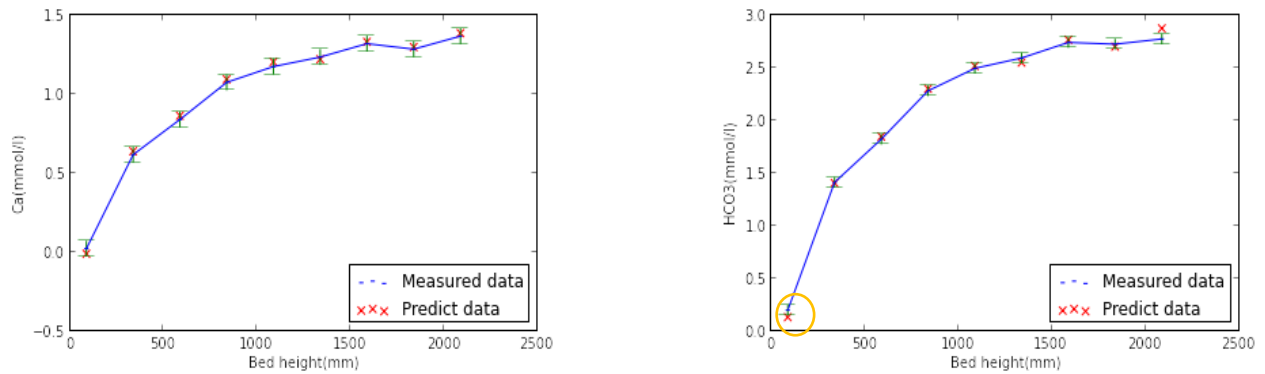


Figure 16. Predicted calcium and bicarbonate based on pilot-EC meter and measured data in the filter with grain size 1-2 mm and a velocity of 5 m/h. The error bars mark a deviance of 5% from the actual data

As can be seen in Figure 15 and Figure 16, the predicted data fell between the acceptable deviations of 5% from the actual data, which confirms the reliability of these two relations. At low concentrations of calcium, however, the error percentage could cross that threshold of 5%. This is because the EC will be affected by low pH values. This relation was further investigated in detail using a PhreeqPython simulation, as can be seen in appendix III. This relation will be used to calculate the calcium and bicarbonate concentrations in run 2 for extra CO₂ dosage experiments.

Another important factor that affects the EC is temperature. A higher temperature implies a lower viscosity, which results in an increase in the mobility of ions and consequently of the EC (Baron and Ashton, 2005). Furthermore, the temperature coefficient is dependent on the type of solution and is expressed as a percentage of EC increase when the temperature increases by 1 °C (Baron and Ashton, 2005). The RO permeate water composition is almost constant, while the water temperature changes between 12-14 °C. Therefore, to extract the effect of temperature variations on the EC, a temperature compensation of 2% was applied to the EC sensor, which converted the EC at any temperature to the EC at the reference temperature of 25 °C.

3.3.3 Tracer test on the calcite filter

The dispersion of a fluid in the filter may lead to less contact time and consequently a lower degree of calcium dissolution. However, the effect of axial dispersion is expected to be negligible, since several studies have shown that the dispersion is minor when the diameter to length ratio of the column is small (Klinkenberg et al., 1953; Miller et al., 2004; Delgado, 2006). In order to confirm the effects of longitudinal dispersion on calcite dissolution and to exclude these possible effects from the dissolution rate, a tracer test was conducted. The following steps were taken:

- Filters 1 and 2 were filled with grain size 1-2 mm and 0.5-1.2 mm respectively.
- Both filters were operated at same velocity of 5 m/h.
- Two sample points were chosen where the EC in the filter was continuously measured. To exclude the possible effects of mix flow in the water above the filters, the sample points were chosen to be located just below the calcite layer (see Figure 17). The EC was compared with the EC of effluent water.
- The sodium chloride brine was used as a tracer and was pumped through the filter from the sampling point behind the filter by impulse injection, i.e., the pump was active for 2 minutes.

- Since the EC is also influenced by the dissolution of calcium and bicarbonate, it is crucial to apply a high concentration of salt to provide a noticeable peak.

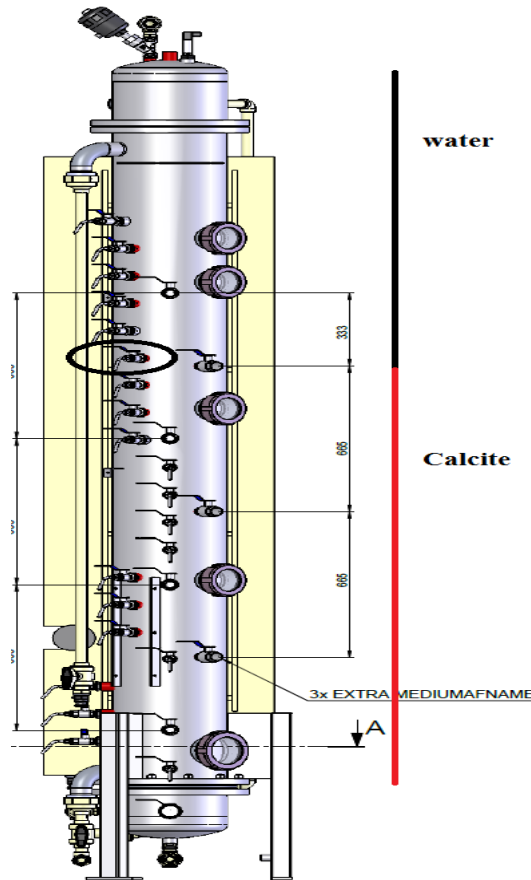


Figure 17. The filter filled with calcite where the sample point EC was measured

Figure 18 and Figure 19 depict the results from filter 1 and filter 2 respectively. Readjusting for the phase difference between the curves and removing the extra EC that was generated by the calcite dissolution in each figure, the two curves almost overlap, showing that the effect of dispersion was negligible in both filters. The slight differences between the EC values in the filter containing calcite grain size 1-2 mm could be explained by equation (2.31 provided by Levenspiel et al. (1972), as $N_D < 0.01$. Based on this relation, a larger diameter results in a greater dispersion.

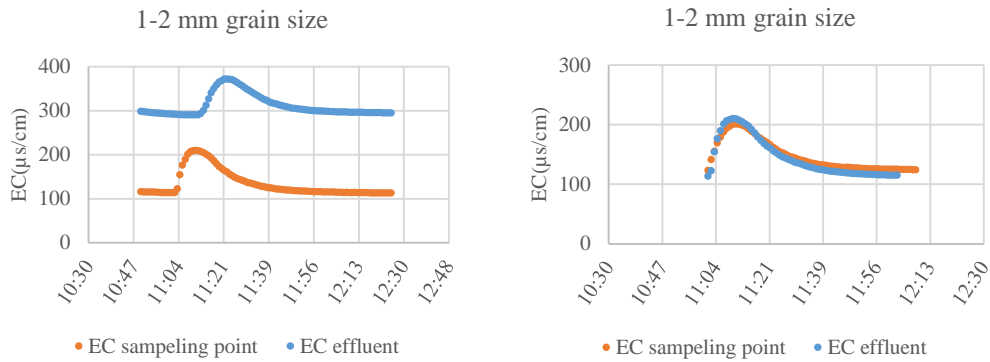


Figure 18. The figure on the left shows the original values of EC measured for filter 1 with grain size 1-2 mm while the figure on the right shows the same but the extra EC from calcite dissolution is excluded and the time phase between the two samples is removed

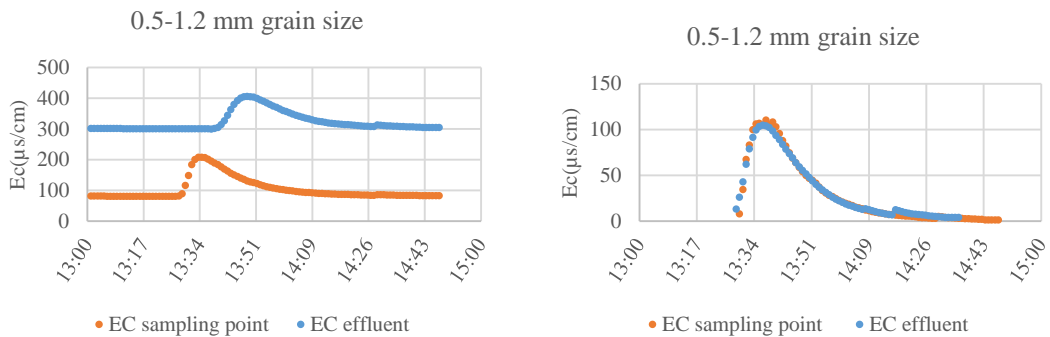


Figure 19. The figure on the left shows the original values of EC measured for filter 1 with grain size 0.5-1.2 mm while the figure on the right shows the same but the extra EC from calcite dissolution is excluded and the time phase between the two samples is removed

3.3.4 Ca vs. HCO₃

To investigate the stoichiometric ratio between calcium and bicarbonate, which was assumed to be 1:2, the results of the measured bicarbonate were plotted against the bicarbonate concentration that was calculated based on the calcium concentration. As can be seen from the Figure 20, the experimental data confirm the 1:2 ratio between calcium and bicarbonate. These results could be used to calculate the bicarbonate based on the calcium concentration.

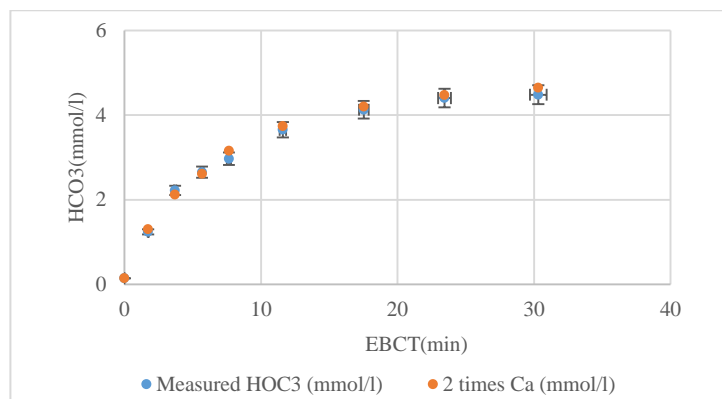


Figure 20. The measured and calculated bicarbonate concentration at various heights over the filter with grain size 0.5-1.2 mm. The error bars mark a deviance of 2% from the measured data

3.4 Overview of experiments

Several parameters affect the calcite dissolution rate. Various experiments were conducted to measure important physical characteristics of the packed-bed contactors and to investigate their effects on the calcite dissolution rate at a low temperature.

3.4.1 Velocity

In order to study the influence of the incoming flow rate, two sets of velocity tests were conducted. For this purpose, both reactors/columns were fully packed with calcite grains with a diameter of 0.5-1.2 mm for set 1 and 1-2 mm for set 2. Each set of experiments consisted of six different velocities: first 5, 10, 15, 16.5 m/h, and on a different day 20 and 30 m/h. During each test, the two filters were run under equal conditions to create duplicate data. Samples were collected from 13 sampling ports positioned along the height of the column, starting from the top of the column and moving downwards to avoid interference in the flow rate during sampling. Each sample was analyzed to determine its bicarbonate and calcium concentrations.

3.4.2 EBCT

The aim of the EBCT experiment was to find the EBCT at which equilibrium was reached. This experience was repeated three weeks later to investigate the effects of different calcite filter runtimes. The EBCT is a function of bed height and flow rate. During the velocity test experiments, the velocity was kept constant while the EBCT was calculated by changing the bed height. In this experiment, the EBCT was adjusted by changing the flow rate and could be calculated using $EBCT = V/Q$.

For this purpose, EBCT ranging between 10-40 minutes and corresponding to flow velocities between 3.0-12.0 m/h were tested. The experiment was conducted at a constant temperature of 12 °C and a bed height of 2 m, while the filters were operated for 3 hours for each specific flow condition.

3.4.3 Carbon dioxide dosage

The effects of the concentration of inlet CO₂ on the dissolution rate were examined under the following conditions:

- Both filters were filled with calcite grain size 0.5-1.2 mm and 1-2 mm in the first and second run respectively.
- To confirm the reliability of the results, both filters were operated under the same conditions for an hour before samples were taken.
- During both runs, the temperature was approximately constant at 12±2 °C.
- During the first run, 9 samples were taken per carbon dioxide concentration test from sampling points along the height of each column, while in the second run samples were taken from all 16 sampling points along the filters.
- The calcium, carbon dioxide, and bicarbonate contents were measured in the laboratory during the first run. However, since the reliability of the relation between EC and the concentrations of calcium and bicarbonate was proven by previous experiments, this relation was used to estimate the calcium and bicarbonate concentrations in the second run.
- The EBCT was adjusted by changing the bed height at a constant filtration velocity of 3.8 m/h.

- The bed heights were measured with measuring tape through the sight glasses in the first run and with bed height sensors during the second run.
- The carbon dioxide efficiency is calculated as follows:

$$\text{CO}_2 \text{ efficiency \%} = \frac{\text{Ca}_{\text{in}} - \text{Ca}_{\text{out}}}{\text{CO}_2 \text{ initial} + \text{CO}_2 \text{ dosing}} \quad (3.5)$$

Where Ca_{in} , Ca_{out} are the initial and effluent calcium concentrations respectively.

- The initial CO_2 concentration was measured by the CO_2 sensor at the pilot plant, while a correction of 9% is used as the inlet CO_2 concentration.
- The CO_2 concentrations of samples at other bed heights were calculated by the laboratory based on the bicarbonate, calcium, EC, and Ph levels, and the temperature of each sample using NPR 6538, NEN 6533.
- During each run, additional CO_2 concentrations of 2, 4, 6, and 8 mmol/l were injected into the inlet flow using a mass flow controller (MFC).

3.5 Software used

To prevent the complicated and time-consuming chemical calculations to find the equilibriums, reactions were simulated in the chemical simulation environment of PhreeqPython (Heinsbroek, 2017). PhreeqPython is an object-oriented wrapper around the VIPhreeqc extension of the Phreeqc chemical modeling environment (Parkhurst & Appelo, 1999) written in Python. PhreeqPython uses the STIMELA database and is partly derived from the PhreeqPy extension for Iphreeqc (Müller et al., 2011). Moreover, Phreeqc is a modeling environment for standardized mathematical models of drinking water treatment processes developed by Omnisys and the Delft University of Technology as part of the STIMELA modeling environment (Van der Helm & Rietveld, 2002). The modified Yamauchi model (Chapter 5) was also implemented in PhreeqPython to calculate the kinetics of dissolution reactions. The main advantage of PhreeqPython over Phreeqc (Parkhurst & Appelo, 1999) is that it combines Phreeqc and Python in one programme. This has made it possible to gather the chemical reaction results from Phreeqc and the dissolution rate from the modified Yamauchi model in one place and to simulate the final water quality in Python in the form of graphs or tables. In other words, the user only needs to add the initial water quality and the operational parameters of the calcite filter, such as the velocity, grain size, porosity, and bed height in the excel sheet. The user can then run the model in PhreeqPython, where all calculations will be done in the background and the output will consist of the final water quality with regards to its calcium and bicarbonate concentration.

4 Results of pilot plant experiments

In this chapter, the results of the performed tests are presented. The influence of each parameter is further investigated through sensitivity analyses in Chapter 7.

4.1 Velocity tests

The results of the velocity variation tests are depicted in Figure 21. In order to make the data comparable, it was crucial to keep the other operating parameters constant. However, due to the configuration of the wells, CO₂ concentrations fluctuated during the experiments as well as in between the velocity tests. This also affected the calcite dissolution. To rule out the effect that this could have, the calcium concentration was divided by the corresponding calcium saturation concentration for each sample as calculated in PhreeqPython.

In all velocity tests, most of the calcite dissolution took place in the first 50 cm of the reactor, as a high concentration of carbon dioxide was present there. It was found that after five minutes of EBCT in the filter with small grain sizes, the concentration of dissolved calcite reached 62-72% of the maximum potential mass that could be dissolved, i.e., the calcium concentration equilibrium. For the larger grain sizes, this value was between 32-52% when the CO₂ concentration was below 1.5 mmol/l.

As shown in Figure 21, the dissolution rate slows down considerably when water reaches the last third of the reactor volume. Furthermore, when comparing the calcium concentrations in the last section of reactors, it becomes evident that an increase in velocity causes a reduction in the calcium concentration, as it results in less EBCT.

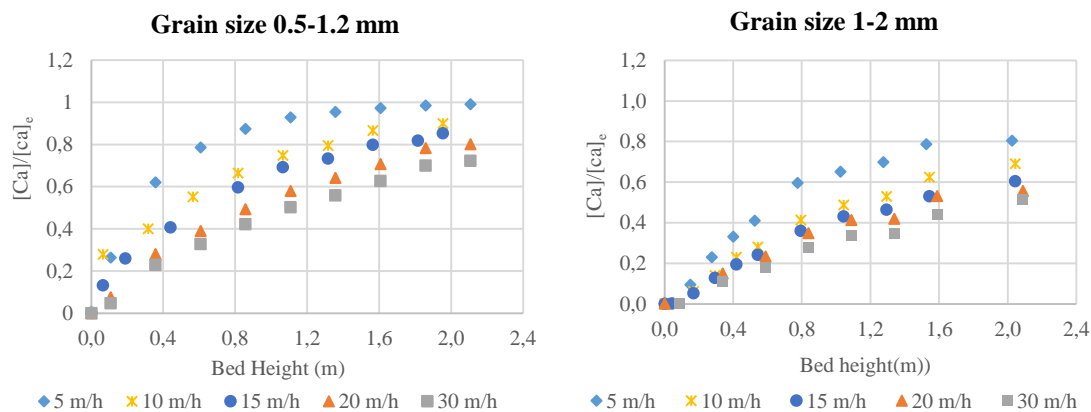


Figure 21. Measured $[Ca^{2+}]$ concentration divided by the equilibrium concentration of calcium calculated by PhreeqPython as a function of bed height for the five tested velocities of 5, 10, 15, 20, and 30 m/h flow rates and a CO₂ concentration of less than 1.5 mmol/l

Figure 22 and Figure 23 show the results of the velocity tests corresponding to run 1, grain size 0.5-1.2 mm, and run 2, grain size 1-2mm, respectively. Here, the EBCT was calculated based on the position of each sample over the bed height.

The calcite dissolution rate is represented by the slope ($R = dCa/dt$) in Figure 22 and Figure 23. To depict the variation between the slopes more clearly, the first 10 minutes of the reaction are magnified on the right. Comparing the experimental results from both ranges of grain sizes, it is evident that the bigger grain size was more sensitive to the velocity variation than the smaller one, indicating a diffusion limitation at lower velocities. The effects of the flow rate on calcite dissolution will be further investigated in the model.

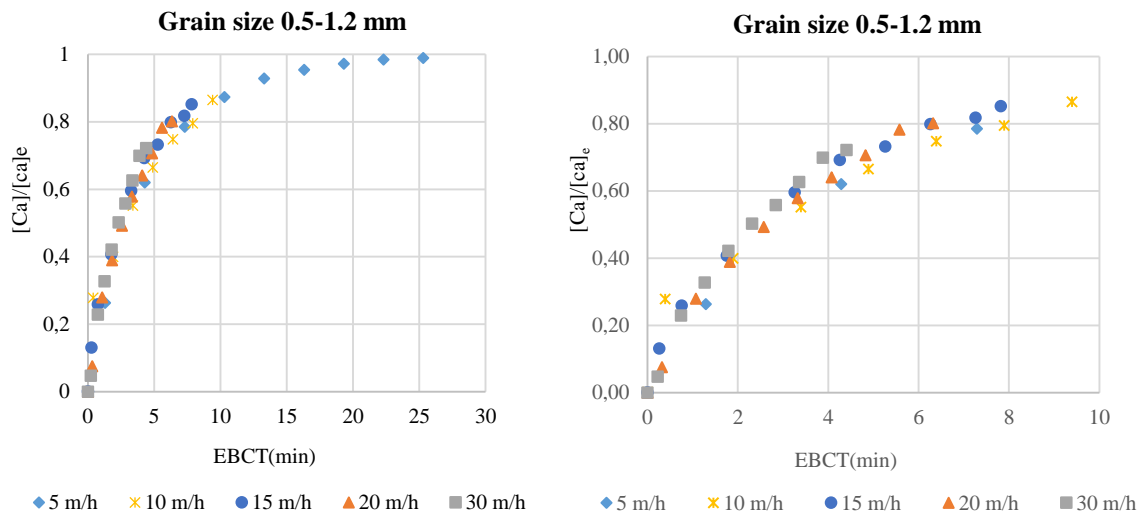


Figure 22. Measured $[Ca^{2+}]$ concentration divided by the equilibrium concentration of calcium calculated by PhreeqPython as a function of retention time for the five tested velocities of 5, 10, 15, 20, and 30 m/h flow rates and a CO_2 concentration of less than 1.5mmol/l

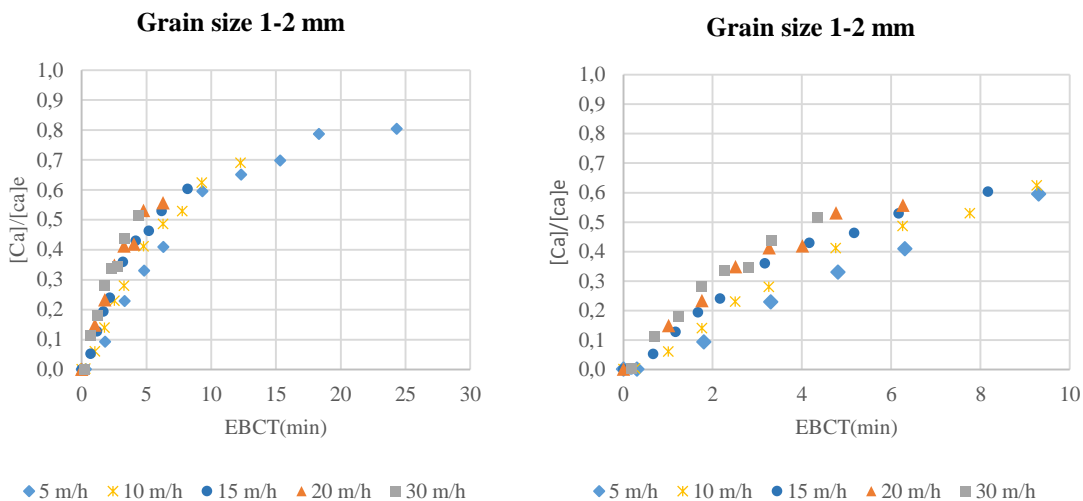


Figure 23. Measured $[Ca^{2+}]$ concentration divided by the equilibrium concentration of calcium calculated by PhreeqPython as a function of retention time for the five tested velocities of 5, 10, 15, 20, and 30 m/h flow rates and a CO_2 concentration of less than 1.5mmol/l

What can be concluded from Figure 22 and Figure 23 is that the dissolution rate in the calcite filter with grain size 0.5-1.2 mm was clearly higher than in the other filter. This can be explained by equations (2.8 and (2.9, since the smaller grain has a higher specific surface area (A/V), resulting in a higher dissolution rate. Moreover, as a result of the faster reaction velocity, the smaller calcite size reaches the equilibrium quicker than the bigger grain size, making it the more efficient size to use.

Furthermore, the EC of the effluent water was monitored for seven consecutive days while filters 1 and 2 were filled with the 1-2 mm and 0.5-1.2 mm grain sizes respectively. Both filters were operated under the same conditions. The results confirmed the effect of grain size on calcite dissolution rates, as a higher EC represents higher calcium

concentrations. However, from the experiment it appeared that the effect of grain size is more significant at higher inlet concentrations of CO₂.

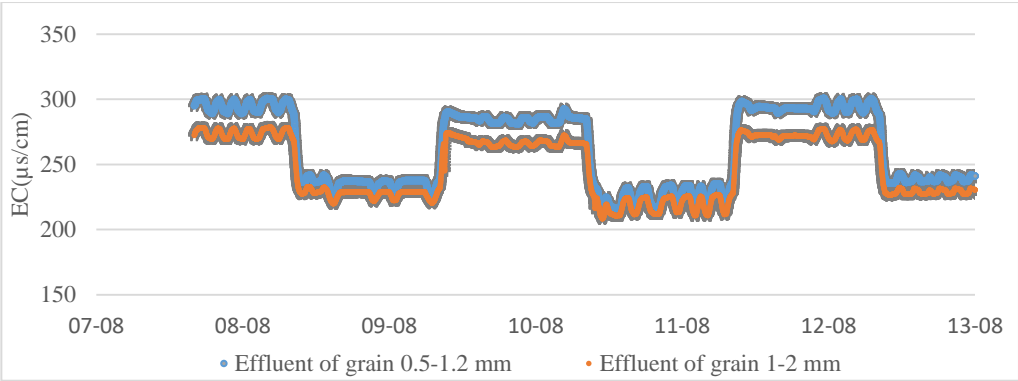


Figure 24. Effluent EC converted to the reference temperature of 250 °C measured at the pilot plant for 7 consecutive days. Filter 1 and 2 contain grain size 1-2 mm and 0.5-1.2 mm respectively

4.2 EBCT effect

As mentioned in Chapter 3.4.2, the bed height was kept the same in this experiment and the EBCT was adjusted by changing the flow rate. Effluent water qualities were compared. Moreover, the experiments were repeated after approximately three weeks to investigate the effect of the filter runtime on calcite dissolution. These results are depicted in Figure 25. The main observations are:

- The grain size of 1-2 mm approached the equilibrium after 25 minutes when the CO₂ concentration was low but saw a slight increase when the CO₂ concentration rose. However, the grain size of 0.5-1.2 mm only required approximately 15 minutes to reach the equilibrium at high CO₂ concentrations as is depicted by the yellow line.
- The performance of filters does not change noticeably after three weeks of runtime.
- Both ranges of grain size met the target calcium concentration of 0.625 mmol/l in all tested EBCT.

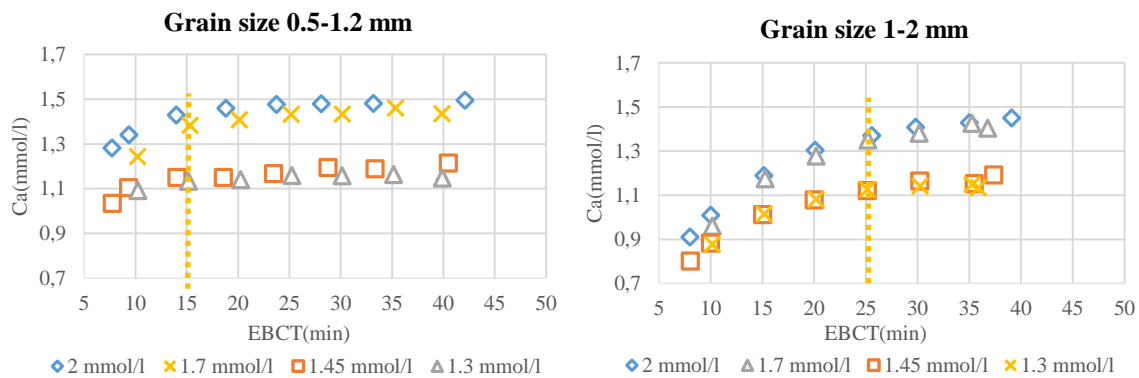


Figure 25. The calcium concentration at various EBCT at the beginning of the running period with CO₂ concentrations of 2 and 1.45 mmol/l and after 3 weeks with CO₂ concentrations of 1.3 and 1.7 mmol/l

4.3 Carbon dioxide concentration effect

Based on a reaction equation, the carbon dioxide concentration is expected to have a noticeable effect on calcite dissolution. This can be seen in Figure 25, where it is shown that the CO₂ concentration fluctuated between 1.3-2 mmol/l. As mentioned in Chapter 3.4.3, to investigate the effects of the initial CO₂ concentration, various CO₂ concentrations were dosed to the water before it entered the calcite filter. The influent water thus contained various amounts of CO₂. What is reported here, however, is the total CO₂ content: both the influent and the dose content. The results of these experiments are shown below.

An overview of the calcite dissolutions with grain sizes between 0.5-1.2 mm and between 1-2 mm are depicted in Figure 26. The main observations are:

- There is a clear connection between the amount of CO₂ dosing and the calcium production. However, the increase in calcium concentration slows down over time as the calcium concentration approaches the equilibrium concentration. This equilibrium value depends on the initial CO₂ concentration that was applied before filtration.
- When the CO₂ concentration increases, the required EBCT also elevates.

The maximum efficiency for grain size 0.5-1.2 mm was around 81%, while grain size 1-2 mm cannot reach an efficiency higher than 74% within the given EBCT.

- The slope of the graphs represents the calcite dissolution rate ($R = dCa/dt$). As can be seen from Figure 26, increasing the carbon dioxide concentration also elevates the calcite dissolution rate noticeably, especially during the first 10 minutes.
- Additional CO₂ dosage accelerates the calcite dissolution but results in a CO₂ efficiency drop, as shown in Figure 27. Subsequently, more effort is required to correct the pH value following filtration, due to a high concentration of unreacted CO₂.

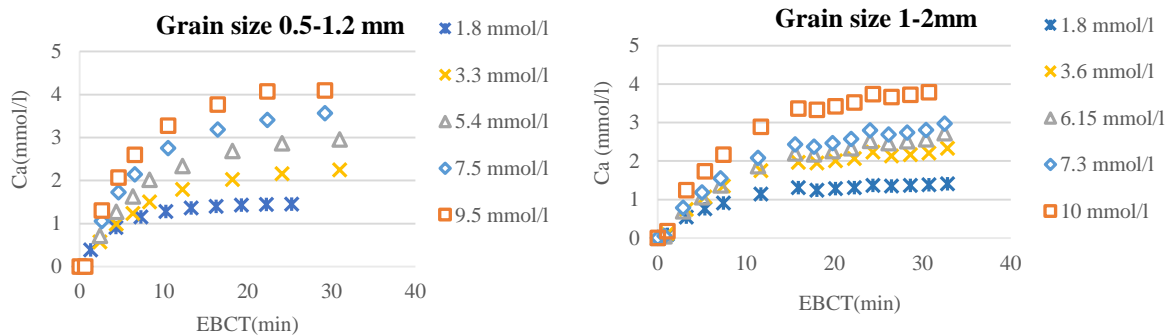


Figure 26. The effect of the initial CO₂ concentration on the calcite dissolution rate

As depicted in Figure 27, increasing the CO₂ dosage decreases the maximum CO₂ efficiency. Furthermore, the CO₂ efficiency for grain size 1-2 mm is less than for grain size 0.5-1.2 mm at the same operation conditions, among which EBCT. This is reasonable, as there is less reaction surface area available for this grain size.

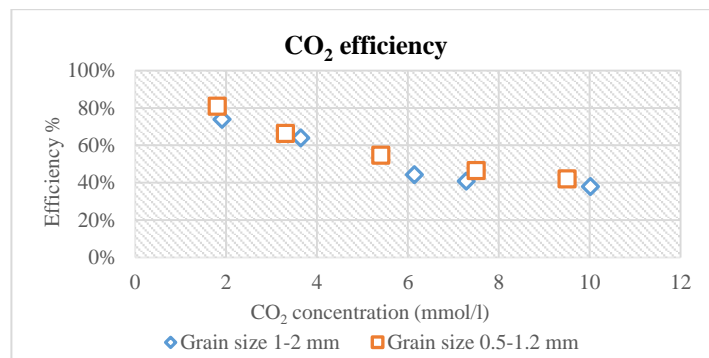


Figure 27. The CO₂ efficiency for calcite grain sizes at various carbon dioxide concentrations at constant EBCT of 30-33 minutes

Figure 28 shows the CO₂ efficiency at various EBCT for different inlet CO₂ concentrations. As can be seen, the CO₂ efficiency drops below 80% when reducing the EBCT to below 15 minutes. This is because at a shorter EBCT, part of aggressive CO₂ leaves the filter unreacted. If the EBCT is sufficient, however, it will be converted to calcium and will result in an increase of the CO₂ efficiency.

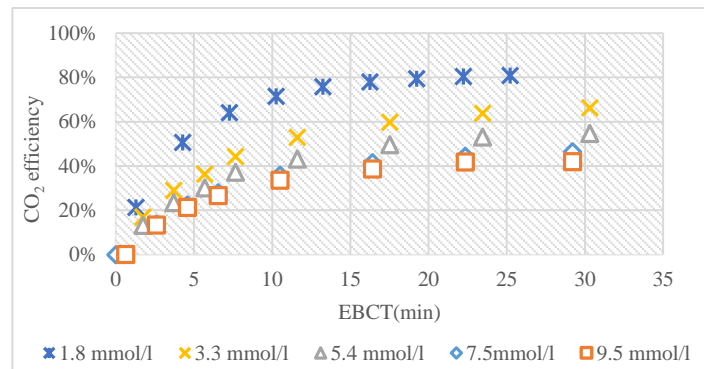


Figure 28. The CO₂ efficiency versus the EBCT where the EBCT changes by adjusting the bed height for grain size 0.5-1.2 mm and constant velocity

A high CO₂ efficiency is preferable to limit the use of chemicals, such as the NaOH that is required to correct the pH. However, efficiency could never reach 100% because:

1. The chemical equilibrium is never achieved in practice when given a finite contact time (Yamauchi et al., 1987). As CO₂ dissipates from the water, the kinetics of the process decrease. Consequently, a realistic contact time is insufficient to convert all the aggressive CO₂ in practice.
2. Based on the Tillman's curve of Figure 2, part of the CO₂ will not participate in the reaction because it is present as non-aggressive CO₂. Water in chemical equilibrium always contains a certain amount of non-aggressive CO₂ that is relative to the amount of HCO₃ present in the water. Therefore, the process becomes inefficient as the bicarbonate content in the water increases (Letterman et al., 1991).

5 Mathematical model

The kinetics of calcite dissolution play a fundamental role in the effectiveness of the remineralization process in practice. Therefore, it is crucial to develop a kinetics model that can predict calcite dissolution with a high accuracy. This model could be utilized to predict the calcite dissolution rate as a function of design parameters. Subsequently, it could be used to improve the design and operation conditions of the production process of high-quality, cost-efficient product water. In general, the objectives of using the mathematical model are:

1. To calculate the effluent water quality based on the initial water quality data after calibration of the model;
2. To determine the optimal design aspects and operational variables of a calcite filter.

In order to model the remineralization process from the beginning until the point of equilibrium, three steps were taken:

1. Simulating the chemical reactions in calcite filters using PhreeqPython;
2. Determining the reaction rate based on the model provided by Yamauchi, since the PWP model used by Phreeqc is not compatible with Oasen's low-pH systems (Hasson & Bendrihem, 2006; Bang, 2012; Shemer et al., 2013);
3. Fitting the model to pilot experimental data.

5.1 Simulation of chemical reactions

The inlet water of the filters was permeate water with a low and constant ion content. In our simulation, the average water quality provided in Table 5 was used. The initial concentrations of calcium and bicarbonate were measured by the laboratory for each run. The CO₂ concentrations were measured at the pilot plant using CO₂ meters. This information was used to calculate the calcium concentrations at the equilibrium using the implemented Phreeqc in PhreeqPython.

5.2 Reaction rate based on Yamauchi model

To calculate the kinetics of the calcite dissolution reaction, the Yamauchi model (Yamauchi et al., 1987), extensively described in Chapter 2.4.2, is used. According to Yamauchi et al. (1987), aggressive CO₂ is the driving force behind the reaction.

Based on Yamauchi's equation (2.32), there is a linear relationship between $\ln \frac{([x]_e - [x]_i)}{([x]_e - [x]_o)}$ vs. the EBCT, where X represents either [HCO₃] or [Ca] and the subscripts 0, L, and e stand for inlet, bed height, and equilibrium concentrations respectively. The slope of this line gives the $-k \frac{6(1-\varepsilon_L)}{(D_p^* \varphi)}$ equation. By replacing the corresponding diameter and porosity, the Ya coefficient could be calculated experimentally. It should be noted that the Ya coefficient is a calcite dissolution rate coefficient which contains the form factor as well. Therefore, there is no need to measure or calculate the form factor separately. To calculate

the Ya coefficient, the results from the velocity tests for both grain sizes were used. The results are shown in Figure 29 and Figure 30.

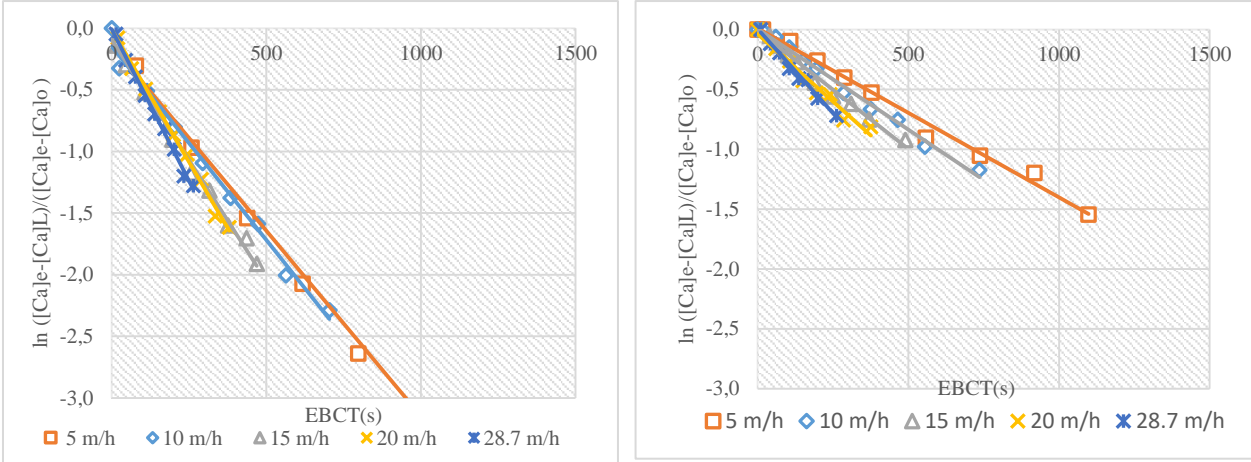


Figure 29. The linear plot of $\ln \frac{([Ca]_e - [Ca]_L)}{([Ca]_e - [Ca]_o)}$ vs. EBCT for grain size 0.5-1.2 mm on the left and 1-2 mm on the right, where $R^2 > 0.99$ for grain size 0.5-1.2 mm and $R^2 > 0.98$ for grain size 1-2 mm.

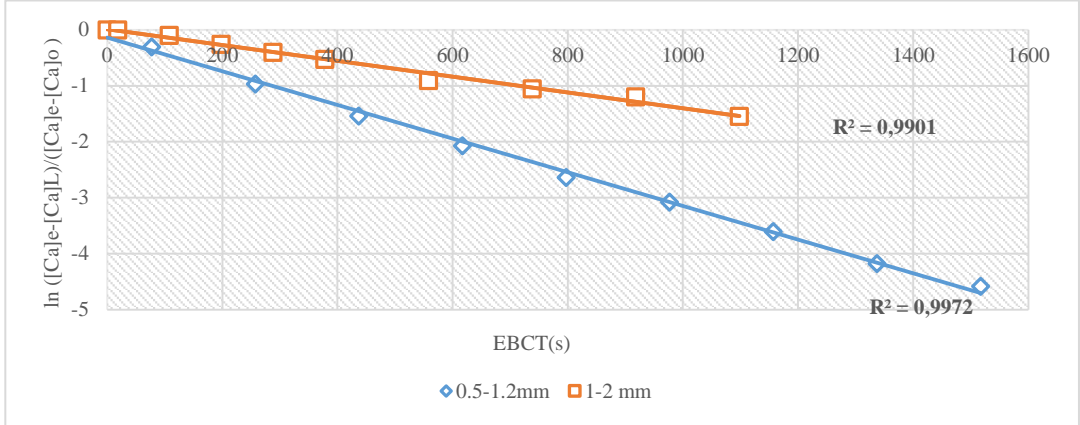


Figure 30. The linear plot of $\ln \frac{([Ca]_e - [Ca]_L)}{([Ca]_e - [Ca]_o)}$ vs. EBCT for various grain sizes at the velocity of 5 m/h and 13 °C

The main observations from the figures above are:

- The experimental data confirms the linear relation provided by Yamauchi et al. (1987), since the result follows the straight line with a correlation coefficient of $R^2 > 0.98$ identically.
- The filtration rate was found to have a converse effect on the calcite dissolution rate as increasing the velocity decreases the necessary contact time to reach equilibrium. This effect can be seen in Figure 29, but it is more obvious in the range of calcite grain sizes between 1-2 mm. This observation was also made by Yamauchi et al. (1987), but they did not take the effect of velocity on Reynolds number into account. The turbulence of the flow increases with an increasing filtration rate based on a Reynolds number equation. More turbulence accelerates the transfer of substances from solid surface to bulk solution (Lehmann et al., 2013).
- Figure 30 depicts the effect of calcite grains on the dissolution rate constant, which reaffirms the model provided by Yamauchi et al. (1987). As can be seen, the smaller particle has a steeper slope, corresponding to a greater Ya coefficient. This can be

explained by the fact that the smaller particles have larger surface reaction which accelerate their dissolution.

- The Y_a coefficient, determined from the velocity test, ranged between 4.86×10^{-3} and 7.78×10^{-3} for grain size 0.5-1.2 mm and between 4.12×10^{-3} and 8.24×10^{-3} for grain size 1-2 mm when the velocity ranges from 5 to 28.7 m/h. The differences between the Y_a coefficients can be explained by diversity in the form factor of each grain size.

Table 8 compares the calcite dissolution rate based on the Yamauchi model derived from previous studies, while the dissolution rate constant is derived from our experimental data. The results show that the dissolution constant is strongly affected by a change in temperature. As shown in Figure 31, the dissolution rate increases by a factor of 2 when elevating the temperature from 22 °C to 30 °C (Shemer et al., 2013). However, the dissolution rate constant derived from the study by Shemer et al. (2013) at a temperature of 22 °C is comparable to our experimental data. Since the temperature was approximately constant in our case, the temperature effect on calcite dissolution was neglected.

Table 8. The calcite dissolution rates (Y_a coefficient) from previous studies regarding their operational conditions and our experimental data

	Hasson(2006)	Shemer(2013)	Shemer 2013	Shemer(2013)	Hasson(2013)	Hasson(2013)	Orly(2013)	Yamauchi(1989)	Ghanbari 2017	Ghanbari 2017
D_p (mm)	2.85	2	2	2	2	2	2	1.34-1.37-1.96	0.5-1.2 mm	1-2mm
ϵ	38%	?	?	?	56%	51%	56%	40-44%	50%	49%
Velocity(mm/s)	2.07	2.75	4.56	4.56	4.56	4.56	2.7	2.5	2.77	2.77
	4.14	4.56	-	-	-	-	-	8,6	4.58	4.58
	6,22	7,57	-	-	-	-	-	-	7.97	7.97
Column diameter(mm)	32	98	98	98	98	98	3880	100	318	318
Bed height(m)	2	1,8	1,8	1,8	0,94	0,94	3,5	0.5-2.4	2-2.1	2-2.1
Temperature($^{\circ}$ C)	30	22	22	30	28.6	28,6	24	40	12 \pm 2	12 \pm 2
CO ₂ concentration(mmol/l)	0.5-2	4,3	3.4-4.3-6.8	0.25-0.75-1.4	3-4.5-6.4	3-4.5-6.4	0.95-2.16-3-3.6	1.2-2.5	1.45-1.8	1.45-1.8
pH	5.2-6.2	?	?	?	?	?	?	?	5.43-5.51	5.43-5.51
$k_6(1-\epsilon)/D_p^* \Phi$	5,50E-03	?	?	?	2,31E-03	?	-	-	-	-
$6k/\Phi$	2,53E-02	6,95E-03		1,20E-02	1,05E-02	1,76E-02	8,36E-03		4,89E-03	4,80E-03
	-	7,13E-03	6.59 \pm 0.67E-03	-	-	-	-	3,10E-02	6.29E-03	6.1E-03
	-	7,31E-03		-	-	-	-	-	8.3E-03	8.2E-03
Calcite purity	98%	96%	96%	96%	96%	97.5%	?	?	99%	99%

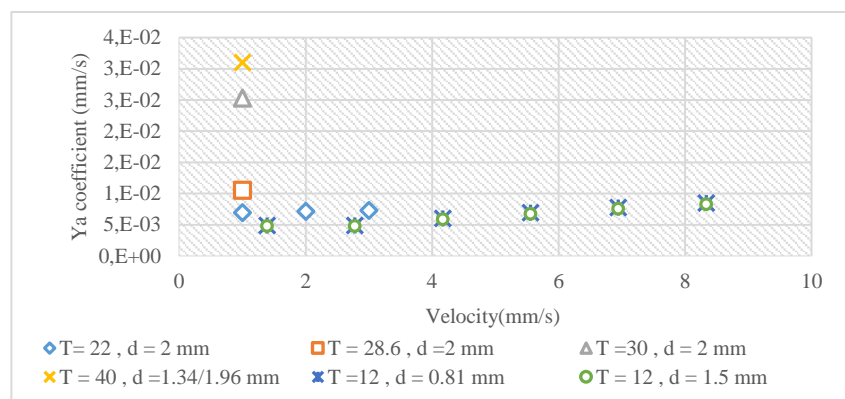


Figure 31. Recap from previous studies on calcite dissolution rates using the Yamauchi model

5.3 Calibration of Yamauchi model

The effects of velocity on the dissolution rate constant were further investigated in order to find a unique relation that fit the velocity data. For this purpose, the least-squares method was used. The results from these fitting data are shown in Figure 32.

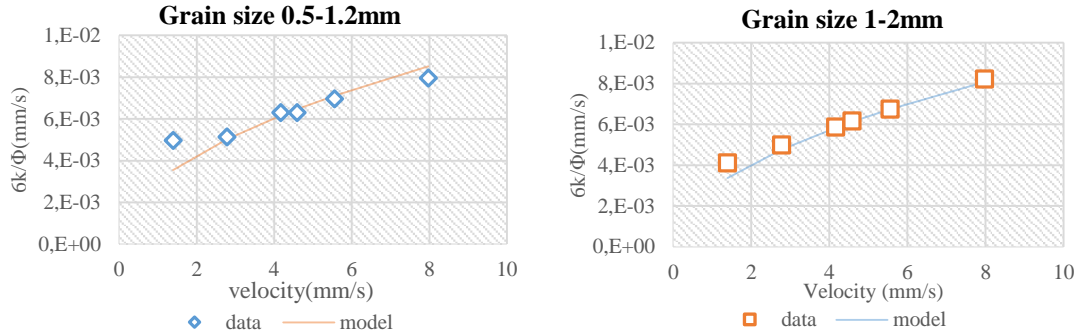


Figure 32. Reaction rate constant plotted as a function of velocity. Points were obtained from a velocity test and the Yamauchi model, and the line was fitted to data by method of least squares

The calcite dissolution rate coefficients $6k/\Phi$, obtained by analyzing the data from 10 velocity runs, consisting of 5 different velocities for each grain size, were found to fit the following correlations:

$$\frac{6k}{\Phi} \left(\frac{mm}{s} \right) = 2.96 \times 10^{-3} \sqrt{U_L (mm/s)} \quad (4.1)$$

This equation will be used to calculate the Ya coefficient in the Yamauchi model. However, as can be seen from Figure 32, this correlation underestimates the dissolution rate coefficient ($6k/\Phi$) at the low velocity of 5 m/h, especially for the smaller grain size. When comparing the dissolution rates obtained from the 5 m/h and 10 m/h velocity tests depicted in Figure 29, it can be concluded that, at such low flow rates, the dissolution rate was not a function of the flow velocity, as the slopes of the dissolution rate curves of both velocities were almost identical. In other words, under the conditions tested, increasing the flow rate from 5 m/h to 10 m/h did not have a visible effect on the dissolution rate.

By replacing the velocity correlation in the Yamauchi model shown in (4.1), the modified Yamauchi expression is as follows:

$$\ln \frac{([Ca]_e - [Ca]_l)}{([Ca]_e - [Ca]_o)} = 2.94 \times 10^{-3} \sqrt{U_L (mm/s)} \frac{(1 - \varepsilon_L)}{D_p} * \frac{z_L}{U_L} \quad (4.2)$$

The input data of the model consists of two main parts: the initial water quality before filtration to calculate the calcium concentration at equilibrium using PhreeqPython, and the operational parameters such as the velocity, bed height, and calcite grain size. To make all calculations more organized and to gather them in one place, the model has been implemented in PhreeqPython.

5.3.1 Result from modified model

The results from the duplicated velocity test and CO₂ test were used to validate the modified Yamauchi model. Figure 33 and Figure 34 show the results of the calcium concentrations

predicted by the modified Yamauchi model for grain size 0.5-1.2 mm and 1-2 mm respectively.

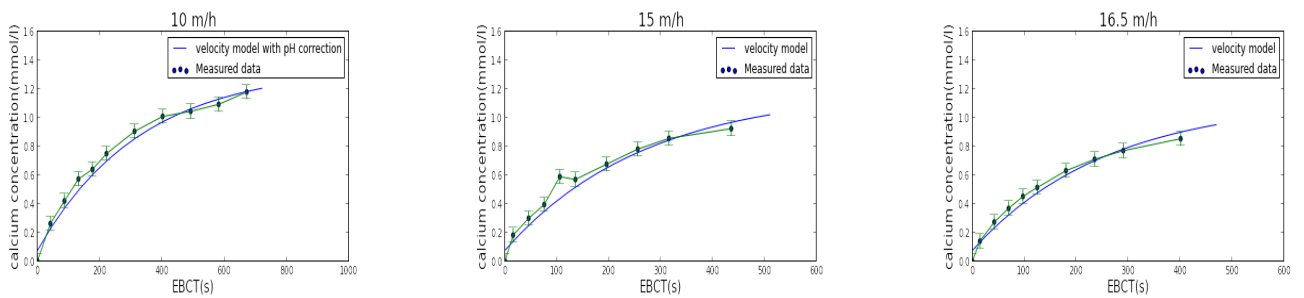


Figure 33. Modeling data using the modified Yamauchi model for grain size 0.5-1.2 mm. The error bars mark a deviance of 5% from the measured data

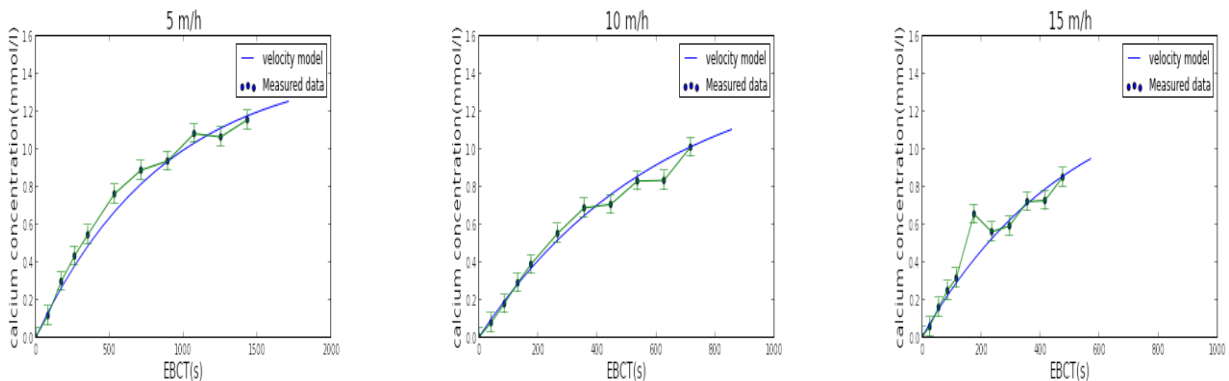


Figure 34. Modeling data using the modified Yamauchi model for grain size 1-2 mm. The error bars mark a deviance of 5% from the measured data

As shown in Figure 33 and Figure 34, the model can predict the calcium concentration at each EBCT with an error percentage of less than 5% except for the velocity of 5 m/h, which sometimes shows an error of around 8%. This is because, as mentioned before, the velocity correlation underestimates the dissolution rate as shown in Figure 32. Figure 35 depicts the small grain size CO₂ experiment simulation using the modified Yamauchi model in PhreeqPython. The PhreeqPython codes of these simulations are shown in appendix VIII.

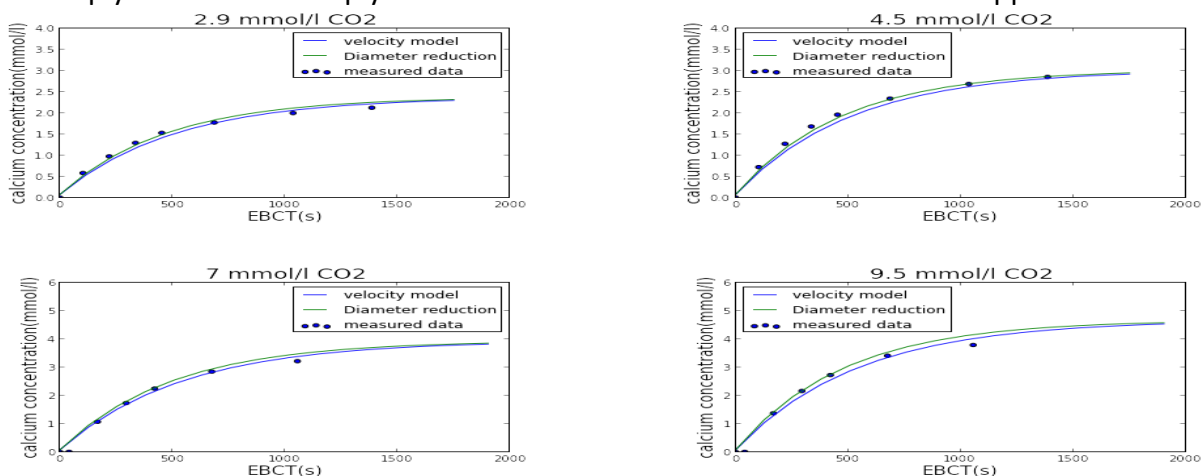


Figure 35. Modeling data using PhreeqPython, grain size 0.5-1.2mm, CO₂ test, and filter 1 at constant flow of 3.8 m/h

In conclusion, the results of the pilot study confirmed the validity of the modified Yamauchi model for desalinated water from RO with changing operational variables such as the calcite grain size, velocity, EBCT, and the initial carbon dioxide and calcium concentrations at low temperatures. The results show an approximate error of only 5%. This error can be explained by several reasons, listed below:

- As shown before, one of the important parameters affecting the calcite dissolution is the initial CO₂ concentration. Therefore, accurate measurements of initial CO₂ concentrations are crucial to predicting the calcium concentrations when using the model. However, the permeate water contains a variable amount of CO₂, which was measured with a CO₂ meter at the pilot plant with an accuracy of ±5%. This error in measurement could cause a deviation between measured and predicted data.
- The other reason behind a possible error in the simulation values is the calcite grain size. The model used the average grain size found by sieving analyses, while there is a range of grain sizes inside the filter that could cause small deviations between predicted and measured data.
- As mentioned in Chapter 3.2.1, the bed heights during the first run with grain size 0.5-1.2 mm were measured using measuring tape on the outside of the filters, which may result in inaccuracies in height measurement and consequently in the model.

5.3.2 Testing the Yamauchi assumptions

As previously mentioned, the calcite dissolution rate is proportional to the specific surface area. Yamauchi et al. (1987) assumed the calcite filter as a one-layer plug flow model, in which the effects of calcite dissolution on grain size and subsequently on specific surface area were neglected. In the following part, the validity of these two assumptions will be tested.

As can be seen from Figure 36, most of the dissolution took place in first 50 cm of the calcite filter, and it diminishes over the bed height. This part will be refilled frequently with fresh calcite grains to keep the design EBCT constant. The frequency of refilling can be calculated using model based on calcite reduction. This will be explained in Chapter 6. It is recommended to reload the filter when the initial calcite level is reduced by 10% or more to maintain the design EBCT (Ludwig & Hetschel, 1986).

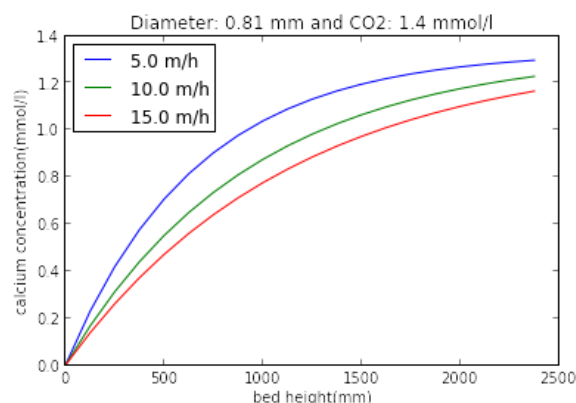


Figure 36. Calcite dissolution simulation at constant water quality and grain size using the modified Yamauchi model

Before refilling the filter, it is necessary to estimate the diameter reduction. To do this, it is assumed that the number of calcite grains in a specific volume does not change during the calcite dissolution. To simplify the calculations, it is also assumed that the calcite grains are

spherical. Using these assumptions, the number of calcite grains in the filter can be calculated with median diameters of 0.81 mm and 1.5 mm for the two respective ranges of grain sizes as follows:

$$V_{\text{calcite packed}} = \frac{\text{No. calcite bag} * \text{Weight of each bag} * \text{Purity of calcite}}{\text{bulk density of calcite}} \quad (4.3)$$

$$\text{No. calcite grains} = \frac{V_{\text{calcite packed}}}{\frac{2}{3} \pi \left(\frac{d_p}{2}\right)^3} \quad (4.4)$$

Subsequently, the reduction volume can be calculated by equation 4.6. This equation is based on a bed height drop of 10%, since the filter will be reloaded after this point.

$$H_{\text{After reduction}} = \frac{V_{\text{calcite packed}}}{\text{Surface area of the filter}} * \text{Porosity} * 0.9 \quad (4.5)$$

If the number of calcite grains stays constant, the new diameter can be calculated with equation (4.4) by replacing the volume of calcite packed after the reduction. The diameter of calcite following a 10% reduction in the bed height is equal to 0.76 mm from the initial diameter of 0.81 mm. Subsequently, the calcite concentration over the bed height was simulated using the modified Yamauchi model to see the effects of the calculated diameter reduction on calcite dissolution.

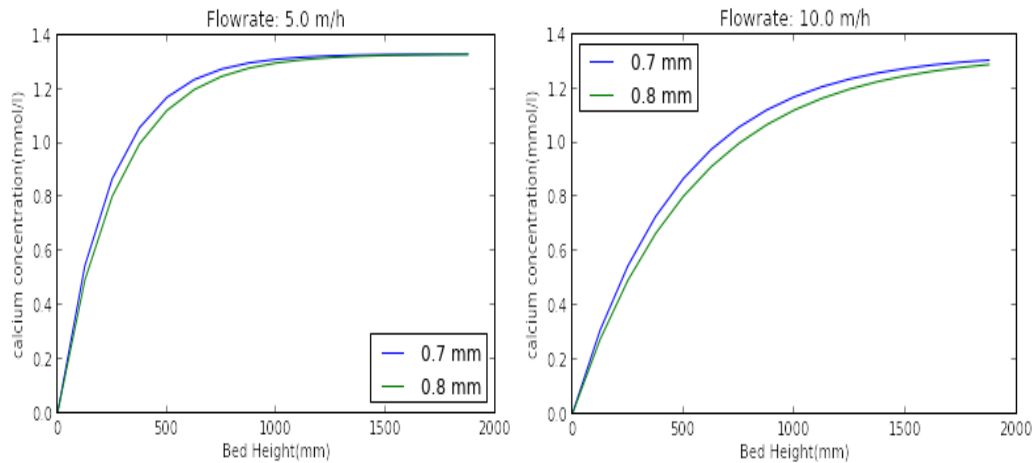


Figure 37. Calcite dissolution simulation at constant water quality and grain size reduction using PhreeqPython

As can be seen in Figure 36, the effect of a diameter reduction on the calcite dissolution rate is not large. This reaffirms the assumption made by Yamauchi et al. (1987) regarding the negligible effect of calcite dissolution on calcite grain size during the operation period.

In order to further examine the necessity of a more complex model based on a multilayer concept, an existing multilayer model is used (G. Zweere, 2016). The model was built in PhreeqPython under the assumption that stratification of grain sizes over the bed height will occur after each backwash. In this model, as in the Yamauchi model (Yamauchi et al., 1987), the aggressive CO_2 is defined as the driving force behind calcite dissolution in water. As a starting point, first-order reaction kinetics are used to describe the dissolution process:

$$-\frac{dc}{dt} = k(C - C_s) \quad (4.6)$$

Since the half-life of a first-order reaction is a constant, the equation can be recalculated by calculating the half concentration of aggressive CO₂ using the rate constant (k) below:

$$[\text{CO}_2] = \frac{1}{2}[\text{CO}_2]_0 \rightarrow \frac{[\text{CO}_2]}{[\text{CO}_2]_0} = \frac{1}{2} = e^{-kt} \rightarrow t = \frac{\ln 2}{k} = \frac{0.693}{k} V \quad (4.7)$$

Subsequently, the half concentration of aggressive CO₂ can be calculated using equation (4.8):

$$1/2 = K_{\text{solving}} * v_f^{0.65} * \varphi * p * d^{1.1} / \text{rho} \quad (4.8)$$

Where:

- rho = density of calcite grains (2,500-2,700 kg/m³)
- p = porosity of the bed (0.32-0.5)
- d = grain size
- φ = granular shape factor = (0.9 to 0.665)
- V = filtration velocity (contact time)
- K_{solving} = correction factor

Subsequently, the particle size distribution over the bed height is assumed to be in the order of the smallest to the largest diameter in a downward direction. Finally, the bed height is divided into approximately 100 layers of 0.025 m per layer in this particular case. This is assumed in such a way that the water quality calculated for a layer becomes the inlet water quality for the layer located directly below. This information is used to build the model in PhreeqPython. However, a further in-detail description of the model is beyond the scope of this research.

To compare the results from both models, the velocity experiment of 16.5 m/h for grain size 0.5-1.2 mm was chosen. The calcite dissolution rate over the bed height was simulated with both the modified Yamauchi model as well as the multilayer model. The simulation data is shown in Figure 38. As can be seen, there is no considerable variation in the accuracy of the results simulated by the modified Yamauchi model. As it can simulate the calcite dissolution with an accuracy of 95% or more, there is no need for a multilayer model. This confirms the single layer model provided by Yamauchi, which is also the base model used in this study.

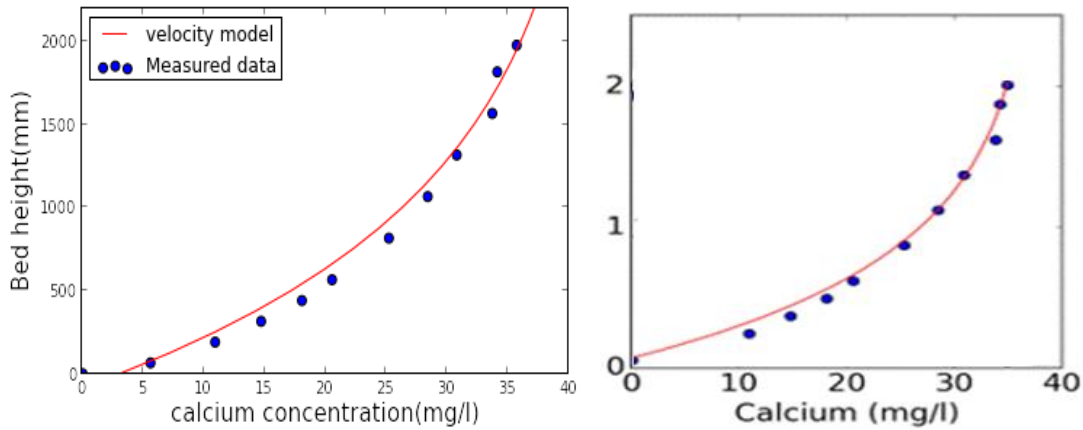


Figure 38. The simulation result from the multilayer model by G. Zweere (2017) on the left and the modified Yamauchi model from this study on the right where the velocity, water quality, and grain size are the same

5.3.3 Model application regarding operational variable

Finally, the model was used to predict the final calcite concentration. Figure 39 shows the simulation of the modified Yamauchi model with an average initial water quality, a bed height of 2 m, and grain sizes ranging between 0.5-1.2 mm. This simulation illustrates the influence of operational parameters on the calcium concentration after filtration. The colored bar shows the calcium concentration in mg/l. Elevating the velocity, diameter, and porosity causes a reduction in the calcium concentration. Furthermore, when replacing the diameter of 0.81 mm and porosity of 50%, it can be seen that, with this carbon dioxide concentration and water quality, the required calcium concentration of 25 mg/l can be reached as long as the velocity is higher than 10 m/h. This holds true when there is no bypassing and 100% of the water goes through the filter. If 53% bypassing is wanted, for example, the treatment water should contain a calcium concentration of 51.2 mg/l, which is only possible at a velocity below 10 m/h.

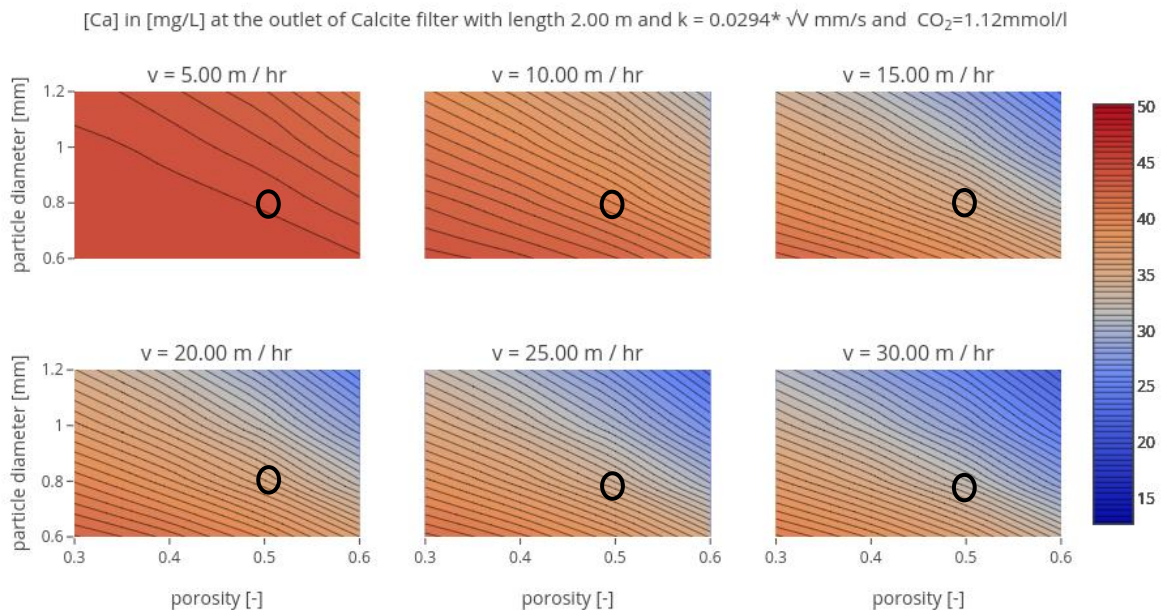


Figure 39. Sensitivity analyses based on the Yamauchi model (Yamauchi et al., 1987) with various levels of porosity, diameter, and velocity created using Python and Plot.ly (<https://plot.ly/create/?fid=sara.ghanbari>)

6 Application and optimal design

6.1 Introduction

The design of a calcite filter should ensure that the product water complies with predefined water quality standards. Table 9 lists the current guidelines that Oasen sets for the quality of remineralized water. The required magnesium concentration will be reached by adding magnesium chloride, $MgCl_2 \cdot 6H_2O$, to the filtered water. The parameters affecting the design and operational costs of calcite filters consist of the EBCT, the inlet CO_2 concentration, and the bypass ratio. In this chapter, various design scenarios will be discussed to determine the most cost-efficient design. The cost calculation will only include the calcite filtration step, not the cost for dosing magnesium chloride to the water.

Table 9. Oasen water quality regulations

Parameter	Oasen standard
Total Hardness	1 mmol/L
HCO_3^-	1.25 -1.45mmol/L
Calcium	0.625 mmol/L
Magnesium	0.375 mmol/L

6.2 General process scheme

Oasen plans to build its first full-scale RO plant at drinking water treatment plant (DWTP) “De Hooge Boom” in Kamerik. For this purpose, the capital expenditures (CAPEX) and operating expenses (OPEX) of each design scenario will be estimated based on this DWTP. This is done with the purpose of finding the optimal process parameters that bring the costs down to a minimum. Figure 40 depicts the main water flow scheme based on a reference scenario consisting of four parallel units to guarantee the required water treatment capacity and redundancy of the system. Table 10 lists the water quality and water demand data of DWTP “De Hooge Boom” in Kamerik.

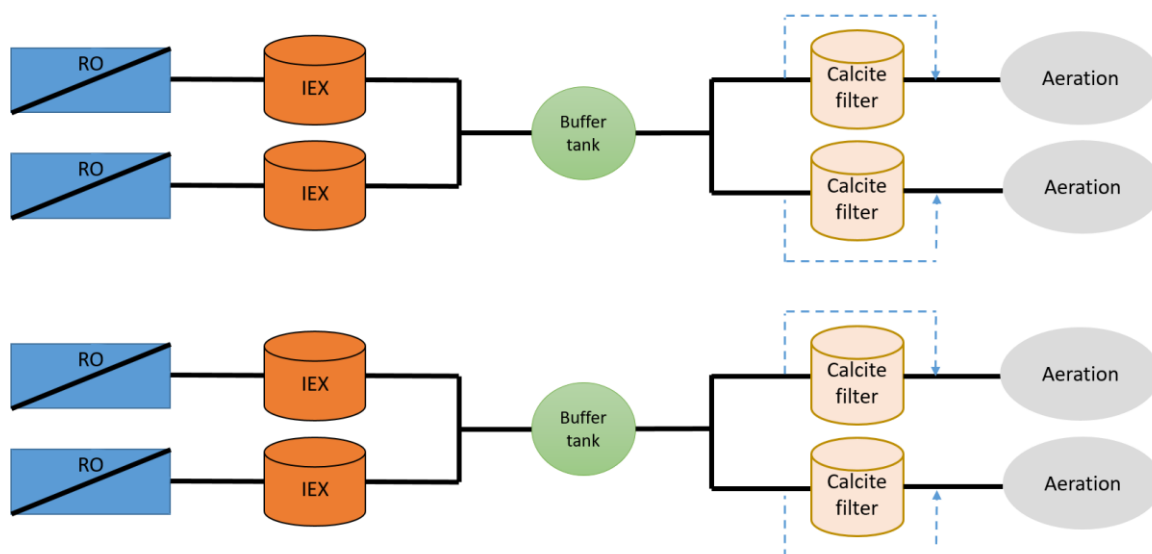


Figure 40. General treatment process scheme for the new to build DWTP “De Hooge Boom”

Table 10. Design parameters for the full-scale treatment plant “De Hooge Boom” in Kamerik

Design parameter	value	Unit
Annual production	2,628	million m ³ /year
Average production	300	m ³ /hour
Peak factor	1.4	-
Maximum capacity	420	m ³ /hour
Redundancy	N+1	At average production
Number of units	4	
Average capacity per unit	105	m ³ /hour
Hydraulic capacity per unit	140	m ³ /hour
CO ₂ in RO permeate (max)	1.8	mmol/l
CO ₂ in RO permeate (min)	1.25	mmol/l
CO ₂ in RO permeate (average)	1.5	mmol/l
CO ₂ dose ²	0	mmol/l
CO ₂ efficiency	80%	-
Contact time	15	minutes

The total cost of an installation depends on the costs of the mechanical components of an installation. In these calculations, the costs for mechanical components are based on reference values from projects that have already been implemented. Besides the construction expenses, CAPEX include 35% of the additional costs for the project management, design, construction supervision, and interest during construction. The costs for interest and depreciation (I&D) and for operation and maintenance (O&M) were determined as a ratio of the construction costs. These factors are listed in Table 11. The costs used for chemicals, energy, and operational parameters are shown in Table 12. The actual calculations can be found in the Excel workbook “20180105–Businesscase-Oasen.xlsx”

Table 11. Factors used for interest and depreciation, operation, and maintenance (Van Der Laan et al., 2016)

Costs		
Interest & Depreciation		
Building	6,6%	(40 years, 6% annuity)
Mechanical + Piping	8,7%	(20 years, 6% annuity)
Electrical	10,3%	(15 years, 6% annuity)
Operation & Maintenance		
Building	0,5%	
Mechanical + Piping	2,0%	
Electrical	4,0%	
Additional costs	35%	of construction costs

² There is at average 1.5 mmol/L CO₂ in the RO effluent, which is more than sufficient to dissolve 0.625 mmol/L of CaCO₃.

Table 12. Cost for chemicals, energy, and other operational parameters (Van Der Laan et al., 2016)

Calcite granular per ton	€74
CO ₂ per ton	€102
Energy per kWh	€0.11

6.3 Assumptions and boundary conditions

In this part, the technical starting points of the design are discussed.

Design capacity

The design capacity should be able to achieve the maximum capacity with 4 units in operation and the average capacity with 3 units in operation. This will guarantee an adequate redundancy in case one unit fails or needs to be shut down for maintenance. In this design, determining the filter dimensions is done by calculating the capacity per unit using equation (5.1). This equation will prevent oversizing the filters. It is possible that one unit fails at the maximum capacity. Should this happen, it should still be able to achieve the capacity by operating at a shorter contact time.

$$Q_{\text{per unit}} = \text{Max}\left(\frac{Q_{\text{Max}} \times \text{treatment \%}}{(\text{Number of units})}; \frac{Q_{\text{Average}} \times \text{treatment \%}}{\text{Number of units} - 1}\right) \quad (5.1)$$

Filter dimensions

The calcite bed height should be range between 1.5-3 m (Voutchkov, 2013). Due to practical difficulties regarding the transport of the filters to the production location, the diameter of the filters should not be above 3.5 m. This maximum diameter will avoid exorbitant transportation costs. Besides that, a decrease in the ratio of column diameter to length will minimize the possible dispersion effect (Delgado, 2006).

Calcite grain size

From the experimental results, it was concluded that the calcite grain size range of 0.5-1.2 mm accelerates the calcite dissolution kinetics due to its larger specific surface area (A/V). Therefore, this range of calcite grain sizes will be used in the design.

CO₂ concentration in the RO permeate

As discussed before, the carbon dioxide concentration at “De Hooge Boom” production facility fluctuates from day to day due to the various well configurations. However, in this design the average CO₂ concentration of 1.5 mmol/L will be used as the CO₂ concentration in the permeate water. This average concentration can be achieved by changing the combination of the wells in such a way that the amount of carbon dioxide is kept as constant as possible in all configurations.

Furthermore, the modified Yamauchi model developed in this study will be used to determine the minimal CO₂ concentration necessary to achieve the target calcium concentration, as well as to comment on various scenarios with different bypass ratio.

The CO₂ efficiency is another important factor to determine the optimal CO₂ concentration. The results from the pilot study show that the CO₂ efficiency decreases by increasing the CO₂ concentration and reducing the EBCT. It should also be noted that higher CO₂ dosages require a higher pH correction after filtration. Here, it is assumed that the aeration step will provide a sufficient capacity to remove the residual CO₂. In order to determine the optimal CO₂ dosage, the subsequent aeration step will therefore not be taken into consideration.

EBCT

From a process control point of view, there are several advantages to having effluent water that has closely approached the chemical equilibrium. From the experimental results, it was observed that after 15 minutes of EBCT, there will be no further significant change to the calcium concentration. This means that equilibrium is practically reached after 15 minutes. There are three main advantages to achieving a complete reaction:

1. The contact time is not critical: a slight decrease in the height of the filter bed does not affect the calcium and bicarbonate concentrations of the effluent water from the filter. Therefore, refilling the filter bed does not require a very high accuracy or frequency.
2. Short production interruptions or changes in the production flow rate do not have a noticeable influence on the calcium and bicarbonate concentrations in the effluent water from the filter.
3. The calcium and bicarbonate concentrations can be controlled with just the CO₂ dosage instead of both the CO₂ dosage and the EBCT, because the EBCT can always be considered to be sufficiently large. This makes process management simpler and more robust.

Moreover, an EBCT of less than 15 minutes is not desirable, as this will cause the CO₂ efficiency to decrease, especially at higher CO₂ concentrations. The design is therefore based on an EBCT of 17 minutes, to ensure that the minimum EBCT of 15 minutes necessary for the most efficient design capacity is still reached when the bed height has dropped.

Velocity

In order to maintain the minimum EBCT of 15 minutes at design capacity for a fixed bed height of 2.7 m, i.e., the bed height of 3.0 m minus a 10% reduction, the velocity should not be more than 10.8 m/h. This can be calculated as follows:

$$EBCT = \frac{Volume}{Q} = \frac{Area \times H}{Area \times v_{velocity}} = \frac{H}{v_{velocity}} \Rightarrow V_{Max} = \frac{2.7}{\frac{15}{60}} = 10.8 \text{ m/h} \quad (5.2)$$

Dispersion effect

To investigate the effects of non-plug flow on a practical level, results from a tracer test performed at the Kolff production location of Vitens are used (Zweere & Teunissen, 2015). To determine how the water flows through the filter, a tracer test has been carried out on a filter with a packed bed height of 2.85 m, a flow rate of 220 m³/h, a surface of 23.7 m² and a porosity of 0.47. During the experiment, the EC was measured every 90 seconds from 8

sample points along the filter bed. The results from a sample point located at 2.6 m from the ground were then taken as a starting point and the flow was modeled with the assumption of plug flow. Subsequently, the calculated results from the model were compared with the measured data. The results from two sample points at heights of 2.1 m and 0.6 m respectively are shown in Figure 41 and Figure 42. The results of this experiment confirmed the almost ideal plug flow through the filter. As a result, the effect of dispersion will be also neglected in translating the pilot model to full-scale application.

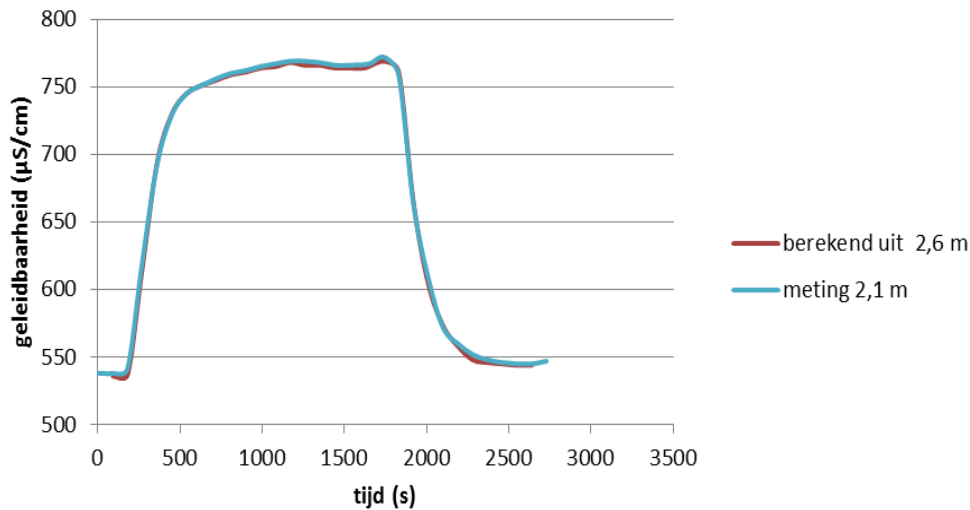


Figure 41. Predicted and actual EC values at 2.1 m (tracer test Zweere & Teunissen, 2015)

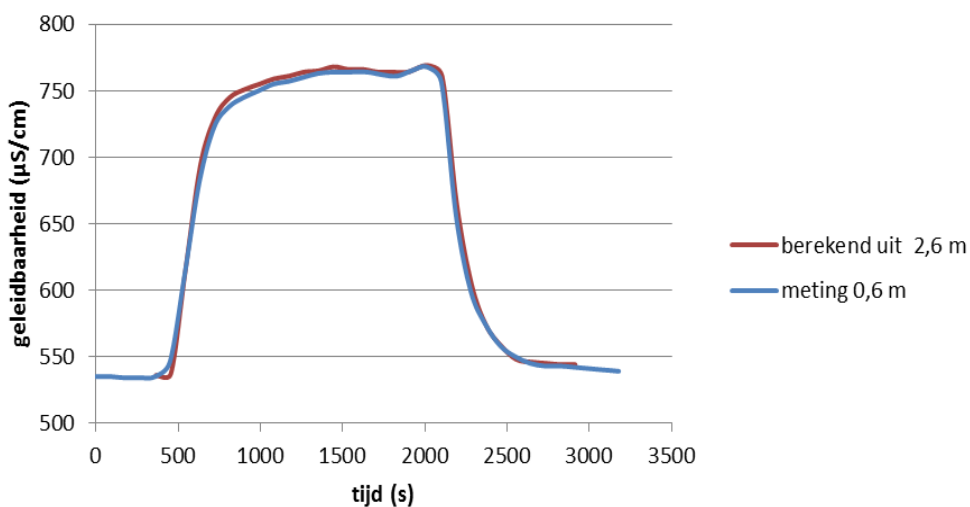


Figure 42. Predicted and actual EC values at 0.6 m (tracer test Zweere & Teunissen, 2015)

6.4 Model application

The calculations that were done were based on the modified Yamauchi model to determine the calcium concentration and subsequently to determine the percentage of bypass. Furthermore, a cost-effectiveness analysis was carried out. The calcium concentration at the design operation was used to calculate the bed refilling frequency.

In short, the key parameters of this design are:

- A design capacity of 420 m³/h
- An average capacity of 300 m³/h
- An EBCT of 15-17 minutes
- A maximum velocity of 10.8 m/h
- An average water quality, shown in Table 7
- An average carbon dioxide concentration of 1.5 mmol/l
- A maximum filter diameter of 3.5 m

Based on these design parameters, the calcium concentration was calculated using the modified Yamauchi model. The minimum level of carbon dioxide required to reach the calcium target was also determined. As illustrated in Figure 43, the calcium concentration almost reached the equilibrium at an EBCT of 15 minutes. A minimum CO₂ concentration of 0.65 mmol/l is required to reach the calcium target. Since there is always a higher concentration of CO₂, namely 1.5 mmol/l, present in the permeate water, a treatment with 100% calcite filtration would result in a calcium concentration of 1.3 mmol/l. In the following cost-calculation scenarios, the design is therefore based on a constant bypass flow.

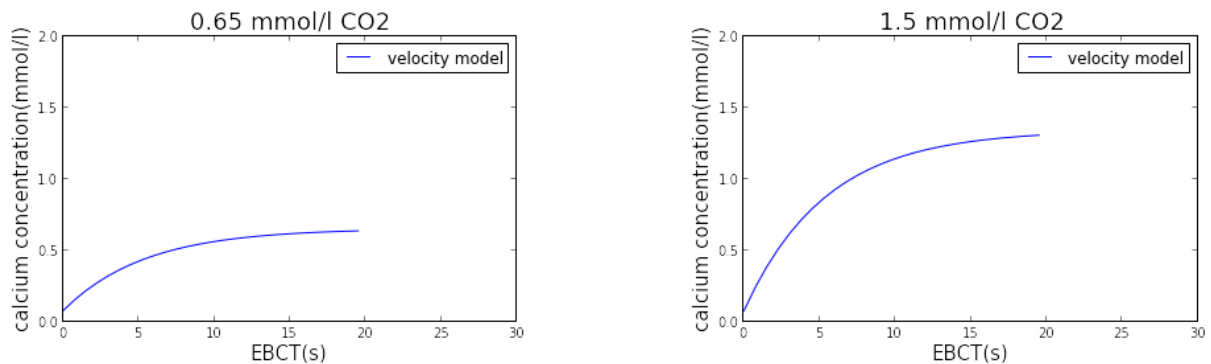


Figure 43. The result from the Yamauchi model at the minimum required concentration and average concentration of CO₂

The treatment percentage was calculated as follows:

$$x \cdot 1.28 + (1-x) \cdot 0.04 = 0.625 \quad (5.3)$$

Where:

0.04 mmol/l = the initial calcium concentration of water

1.28 = the predicted calcium concentration, using the model, when the inlet CO₂ concentration is 1.5 mmol/l

x = the treatment percentage of 47%

This was used as the treatment percentage in scenarios 1-4, where no extra CO₂ was dosed in the system.

Refilling frequency

To calculate the refilling frequency, the following steps should be taken. First, the produced calcium will be calculated using the model, which is 1.28 mmol/l in our case. Using this value, the calcite consumption can be calculated using equation (5.4):

$$\text{CaCO}_3 \text{ consumption with 100\% purity } \left(\frac{\text{mg}}{\text{l}}\right) = 1.28 \text{mmol}_{\text{Ca}} \times 1 \frac{\text{mmol}_{\text{CaCO}_3}}{1 \text{mmol}_{\text{Ca}}} \times \frac{100 \text{mg}_{\text{CaCO}_3}}{1 \text{mmol}_{\text{CaCO}_3}} \quad (5.4)$$

This shows calcite consumption in cases where the calcite is 100% pure. In our case, we have a purity of 99.1%:

$$\text{CaCO}_3 \text{ consumption with 99.1\% purity (mg/l)} = \frac{\text{CaCO}_3 \text{ consumption with 100\% purity } \left(\frac{\text{mg}}{\text{l}}\right)}{\text{purity percentage}} \quad (5.5)$$

Using the average capacity, the calcite consumption per hour can be calculated as follows:

$$\text{CaCO}_3 \text{ consumption } \left(\frac{\text{kg}}{\text{h}}\right) = \text{result of 5.5} \times \text{treatment \%} \times \text{Average capacity} \quad (5.6)$$

To calculate the reduction bed per filter, equation (5.7) can be used:

$$\text{Bed reduction } \left(\frac{\text{m}}{\text{h}}\right) = \frac{\text{CaCO}_3 \text{ consumption } \left(\frac{\text{kg}}{\text{h}}\right)}{\text{Number of filters (4)} \times \text{specific weight of calcite } \left(1350 \frac{\text{kg}}{\text{m}^3}\right) \times \text{surface area of the filter}} \quad (5.7)$$

Finally, assuming an allowed reduction of 10%, the refiling frequency can be calculated:

$$\text{Refiling frequency (day)} = \frac{\text{Allowed bed reduction (10\% of initial bed) } m}{\text{Bed reduction } \left(\frac{m}{h}\right) \times 24h} \quad (5.8)$$

6.5 Design scenarios

To find out the most cost-effective design at the key design parameters, the following scenarios are compared:

Table 13. Various operational scenarios

Scenarios	Parameters	Hypotheses
Scenario 0 (reference)	4 parallel units with a treatment percentage of 47% H = 3 m, D = 2.4 m, CO ₂ = 1.5 mmol/l	High redundancy
Scenario 1	3 parallel units with a treatment percentage of 47% H = 3 m, D = 2.9 m, CO ₂ = 1.5 mmol/l	Cheaper/less redundancy
Scenario 2	4 parallel units with a treatment percentage of 47% H = 1.7 m, D = 3.2 m, CO ₂ = 1.5 mmol/l	Lower refiling frequency due to the larger surface area of the filters. Higher production capacity, the maximum capacity can be reached with 3 filters
Scenario 3	4 parallel units with a treatment percentage of 47%	Smaller filters and lower investment cost

	H = 3.5 m, D = 2.3 m, CO ₂ = 1.5 mmol/l	
Scenario 4	4 parallel units with a treatment percentage of 47% H = 3 m, D = 2.4m, CO ₂ = 1.5 mmol/l – with CO ₂ standby system	Lower treatment percentage if necessary => High redundancy where the maximum capacity is obtained using 3 filters

Table 14, Figure 44, and Figure 45 present the outcomes of the cost comparisons of the various cost scenarios. As can be seen, the scenario with fewer filters results in a lower investment cost. However, this option may be less preferable due to its low redundancy. In other words, in case that one filter fails or is shut down for maintenance, the design capacity has to be reached with just two filters. Scenario 4 illustrates the cost of the process with a CO₂ dosing installation that serves to increase the redundancy of system. This will increase the investment cost by 12%, yet it may only be useful if one filter fails at the maximum capacity, or if multiple filters fail simultaneously.

In a previous study done by Oasen on remineralization techniques (Van Der Laan et al., 2016), the cost of treatment per m³ was found to be €0.076 for calcite filtration, which is higher than all the scenarios discussed here. The difference is found in the assumption of a treatment percentage of 100% with a calcium concentration of 1 mmol/l compared to the 0.625 mmol/l of this study. Moreover, there is less than 1% difference between the reference scenario and scenario 3, which has a longer bed height and a smaller filter, showing that the effect that filter dimensions have on the final cost is minor. However, when one filter is eliminated, the general cost of process is reduced by 16%.

Table 14. Comparison of various calcite filter scenarios

Tested scenarios	Reference scenario	Scenario 1	Scenario 2	Scenario 3	Scenario 4	Van der Laan (2016)
Treatment percentage	47%	47%	47%	47%	47%	100%
Investment	€1,351,000	€1,112,000	€1,446,000	€1,332,000	€1,522,000	€1,693,000
Annual costs						
Interest and Depreciation	€113,000	€92,000	€119,000	€112,000	€128,000	€139,000
Operation and Maintenance	€18,000	€14,000	€18,000	€18,000	€20,000	€21,000
Energy	€8,000	€8,000	€8,000	€8,000	€8,000	€17,000
Chemicals	€12,000	€12,000	€12,000	€12,000	€14,000	€23,000
Total	€151,000	€127,000	€157,000	€149,000	€169,000	€200,000
Costs per m³	€0.057	€0.048	€0.060	€0.057	€0.064	€0.076
Deviation from reference scenario	0%	-16%	4%	-1%	12%	32%

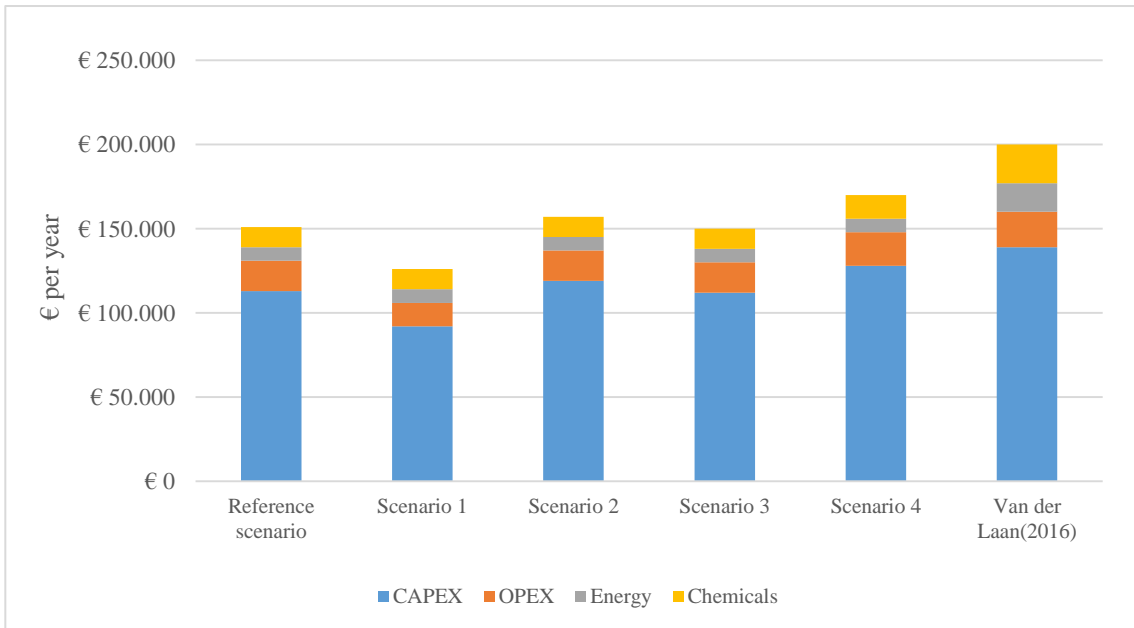


Figure 44. Cost comparison in € per year for different scenarios

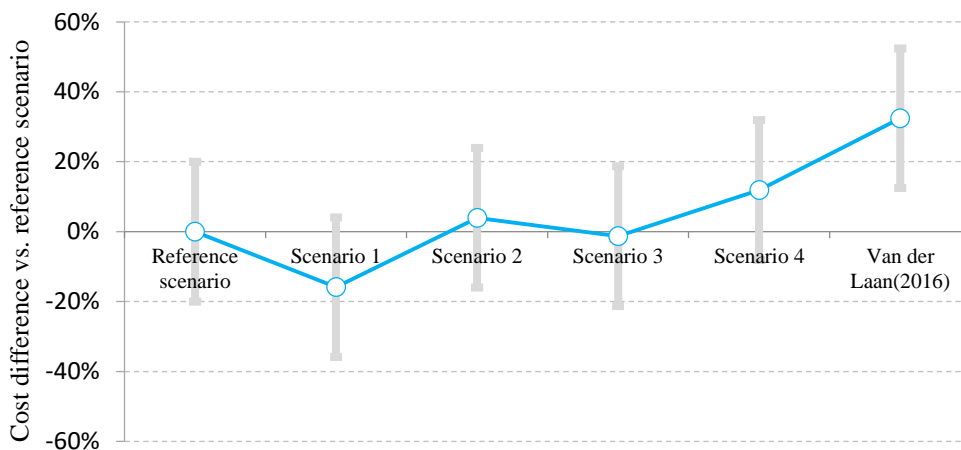


Figure 45. Cost difference in percentage related to the reference scenario where gray error bars indicate the general uncertainty in the cost model of +/- 20%

It should be noted that all of the above scenarios ensure the sufficient calcium concentration of 0.625 mmol/l. Since Ca:HCO₃ is always 1:2 based on Chapter 3.3.4, the bicarbonate concentration of 1.25 mmol/l will also be achieved.

The calcium concentration at the average capacity was used to calculate the bed refilling frequency using the provided calcium concentration. For this purpose, it is assumed that the beds are refilled when the bed height decreases by 10%. This is because a reduction of more than 10% will result in an EBCT of less than 15 minutes, which is not desirable as it eliminates the equilibrium and reduces the CO₂ efficiency. The results from these calculations show that each calcite filter should be refilled every 17 days, which means that one filter should be refilled and backwashed every week in order to prevent the refilling of multiple filters at the same time. In total, 160 tons of calcite are needed per year, which can partially be stored in two silos at the treatment plant.

As a conclusion of these cost analyses, scenario 3 is the recommended scenario. It is the optimal scenario with regards to its high redundancy and low costs compared to the scenarios with 4 parallel units. However, as shown above, the effect of a taller bed height on the investment costs is not big, as shown above. Therefore, the reference scenario can also be considered a good option. These two options will give the operator flexibility in choosing to either adjust the bed height or the diameter of the filters. The major components of this scenario are listed in Table 15.

Table 15. Major components of calcite filtration

Design parameter	Value	unit
number of contactors	4	-
calcite bed volume	14	m ³
diameter	2.3-2.4	m
bed height	3-3.5	m
calcite silos	2	-
calcite use	160	ton/year
number of silos	2	-
volume per silo	30	m ³
backwash pumps	2	-
capacity each	48.3	m ³ /h

6.5.1 CO₂ dosing for DWTP with higher capacity

In general, additional CO₂ dosing is beneficial when the treatment capacity is high and a high number of filters is needed. By increasing the inlet CO₂, the calcium dissolution also increases, which results in a higher bypass ratio and consequently in a lower number of filters. However, the treatment capacity of DWTP “De Hooge Boom” in Kamerik is relatively low, and it is not possible to reduce the number of filters to less than 4, as this would have a negative effect on the redundancy of the system. To investigate the effects of extra CO₂ dosing, therefore, the high design capacity of 5000 m³/h was chosen. The results are compared below at situations of 53% bypass vs. 75% bypass. Table 16 and Figure 46 show the outcome of a cost comparison between the two scenarios. As can be seen, dosing 1.7 mmol/l extra CO₂ will decrease the investment cost of the process by half. This is because the required number of filters will decrease by increasing the CO₂ concentration, which will result in an increase of the bypass ratio of the filter. Another interesting find from this comparison is the low cost of treatment per m³ in comparison with our case study. This shows that a higher treatment capacity reduces the treatment price per m³ of treated water.

Table 16. Comparison of the system with and without the CO₂ dosing system at a treatment capacity of 5000 m³/h

Tested scenario's	Reference scenario	Extra CO ₂ dosage
Treatment percentage	53% bypass	75% bypass
Investment	€10,133,096	€5,810,021
Annual costs		
Interest and Depreciation	€827,000	€476,000
Operation and Maintenance	€121,000	€71,000
Energy	€136,000	€74,000

Chemicals	€277,000	€391,000
Total	€1,361,000	€1,012,000
Costs per m³	€0.031	€0.023
Deviation from reference	0%	-26%

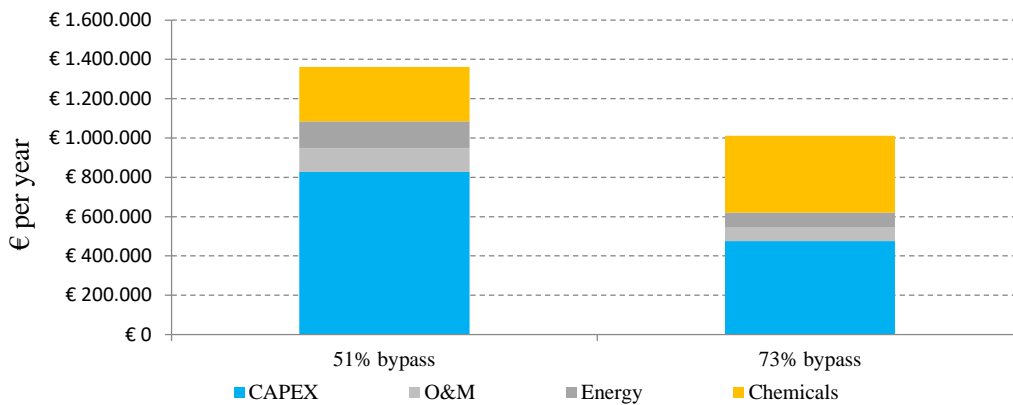


Figure 46. Cost comparison in € per year determined for both with and without additional CO₂ dosage at a high design capacity of 5000 m³/h

7 Conclusions and recommendations

7.1 Conclusions

7.1.1 Pilot study and modeling

As is known from available scientific literature, the calcite dissolution rate depends on the chemical driving force and the specific surface area of the calcite grains. Among several studies investigating the calcite dissolution kinetics, the empirical model provided by Yamauchi et al. (1987) was found to offer the most convenient expression describing the calcite dissolution based on aggressive CO₂ as the driving force. Although the reliability of this model was confirmed by several authors (Hasson & Bendrihem, 2006; Shemer et al., 2013; Hasson et al., 2013; Shemer et al., 2015), none of these previous studies investigated the calcite dissolution rate at a low temperature (<22 °C) and with calcite grain sizes smaller than 2 mm. Between the period of May to August 2017, various experiments were therefore conducted to test the effects of various operational parameters on the calcite dissolution rate at a water temperature of 12 °C.

The experimental data gathered from this study confirmed the reliability of the Yamauchi et al. (1987) model to express the kinetics of calcite dissolution at a low temperature of 12 °C. However, it was found that the effect of the flow rate on the diffusion boundary layer encompassing the calcite grains had not been taken into account in the study carried out by Yamauchi et al. (1987). Therefore, the effect of velocity on the calcite dissolution coefficient was investigated at five different velocities: 5, 10, 15, 20, and 30 m/h.

At this point, a function was developed to describe the correlation between the flow rate and the dissolution rate coefficient, which demonstrates the influence of the filtrate velocity on the diffusion layer and subsequently on the calcite kinetics coefficient. Finally, by incorporating this correlation into the main Yamauchi expression, the modified Yamauchi model was defined.

The experimental data from this study shows that CO₂ efficiency is significantly reduced, to below 60%, when the CO₂ concentration becomes higher than 3 mmol/l. This is because the amount of aggressive CO₂ is reduced by an increase of the concentration of bicarbonate in the water. Moreover, a high CO₂ concentration requires a pH adjustment afterwards, which may increase the consumption of energy or chemicals.

It is shown that the calcite grains ranging between 0.5-1.2 mm in size required a shorter EBCT than the grain size ranging between 1-2 mm in order to reach equilibrium. In general, it was found that the necessary EBCT to reach equilibrium is 15 minutes for grains sized between 0.5-1.2 mm, and 25 minutes for grains sized between 1-2 mm. This can be explained by the fact that the smaller grain size has a larger specific surface area and consequently a faster dissolution reaction. Furthermore, it was found that a reduction in the diameter of the calcite due to the effects of calcite dissolution only resulted in a small effect on the dissolution kinetics over the course of three weeks. Its effects within a filter can thus be neglected.

Comparing the modified Yamauchi model based on a single layer model with a multilayer model that simulates a stratified bed, developed by Zweere (2016), showed no considerable variations in the accuracy of the results. Both models can be used to simulate the calcite dissolution with an accuracy of 95% or more. Therefore, it is concluded that there is no need for a complex multilayer model.

It is important to have reliable sensors to continuously measure the CO₂ concentration. The results from sensor validations verified the reliability of the CO₂ sensor, while the pH sensor was found to be inaccurate in measuring the pH of the permeate water due to its low ion content.

Lastly, the pilot study found a linear relationship between EC and the concentration of calcium, as well as between EC and the concentration of bicarbonate. Therefore, EC sensors can be used to continuously measure the Ca/HCO₃ concentration. This relation has two main advantages over any other model: firstly, the EC is easy to measure and has a high accuracy, and secondly, the EC relation requires no extra data to predict the calcium and bicarbonate, making it an easy and straightforward method.

7.1.2 Practical application

The model was used to design and optimize the calcite filtration stage for a future treatment plant of Oasen located in Kamerik. The "De Hooge Boom" treatment plant has an average capacity of 300 m³/h and is planned to operate at full-scale RO. In this study, the focus was restricted to the step of calcite filtration, which aims to add the target concentration amounts of calcium and bicarbonate at 0.625 mmol/l and 1.25 mmol/l respectively. The required time to reach the equilibrium for grain size 0.5-1.2 mm was found to be 15 minutes, which should also be maintained after a bed reduction at the design capacity. By assuming a bed reduction of 10%, an EBCT of 17 minutes was chosen as the design EBCT. Another key feature of this design is the available CO₂ concentration in permeate water. The average CO₂ concentration of 1.5 mmol/l present at "De Hooge Boom" was used in the design calculations.

To find the optimal calcite design, various operating scenarios were analyzed. The only common feature that all of them shared was a bypass percentage of 53%, which was based on the simulation from the modified Yamauchi model. The calcium concentration in the product water was determined based on an average CO₂ concentration in the permeate water, using the model at the design parameters. From the results, it was found that the initial CO₂ concentration of 1.5 mmol/l provides 1.28 mmol/l of calcium. Therefore, the design had to be based on partial design flow. This resulted in a bypass ratio of 53% to provide the target calcium concentration. Subsequently, several scenarios were tested to find the most cost-efficient option. It was concluded that the design with three parallel units was the cheapest alternative. However, to increase the redundancy of the process for the given design parameters, the scenario with four parallel filters with a diameter of 2.3-2.4 m and an average bed height of 3-3.5 m was found to be optimal. The total treatment cost of this design is €0.057/m³ and the investment cost was found to be €1,351,000.

Furthermore, the refilling frequency was calculated based on calcite consumption as a function of calcium dissolution. It was found that based on a reduction of the filter bed of 10% and an average capacity of 300 m³/h, the filters should be refilled after approximately 17 days to keep the EBCT above the 15 minutes at all times. In order to prevent the refilling of multiple filters at the same time, one of the filters should be refilled and backwashed every week.

7.2 Recommendations

This research focused on parameters that have an effect on the calcite dissolution rate. Based on the results found in this report, the following aspects are recommended:

- The turbidity of the effluent water could limit the maximum velocity, as a high velocity may raise the turbidity above the threshold level. Therefore, it is recommended to test the water turbidity based on various velocities;
- The experiments are sensitive to backwash regimes since the high rate of backwash may result in breaking the particles as a consequence of increasing turbidity, which negatively affects the water quality. Therefore, further investigation should be done to find the optimal backwash flow rate and duration;
- To keep the CO₂ concentration constant, it is recommended that the combination of the wells is changed in such a way that the variation of water quality between configurations is minimized. Otherwise, it is recommended that a sensor is developed using a model to calculate the calcium concentration based on the initial CO₂ concentrations and subsequently to determine the required bypass over time;
- In order to determine the effect of runtime, it is recommended to test the process for a period of at least six months;
- From previous studies, it was concluded that temperature has a strong effect on the calcite dissolution. Therefore, it is recommended that the temperature dependency of the kinetic coefficient is further investigated throughout the pilot study in case the model is used in other locations with different water temperatures.
- The calcite purity is another factor that may affect the kinetic coefficient. Based on literature, the calcite used for remineralization should have a purity higher than 99%; Therefore, it is crucial to study the effect of calcite impurities on the calcite dissolution rate if the calcite source is changed to calcite source of less than 99% purity;

- The next step for Oasen is to make an automatic sensor that uses the data from the CO₂ sensor, the bed height meter, and the flow rate, and calculates the calcium and bicarbonate concentrations using the model to provide continuous control on the water quality. The EC-Calcium and EC-Bicarbonate relation can be used as a reliable, cheaper option to calculate the calcium and bicarbonate concentrations continuously, and to develop a sensor to regulate the bypass ratio based on the EC value.

8 Bibliography

- Bang, D. P. (2012). Upflow limestone contactor for soft and de-salinated water.
- Bear, J. (1988). Dynamics of Fluids in Porous Media. *Soil Science*. 120.
- Benjamin. L.. Green. R. W.. Smith. A.. & Summerer. S. (1992). Pilot Testing a Limestone Contactor in British Columbia.
- Colombani, J. (2008). Measurement of the pure dissolution rate constant of a mineral in water. *Geochimica et Cosmochimica Acta*. <https://doi.org/10.1016/j.gca.2008.09.007>
- Dahaan, S. A. M. Al. Al-Ansari. N.. & Knutsson. S. (2016). Influence of Groundwater Hypothetical Salts on Electrical Conductivity Total Dissolved Solids. *Engineering*. <https://doi.org/10.4236/eng.2016.811074>
- Delgado, J. M. P. Q. (2006). A critical review of dispersion in packed beds. *Heat and Mass Transfer/Waerme- Und Stoffuebertragung*. <https://doi.org/10.1007/s00231-005-0019-0>
- Dow Answer Center.. (2017). Retrieved from dowac.custhelp.com/app/answers/detail/a_id/3215/~/_/filmtec-membranes---cleaning-information.
- Erga, O.. & Terjesen. S. G. (1956). Kinetics of the heterogeneous reaction of calcium bicarbonate formation with special reference to copper ion inhibition. 10. <https://doi.org/10.3891/acta.chem.scand.10-0872>
- Hasson, D.. & Bendrihem. O. (2006). Modeling remineralization of desalinated water by limestone dissolution. *Desalination*. <https://doi.org/10.1016/j.desal.2005.09.003>
- Heinsbroek, A. (2017). Vitens/Phreeqpython. *Vitens*. Retrieved from github.com/Vitens/phreeqpython
- Hubert, E.. & Wolkersdorfer. C. (2015). Establishing a conversion factor between electrical conductivity and total dissolved solids in South African mine waters. *Water SA*. <https://doi.org/10.4314/wsa.v41i4.08>
- Iyasele, J.. & Idiata, D. J. (2015). Investigation of the Relationship between Electrical Conductivity and Total Dissolved Solids for Mono-Valent, Di-Valent and Tri-Valent Metal Compounds. *International Journal of Engineering Research and Reviews ISSN*. 3(1). 2348-697.
- Klinkenberg, A.. Lauwerier, H. .. & Krajenbrink, H. . (1953). Diffusion in a Fluid Moving at Uniform Velocity in a Tube. *Industrial & Engineering Chemistry*. <https://doi.org/10.1021/ie50522a024>
- Lehmann, O.. Birnhack, L.. & Lahav, O. (2013). Design aspects of calcite-dissolution reactors applied for post treatment of desalinated water. *Desalination*. <https://doi.org/10.1016/j.desal.2012.12.017>
- Letterman, R. D. (1995). Calcium Carbonate Dissolution Rate in Limestone Contactors. Retrieved from <https://nepis.epa.gov/Exe/ZyNET.exe/30003X4U.TXT?ZyActionD=ZyDocument&Client=EPA&Index=1995+Thru+1999&Docs=&Query=&Time=&EndTime=&SearchMethod=1&TocRestrict=n&Toc=&TocEntry=&QField=&QFieldYear=&QFieldMonth=&QFieldDay=&IntQFieldOp=0&ExtQFieldOp=0&XmlQuery=>
- Letterman, R. D.. Hadad, M.. & Driscoll, C. T. (1991). LIMESTONE CONTACTORS: STEADY-STATE DESIGN RELATIONSHIPS.
- Levenspiel, O.. Wiley, J.. & Anderson MARKETING MANAGER Katherine Hepburn PRODUCTION EDITOR Ken Santor, W. (1972). Chemical Reaction Engineering Third Edition.

- McDermid, L. (2017). PH Meter Calibration Problems? Check Out These 12 Tips! Retrieved from www.ysi.com/ysi-blog/water-blogged-blog/2013/04/ph-meter-calibration-problems-check-out-these-12-tips
- Miller, Steven. F., & Judson King, C. (2004). Axial Dispersion in Liquid Flow through Packed Beds. *AIChE Journal, American Institute of Chemical Engineers*. <https://doi.org/10.1002/aic.690120425>
- Müller, M., Parkhurst, D. L., & Charlton, S. R. (2011). Programming PHREEQC Calculations with C++ and Python A Comparative Study.
- Parkhurst, D. L., & Appelo, C. A. J. (1999). User's guide to PHREEQC (version 2). Denver: U.S. GEOLOGICAL SURVEY.
- PLUMMER, L. .. PARKHURST, D. L., & WIGLEY, T. M. L. (1979). Critical Review of the Kinetics of Calcite Dissolution and Precipitation. *Chemical Modeling in Aqueous Systems*. <https://doi.org/10.1021/bk-1979-0093.ch025>
- Plummer, L. N. (1978). The Kinetics of Calcite Dissolution in CO₂-Water System at 5°C to 60°C and 0.0 to 1.0 Atm. *Am J Sci*.
- Raymond Letterman Charles T Driscoll. by D., Marwan Haddad Alan Hsu, J. H., & Logsdon, G. S. (1987). LIMESTONE BED CONTACTORS FOR CONTROL OF CORROSION AT SMALL WATER UTILITIES.
- Rietveld, L. C., & van der Helm, A. W. . (2002). Modeling of drinking water treatment processes within the Stimela environment. In *Water Science and Technology: Water Supply*.
- Ruggieri, F., Fernandez-Turiel, J. L., Gimeno, D., Valero, F., García, J. C., & Medina, M. E. (2008). Limestone selection criteria for EDR water remineralization. *Desalination*, 227(1-3), 314-326. <https://doi.org/10.1016/j.desal.2007.07.020>
- Shemer, H., Hasson, D., & Semiat, R. (2013). Design considerations of a packed calcite bed for hardening desalinated water. *Industrial and Engineering Chemistry Research*. <https://doi.org/10.1021/ie302975b>
- Shemer, H., Hasson, D., & Semiat, R. (2015). State-of-the-art review on post-treatment technologies. *Desalination*. <https://doi.org/10.1016/j.desal.2014.09.035>
- Shemer, H., Hasson, D., Semiat, R., Priel, M., Nadav, N., Shulman, A., & Gelman, E. (2012). Desalination and Water Treatment Remineralization of desalinated water by limestone dissolution with carbon dioxide Remineralization of desalinated water by limestone dissolution with carbon dioxide. <https://doi.org/10.1080/19443994.2012.694236>
- Shemer, H., Hasson, D., Semiat, R., Priel, M., Nadav, N., Shulman, A., & Gelman, E. (2013). Remineralization of desalinated water by limestone dissolution with carbon dioxide. *Desalination and Water Treatment*. <https://doi.org/10.1080/19443994.2012.694236>
- Sjöberg, E. L., & Rickard, D. (1983). The influence of experimental design on the rate of calcite dissolution. *Geochimica et Cosmochimica Acta*. [https://doi.org/10.1016/0016-7037\(83\)90051-0](https://doi.org/10.1016/0016-7037(83)90051-0)
- Sjöberg, E. L., & Rickard, D. T. (1984). CALCITE DISSOLUTION KINETICS: SURFACE SPECIATION AND THE ORIGIN OF THE VARIABLE pH DEPENDENCE. *Chemical Geology Elsevier Science Publishers B.V.* 42, 119-136.
- Van Der Laan, H., Van Opijnen, J., Van Houwelingen, G., Sousi, M., Zijp, M., Kok, L., ... Schoonderwoerd, V. (2016). Search for the optimal remineralization technology.
- Vortmeyer, D., & Schuster, J. (1983). Evaluation of steady flow profiles in rectangular and circular packed beds by a variational method. *Chemical Engineering Science*. [https://doi.org/10.1016/0009-2509\(83\)85026-X](https://doi.org/10.1016/0009-2509(83)85026-X)

- Voutchkov. N. (2013). *Desalination Engineering; Planning and Design*.
- Yamauchi. V.. Tanaka. K.. Hattori. K.. Kondo. M.. & Ukawa. N. (1987). Remineralization of desalinated water by limestone dissolution filter. *Desalination*.
[https://doi.org/10.1016/0011-9164\(87\)90218-9](https://doi.org/10.1016/0011-9164(87)90218-9)
- Zweere. G. Model pellet/marmer filtratie deel 1 (2016).
- Zweere. G. Samenvatting resultaten model op RO-gegevens OASEN (2017).
- Zweere. G. .. & Teunissen. P. (2015). *Zoutproef Kolff*.

Appendices

Appendix I : CO₂ Calculations methods

In order to find the most reliable way to measure the carbon dioxide concentration in the water. during 17 till 20 July 2017. eight samples from permeate water were taken and the carbon dioxide concentration of each sample was measured or calculated in several ways.

The calculation steps of CO₂ concentration based on p and m alkalinity:

Assuming the maximum CO₂ concentration of 3 mmol / l. and having a sample bottle with capacity of 550 ml. the required sodium hydroxide solution of 25% with a specific weight of 1300 mg/ml can be calculated as follow:

Add: 3 mmol / l * 0.55 l = 1.65 mmol_{Required NaOH}
1.65 * 40 (NaOH molarity) = 66 mg_{NaOH}
NaOH_{25%} (mg) = 66*44= 264 mg_{NaOH25%}
NaOH_{25%} (ml) = 264(mg) /1300 mg/ml = 0.2ml (important: volume base is negligible relative to sample size)

Performance:

Take the water sample in a bottle with sodium hydroxide solution. As a result. all the CO₂ is converted into CO₃²⁻. Then by measuring p-alkalinity and m-alkalinity. the original CO₂ concentration can be calculated based on Table 17 . However. because the permeate water contains a small amount of HCO₃⁻. which will also convert to CO₃²⁻. bicarbonate was measured in a sample (without NaOH) to correct the result from CO₂ calculation based on p- and m-alkalinity.

Table 17. Calculation of carbonate, bicarbonate, and hydroxyl based on p and m alkalinity

P- and M- Alkalinity	Hydroxyl (OH)	Carbonate (CO ₃)	Bicarbonate (HCO ₃)
P = 0	0	0	M
P < ½ M	0	2P	M – 2P
P = ½ M	0	M	0
P > ½ M	2P – M	2(M – P)	0
P = M	M	0	0

*Based on ("Dow Answer Center." 2017)

CO₂ concentration based on pH and alkalinity:

The CO₂ concentration could also be calculated using pH. alkalinity and electrical conductivity. For this purpose samples were analyzed for their alkalinity and pH and using the average water composition provided in Table 7. the CO₂ concentration was calculated using PhreeqPython. However. it should be noted that an inaccurate measurement of pH

results in an error in CO₂ calculation. These calculations were also repeated using pH value measured at the pilot plant by pH meter at corresponding time of each sample.

Appendix II : EC vs. TDS relation

A relationship between electrical conductivity (EC) and total dissolved solids (TDS) was investigated by several authors (Dahaan et al., 2016; Hubert & Wolkersdorfer, 2015; Iyasele & Idiata, 2015). who showed a positive linear relationship between TDS and EC whereby increasing TDS, raises the EC value. TDS can be estimated using the equation below:

$TDS (mg/l) = k * EC (\mu s/cm)$	A. 1
----------------------------------	------

Where k is a conversion factor with a range between 0.54-1.1 at 25 °C. The conversion factor was found by plotting EC against TDS that was calculated using the sum of ions concentration in the RO permeate. For this purpose, the data from 168 samples in a large range of EC from 19 to 761 $\mu s/cm$ were taken, and the calcium and bicarbonate concentrations corresponding to each sample were measured in the laboratory. The concentration of other ions was measured over 4 different days. The laboratory analyses showed only a small concentration of sodium, chloride and bicarbonate in the water contributing to TDS.

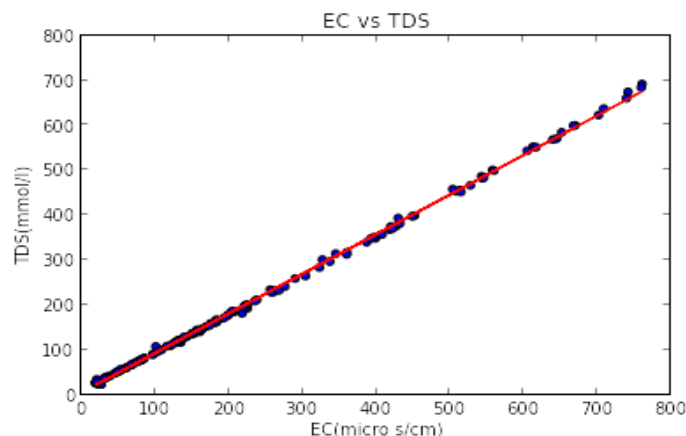


Figure 47. Measured data of EC against TDS fitted in Python. The linear equation is equal to: $TDS = 0.8801 EC + 5.227$

Figure 47 shows the k factor to be 0.88 which supports data provided by Hubert & Wolkersdorfer (2015) for an EC-range of 70-16 000 $\mu s/cm$ and TDS of 50-14 000 mg/l.

By subtracting the initial sodium, chloride and bicarbonate concentration in from total TDS in the water, the sum of calcium and bicarbonate concentration added during remineralization is calculated. However, it should be noted, that various ions had a different mobility affecting the EC (Iyasele & Idiata, 2015). This means that calcium and bicarbonate concentration contributed to the EC and, subsequently, to TDS concentration to a different extent. Fitting data using Excel result in the following equations for calcium and bicarbonate.

$$Ca \text{ concentration (mg/l)} = 0.245 * (TDS - Na - chloride - initial bicarbonate) \text{ (mg/l)}$$

HCO_3 concentration (mg/l) = 0.775 * (TDS- Na - chloride – initial bicarbonate) (mg/l)

It should be noted that 1:2 ratio of calcium and bicarbonate concentration could also be used to predict the final bicarbonate concentration. however. this concentration should be added by initial bicarbonate concentration which in average is an approximately 0.14 mmol/l.

However. as increasing TDS and consequently EC in effluent water from the filter is only the result of the calcite dissolution. it can be concluded that there must be a direct relationship between EC and calcium and bicarbonate dissolved in the water. Therefore. the relationships between these three parameters are further investigated using empirical data.

EC handheld vs. TDS-PhreeqPython code

January 9. 2018

```
In [1]: from openpyxl import load_workbook
import numpy as np
import matplotlib.pyplot as plt
import pandas as pd
from sklearn.linear_model import LinearRegression
from sklearn import datasets, Linear_model
%pylab inline
wb = load_workbook('EC-TDS.xlsx', data_only=True, Read_only=True)
ws = wb['EC']
Populating the interactive namespace from numpy and matplotlib
In [2]: EC = []
for column in ws['G2:G169']:
for cell in column:
EC.append(cell.value)
TDS = []
for column in ws['k2:k169']:
for cell in column:
TDS.append(cell.value)
plt.scatter(EC,TDS)
plt.xlim(0.800)
plt.ylim(0..800)
plt.xlabel('EC(micro s/cm)')
plt.ylabel('TDS(mg/l)')
plt.title('EC vs TDS')
```

Appendix III: EC and Ph relation

The electric conductivity is strongly pH dependent when the pH level is lower than six this is because of a high mobility of the hydrogen ion. Figure 48 shows the EC values at various pH levels simulated by PhreeqPython which depicts when the pH is low. It will be affected the electric conductivity measurement. However. When pH goes above the 6-6.5. it has no effect on electric conductivity. As the pH of effluent water from calcite filter is always higher than 6.5. therefore. The effect of pH on electric conductivity can be neglected. However. This relation is not applicable when samples has low calcium concentration and subsequently low pH.

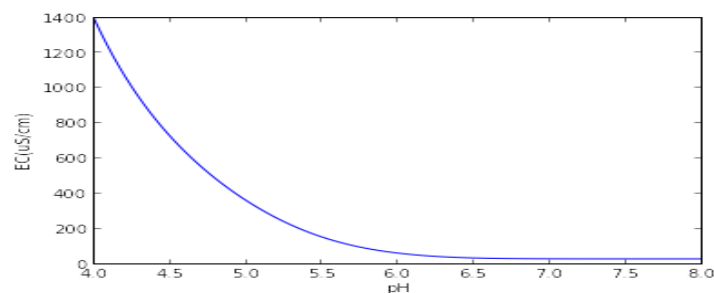


Figure 48. pH vs. EC relation where the water composition is kept constant and pH levels vary between 4 and 8

pH-EC sensitivity-PhreeqPython-code

January 9, 2018

```
In [1]: import phreeqpython
import numpy as np
%pylab inline
pp = phreeqpython.PhreeqPython()
def getresults(ph=5.35):
sol = pp.add_solution_raw({
'pH': ph.
'temp': 13.
'units': 'mg/l'.
'Ca': 0.
'Alkalinity': '7.5 as HCO3'.
'Cl': 1.4.
'Na': 3.35
})
# saturate to Si O
sol.saturate('Calcite'.0)
EC = sol.sc
# cleanup
sol.forget()
return (EC)
ph_range = np.linspace(4.8,100)
results = []
for ph in ph_range:
results.append(getresults(ph))
#deviation = ph_range/4.5
```

```
plt.plot(ph_range.results)
plt.xlabel('pH')
plt.ylabel('EC(uS/cm)')
```

Appendix IV: Phreeqc simulation of EC and Ca/HCO₃ relationship

The reliability of EC relation theoretically is investigated by simulating the reaction in the Phreeqc. The chemical reaction is simulated by applying the initial water quality before the calcite filter in the Phreeqc and forced the reaction to dissolve calcite till above saturation step by step. It should be noted that the temperature of water should be set at reference temperature of 25 °C which measurement data converted to reference temperature of 25 °C. Figure 49 shows the result from this simulation. Figure 50 shows the data from Phreeqc simulation and data derived from pilot measurement in one figure to compare both results. As it can be seen data match exactly with each other. This confirmed the reliability of EC sensor to predict the calcium and bicarbonate concentration independent of the operating conditions such as flow rate and grain size.

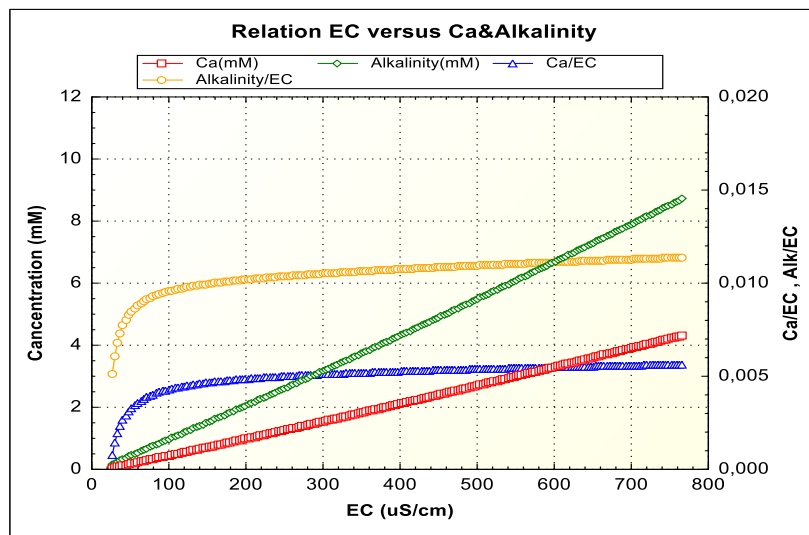


Figure 49. Calcium/alkalinity vs. various EC plotted using Phreeqc (Tony Appelo's Phreeqc version with notepad++ done by Boris van Breukelen)

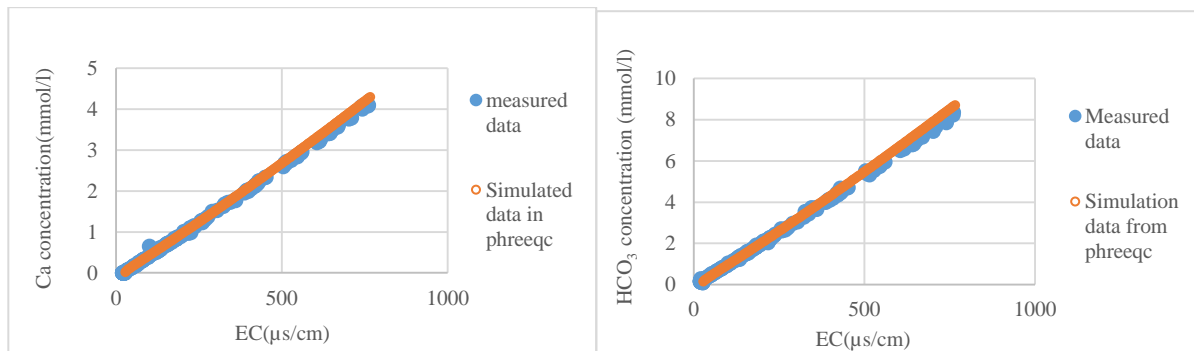


Figure 50. The relation between the calcium/bicarbonate concentration and EC from measured data as well as from theoretical data from the Phreeqc simulation

```
# Theoretical relation between EC and Ca and HCO3 during calcite dissolution
```

```
SOLUTION 1 RO water
units mg/l
Temp 25
Na 3.5
Cl 1.5
pH 4.56
Alkalinity 6.1 as HCO3
END
```

```
USE solution 1
REACTION # Calcite is forced being dissolved even above saturation
Calcite 1
4.3e-3 in 200 steps
USER_GRAPH 1 # plot number 1
-headings EC(uS/cm) Ca(mM) Alkalinity(mM) Ca/EC Alkalinity/EC
-chart_title "Relation EC versus Ca&Alkalinity"
-axis_titles "EC (uS/cm)" "Concentration (mM)" "Ca/EC , Alk/EC"
-axis_scale x_axis 0 800 100
-axis_scale y_axis 0 12 auto auto
-axis_scale sy_axis 0 0.02 auto auto
-connect_simulations true
-initial_solutions false
-start
10 graph_x sc
20 graph_y tot("Ca")*1000
30 graph_y Alk*1000
40 graph_sy (tot("Ca")+1000)/sc
50 graph_sy (Alk*1000)/sc
-end
SELECTED_OUTPUT
-file output.txt
-reset false
USER_PUNCH
-headings step CaCO3_reacted pH Alk(mM) Ca(mM) EC(uS/cm)
-start
10 punch step_no
20 punch RXN
30 punch -la("H+")
40 punch ALK*1000
50 punch tot("Ca")+1000
60 punch sc
-end
END
```

Appendix V : Pilot Components

Appendix V -A : Measurement sensors information

Table 18. pH sensor characteristics

Company	Best Instrument Analytical Solution	Best Instrument Analytical Solution
Online analyzer	Swan	Swan
Type	pH/Redox	pH/Redox
Product. No	A.21.221.050	A.21.221.010
Model	AMI-2	AMI-2
Range	(1-13)	(1-13)
Resolution	0.01pH	0.01pH
Flow range	4-15l/h	5-10l/h
Flow pressure inlet	1bar	Up to 2 bar
Temperature range	(-30-130 °C)	(-30-130 °C)
Temperature resolution	0.01 °C	0.01 °C

Table 19. Electric conductivity characteristics

Company	Best Instrument Analytical Solution
Online analyzer	Swan
Type	Powercon Specific (EC)
Product. No	A.23.441.100
Model	AMI-2
Range	(0.055-1000 micro μ /cm)
Resolution	-/+ 1% reading value
Flow range	5-20l/h
Flow pressure inlet	1bar
Temperature range	(-30-130 °C)
Temperature resolution	0.01 °C

Table 20. Turbidity sensor characteristics

Company	Best Instrument Analytical Solution
Online analyzer	Swan
Type	Turbitrack
Product. No	A.25.4111.200
Model	AMI-2
Range	0.000-100 NTU
Resolution	(+/- 1% Reading)

Flow range	5-20l/h
-------------------	---------

Table 21. CO₂ meter characteristics

Company	DKK-DOA
Type	Turbitrack
Product. No	Handheld carbon dioxide meter
Model	CGP-31
Range	Liquid: 1.49-1490 mg/l / Gas: 0.1-100%
Resolution	(+/- 5% FS)

Appendix V -B : Calcite characteristics

Table 22. Calcite product characteristics

Calcite product characteristics	
Size	0.5-1.2mm
Purity	Approximately 99.1%
Density	2.7 g/cm ³
Bulk density	1500 kg/m ³
Porosity	0.50-0.56
Other components	0.34% SiO ₂ +AlO ₂

Appendix VI: The CO₂ experiment simulations

Appendix VII: PhreeqPython codes

Appendix VII –A PhreeqPython code-velocity test- grain size 0.5-1.2 mm

Modified Yamauchi-model-0.5-1.2mm

January 9, 2018

```
In [1]: import numpy as np
from math import sqrt
import matplotlib.pyplot as plt
%pylab inline
import phreeqpython
pp = phreeqpython.PhreeqPython()
from openpyxl import load_workbook
In [2]: wb = load_workbook('Yamauchi-data.xlsx'. data_only=True. read_only=True)
ws1 = wb['water-quality']
ws2 = wb['operation']
ws3 = wb['measurement-data']
In [3]: #10m/h-filter-1
sol = pp.add_solution_raw({
'temp': ws1['D2'].value.
'units': 'mg/l'.
'pH': ws1['D3'].value.
'Ca': ws1['D4'].value.
'Alkalinity': '8.78 as HCO3'.
'Cl': ws1['D6'].value.
'Na': ws1['D7'].value.
'Fe': ws1['D8'].value.
'Mg': ws1['D9'].value.
'K': ws1['D10'].value.
'Al': ws1['D11'].value.
'S(6)': ws1['D12'].value
})
CO2_0=sol.total('CO2')*1e3
sol.saturate('Calcite'.0)
Cae = sol.total_element('Ca')*1e3
CO2e = sol.total('CO2')*1e3
HCO3 = sol.total('HCO3')*1e3
pH = sol.pH
soln = pp.add_solution_raw({
'temp': ws1['D2'].value.
'units': 'mg/l'.
'pH': ws1['D3'].value.
'Ca': ws1['D4'].value.
'Alkalinity': '8.78 as HCO3'.
'Cl': ws1['D6'].value.
'Na': ws1['D7'].value.
'Fe': ws1['D8'].value.
```

```

'Mg': ws1['D9'].value.
'K' : ws1['D10'].value.
'Al': ws1['D11'].value.
'S(6)': ws1['D12'].value
})
CO2_0n =soln.total('CO2')*1e3
soln.saturate('Calcite'.0)
Caen = soln.total_element('Ca')*1e3
CO2en = soln.total('CO2')*1e3
#15m/h-filter-1
sol2 = pp.add_solution_raw({
'temp': ws1['I2'].value.
'units': 'mg/l'.
'pH': ws1['I3'].value.
'Ca': ws1['I4'].value.
'Alkalinity': '8.7 as HCO3'.
'Cl': ws1['I6'].value.
'Na': ws1['I7'].value.
'Fe': ws1['I8'].value.
'Mg': ws1['I9'].value.
'K' : ws1['I10'].value.
'Al': ws1['I11'].value.
'S(6)': ws1['I12'].value
})
CO2_2_0=sol2.total('CO2')*1e3
sol2.saturate('Calcite'.0)
2
Cae_2 = sol2.total_element('Ca')*1e3
CO2e_2 = sol2.total('CO2')*1e3
#16.5m/h-filter-1
sol3 = pp.add_solution_raw({
'temp':ws1['N2'].value.
'units': 'mg/l'.
'pH': ws1['N3'].value.
'Ca': ws1['N4'].value.
'Alkalinity': '8.5 as HCO3'.
'Cl': ws1['N6'].value.
'Na': ws1['N7'].value.
'Fe': ws1['N8'].value.
'Mg': ws1['N9'].value.
'K' : ws1['N10'].value.
'Al': ws1['N11'].value.
'S(6)': ws1['N12'].value
})
CO2_3_0=sol3.total('CO2')*1e3
sol3.saturate('Calcite'.0)
Cae_3 = sol3.total_element('Ca')*1e3
CO2e_3 =sol3.total('CO2')*1e3
temp= ws1['I2'].value

```

In [4]: Ca_e = sol.total_element('Ca')*1e3 #saturation ca concentration in mmol/l
Caen = soln.total_element('Ca')*1e3

```

Ca_0 = ws1['D4'].value #initial ca concentration in mmol/l
e = ws2['D3'].value #porosity
z = np.arange(0.2100.125) #height in mm
v = ws2['D5'].value #velocity in mm/s
D = ws2['D6'].value
D_reduction = 0.7
EBCT = z/v # EBCT in s
k = 0.00296* math.sqrt(v) #reaction constant in mm/s using velocity model:
Ca = Ca_e - (exp((-k/D)*(1-e)*EBCT)*(Ca_e - Ca_0)) #end ca concentration plt.subplot(2.3.1)
plt.plot(EBCT, Ca, label= 'velocity model with pH correction')
plt.xlabel('EBCT(s)', fontsize=15)
plt.ylabel('calcium concentration(mmol/l)', fontsize=15)
plt.xlim(0.1000)
plt.ylim(0.1.6)
EBCT = []
for column in ws3['B3:B13']:
for cell in column:
EBCT.append(cell.value)
ca = []
for column in ws3['D3:D13']:
for cell in column:
ca.append(cell.value)
plt.subplot(2.3.1)
plt.scatter(EBCT, ca, marker='s', label='Measured data')

err = 0.05*ones(size(ca))
e = errorbar(EBCT, ca, err, ecolor='g', capsize=6)
plt.title('10 m/h', fontsize=18)
plt.legend(loc='best')

#####

Ca_e1 = sol2.total_element('Ca')*1e3 #saturation ca concentration in mmol/l
Ca_01 = ws1['I4'].value #initial ca concentration in mmol/l
e1 = ws2['I3'].value #porosity
z1 = np.arange(0.2200.125) #height in mm
v1 = ws2['I5'].value #velocity in mm/s
D1 = ws2['I6'].value
D1_reduction = 0.7
EBCT1 = z1/v1 # EBCT in s
k1 = 0.00296* math.sqrt(v1) #reaction constant in mm/s using velocity model:
Ca1 = Ca_e1 - (exp((-k1/D1)*(1-e1)*EBCT1)*(Ca_e1 - Ca_01)) #end ca concentration
Ca1_reduction = Ca_e1 - (exp((-k1/D1_reduction)*(1-e1)*EBCT1)*(Ca_e1 - Ca_01)) plt.subplot(2.3.2)
plt.plot(EBCT1, Ca1, label= 'velocity model')
plt.xlabel('EBCT(s)', fontsize=15)
plt.ylabel('calcium concentration(mmol/l)', fontsize=15)
plt.xlim(0.600)
plt.ylim(0.1.6)

```

```
EBCT1 = []
for column in ws3['H3:H12']:
    for cell in column:
        EBCT1.append(cell.value)
ca1 = []
for column in ws3['J3:J12']:
    for cell in column:
        ca1.append(cell.value)
plt.subplot(2.3.2)
plt.scatter(EBCT1.ca1.marker='s'.label='Measured data')
err = 0.05*ones(size(ca1))
e = errorbar(EBCT1.ca1.err.ecolor='g'.capsize=6)
plt.title('15 m/h'.fontsize=18)
plt.legend(loc='best')
```

Modified Yamauchi-model-16.5 m/h

January 9, 2018

```

Ca_e2 = sol3.total_element('Ca')*1e3 #saturation ca concentration in mmol/l
Ca_02 = ws1['N4'].value #initial ca concentration in mmol/l
e2 = ws2['N3'].value #porosity
z2= np.arange(0.2200.125) #height in mm
v2= ws2['N5'].value #velocity in mm/s
D2= ws2['N6'].value
D2_reduction= 0.7
EBCT2 = z2/v2 # EBCT in s
k2 = 0.00296* math.sqrt(v2) #reaction constant in mm/s using velocity model:
Ca2 = Ca_e2 - (exp((-k2/D2)*(1-e2)*EBCT2)*(Ca_e2 - Ca_02)) #end ca concentration Ca2_reduction =
Ca_e2 - (exp((-k2/D2_reduction)*(1-e2)*EBCT2)*(Ca_e2 - Ca_02)) plt.subplot(2.3.3)
plt.plot(EBCT2, Ca2, label= 'velocity model')
plt.xlabel('EBCT(s)'.fontsize=15)
plt.ylabel('calcium concentration(mmol/l)'.fontsize=15)
plt.xlim(0.600)
plt.ylim(0.1.6)
EBCT2 = []
for column in ws3['M3:M12']:
for cell in column:
EBCT2.append(cell.value)
ca2 = []
for column in ws3['O3:O12']:
for cell in column:
ca2.append(cell.value)
plt.subplot(2.3.3)
plt.scatter(EBCT2.ca2.marker='s'. label= 'Measured data')
err = 0.05*ones(size(ca2))
e = errorbar(EBCT2.ca2.err.ecolor='g'.capsize=6)
plt.title('16.5 m/h'.fontsize=18)
plt.legend(loc='best')
plt.subplots_adjust(top=2. left=0.007. right=4.
hspace=0.5. wspace=0.5)
/usr/lib/pymodules/python2.7/matplotlib/collections.py:446: FutureWarning: elementwise 6
if self._edgecolors == 'face':
In [5]: Ca_e = sol3.total_element('Ca')*1e3 #saturation ca concentration in mmol/l
Ca_0 = ws1['N4'].value #initial ca concentration in mmol/l
e = ws2['N3'].value #porosity
z = np.arange(0.2500.125) #height in mm
v = ws2['N5'].value #velocity in mm/s
D = ws2['N6'].value
D_reduction= 0.7
EBCT = z/v # EBCT in s
k = 0.00296* math.sqrt(v2) #reaction constant in mm/s using velocity model:
Ca = Ca_e - (exp((-k/D)*(1-e)*EBCT)*(Ca_e - Ca_0)) #end ca concentration in
Ca_g= Ca*40

```

```
plt.plot(Ca_g, z, 'r', label= 'velocity model')
zm = []
for column in ws3['N3:N14']:
for cell in column:
zm.append(cell.value)
cam = []
for column in ws3['O3:O14']:
for cell in column:
cam.append(cell.value)
cam_g = 40*np.array(cam)
plt.scatter(cam_g, zm, s=35, label= 'Measured data')
plt.ylabel('Bed height(mm)').fontsize=15)
plt.xlabel('calcium concentration(mg/l)').fontsize=15)
plt.ylim(0.2200)
plt.xlim(0.40)
plt.title('16.5 m/h').fontsize=18)
plt.legend(loc='best')
```

Modified Yamauchi-model-1-2mm

January 9, 2018

```
In [1]: import numpy as np
from math import sqrt
import matplotlib.pyplot as plt
%pylab inline
import phreeqpython
pp = phreeqpython.PhreeqPython()
from openpyxl import load_workbook

In [2]: wb = load_workbook('Yamauchi-data-big.xlsx'. data_only=True. read_only=True)
ws1 = wb['water-quality']
ws2 = wb['operation']
ws3 = wb['measurement-data']
In [3]: #5m/h-filter-1
sol = pp.add_solution_raw({
'temp': ws1['C2'].value.
'units': 'mg/l'.
'pH': ws1['C3'].value.
'Ca': ws1['C4'].value.
'Alkalinity': '10.19 as HCO3'.
'Cl': ws1['C6'].value.
'Na': ws1['C7'].value.
'Fe': ws1['C8'].value.
'Mg': ws1['C9'].value.
'K' : ws1['C10'].value.
'Al': ws1['C11'].value.
'S(6)': ws1['C12'].value
})
CO2_0=sol.total('CO2')*1e3
sol.saturate('Calcite'.0)
Cae = sol.total_element('Ca')*1e3
CO2e = sol.total('CO2')*1e3
#10m/h-filter-1
sol2 = pp.add_solution_raw({
'temp': ws1['H2'].value.
'units': 'mg/l'.
'pH': ws1['H3'].value.
'Ca': ws1['H4'].value.
'Alkalinity': '10.31 as HCO3'.
'Cl': ws1['H6'].value.
'Na': ws1['H7'].value.
'Fe': ws1['H8'].value.
'Mg': ws1['H9'].value.
'K' : ws1['H10'].value.
'Al': ws1['H11'].value.
'S(6)': ws1['H12'].value
})
```

```

CO2_2_0=sol2.total('CO2')*1e3
sol2.saturate('Calcite'.0)
Cae_2 = sol2.total_element('Ca')*1e3
CO2e_2 = sol2.total('CO2')*1e3
#15m/h-filter-1
sol3 = pp.add_solution_raw({
'temp':ws1['M2'].value.
'units': 'mg/l'.
'pH': ws1['M3'].value.
'Ca': ws1['M4'].value.
'Alkalinity': '10.65 as HCO3'.
'Cl': ws1['M6'].value.
'Na': ws1['M7'].value.
'Fe': ws1['M8'].value.
'Mg': ws1['M9'].value.
'K' : ws1['M10'].value.
'Al': ws1['M11'].value.
'S(6)': ws1['M12'].value
})
CO2_3_0=sol3.total('CO2')*1e3
sol3.saturate('Calcite'.0)
Cae_3 = sol3.total_element('Ca')*1e3
CO2e_3 =sol3.total('CO2')*1e3
temp= ws1['I2'].value
Ca_e = sol.total_element('Ca')*1e3 #saturation ca concentration in mmol/l
Ca_0 = ws3['D3'].value #initial ca concentration in mmol/l
e = ws2['C3'].value #prosimy
z= np.arange(0.2500.125) #height in mm
v= ws2['C5'].value #velocity in mm/s
D= ws2['C6'].value
D_reduction= 1.4
EBCT = z/v # EBCT in s
k = 0.00296 * math.sqrt(v) #reaction constant in mm/s using velocity model:
Ca= Ca_e - (exp((-k/D)*(1-e)*EBCT)*(Ca_e - Ca_0)) #end ca concentration in plt.subplot(2.3.1)
plt.plot(EBCT, Ca, label= 'velocity model')
plt.xlabel('EBCT(s)').fontsize=15)
plt.ylabel('calcium concentration(mmol/l)').fontsize=15)
plt.xlim(0.2000)
plt.ylim(0.1.6)
EBCT = []
for column in ws3['B3:B13']:
for cell in column:
EBCT.append(cell.value)
ca = []
for column in ws3['D3:D13']:
for cell in column:
ca.append(cell.value)
plt.subplot(2.3.1)
plt.scatter(EBCT.ca.marker='s'.label='Measured data')
err = 0.05*ones(size(ca))
e = errorbar(EBCT.ca.err.ecolor='g'.capsize=6)
plt.title('5 m/h'.fontsize=18)

```

```

plt.legend(loc='best')
#####
Ca_e1 = sol2.total_element('Ca')*1e3 #saturation ca concentration in mmol/
Ca_01 = ws3['J3'].value #initial ca concentration in mmol/l
e1 = ws2['H3'].value #prospity
z1= np.arange(0.2500.125) #height in mm
v1= ws2['H5'].value #velocity in mm/s
D1= ws2['H6'].value
D1_reduction=1.2
EBCT1 = z1/v1 # EBCT in s
k1 = 0.00296* math.sqrt(v1) #reaction constant in mm/s using velocity model:
Ca1 = Ca_e1 - (exp((-k1/D1)*(1-e1)*EBCT1)*(Ca_e1 - Ca_01)) #end ca concentration Ca1_reduction =
Ca_e1 - (exp((-k1/D1_reduction)*(1-e1)*EBCT1)*(Ca_e1 - Ca_01)
plt.subplot(2.3.2)
plt.plot(EBCT1, Ca1, label= 'velocity model')
#plt.plot(EBCT1,Ca1_reduction, label='Diameter reduction')
plt.xlabel('EBCT(s)',fontsize=15)
plt.ylabel('calcium concentration(mmol/l)',fontsize=15)
plt.xlim(0.1000)
plt.ylim(0.1.6)
EBCT1 = []
for column in ws3['H3:H13']:
for cell in column:
EBCT1.append(cell.value)
4
ca1 = []
for column in ws3['J3:J13']:
for cell in column:
ca1.append(cell.value)
plt.subplot(2.3.2)
plt.scatter(EBCT1,ca1,marker='s',label='Measured data')
err = 0.05*ones(size(ca1))
e = errorbar(EBCT1,ca1,err,ecolor='g',capsize=6)
plt.title('10 m/h',fontsize=18)
plt.legend(loc='best')

```

```

Ca_e2 = sol3.total_element('Ca')*1e3 #saturation ca concentration in mmol/
Ca_02 = ws3['P3'].value #initial ca concentration in mmol/l
e2 = ws2['M3'].value #prospity
z2= np.arange(0.2500.125) #height in mm
v2= ws2['M5'].value #velocity in mm/s
D2= ws2['M6'].value
D2_reduction= 1.4
EBCT2 = z2/v2 # EBCT in s
k2 = 0.00296* math.sqrt(v2) #reaction constant in mm/s using velocity model:
Ca2 = Ca_e2 - (exp((-k2/D2)*(1-e2)*EBCT2)*(Ca_e2 - Ca_02)) #end ca concentration Ca2_reduction =
Ca_e2 - (exp((-k2/D2_reduction)*(1-e2)*EBCT2)*(Ca_ Ca_02) Ca_plt.subplot(2.3.3)
plt.plot(EBCT2, Ca2, label= 'velocity model')
plt.xlabel('EBCT(s)',fontsize=15)
plt.ylabel('calcium concentration(mmol/l)',fontsize=15)

```

```

plt.xlim(0.1000)
plt.ylim(0.1.6)
EBCT2 = []
for column in ws3['N3:N13']:
for cell in column:
EBCT2.append(cell.value)
ca2 = []
for column in ws3['P3:P13']:
for cell in column:
5
ca2.append(cell.value)
plt.subplot(2.3.3)
plt.scatter(EBCT2.ca2.marker='s'. label= 'Measured data')
err = 0.05*ones(size(ca2))
e = errorbar(EBCT2.ca2.err.ecolor='g'. capsize=6)
plt.title('15 m/h'. fontsize=18)
plt.legend(loc='best')
plt.subplots_adjust(top=2. left=0.007. right=4.
hspace=0.5. wspace=0.5)

```

Appendix VII –D PhreeqPython code-CO₂ test- grain size 0.5-1.2 mm

Yamauchi-CO₂-Small grain size

January 9, 2018

```

In [1]: import numpy as np
from math import sqrt
import matplotlib.pyplot as plt
%pylab inline
import phreeqpython
pp = phreeqpython.PhreeqPython()
from openpyxl import load_workbook
Populating the interactive namespace from numpy and matplotlib
WARNING: pylab import has clobbered these variables: ['sqrt']
`%matplotlib` prevents importing * from pylab and numpy
In [2]: wb = load_workbook('Yamauchi-CO2.xlsx'. data_only=True. read_only=True)
ws1 = wb['water-quality']
ws2 = wb['operation']
ws3 = wb['measurement-data']
In [3]: #2mole-filter-1
sol = pp.add_solution_raw({
'temp': 13.
'units': 'mg/l'.
'pH': ws1['D3'].value.
'Ca': ws1['D4'].value.
'Alkalinity': '8.113 as HCO3'.
'Cl': ws1['D6'].value.
'Na': ws1['D7'].value.
'Fe': ws1['D8'].value.
'Mg': ws1['D9'].value.

```

```

'K' : ws1['D10'].value.
'Al': ws1['D11'].value.
'S(6)': ws1['D12'].value
})
CO2_1_0=sol.total('CO2')*1e3
sol.saturate('Calcite'.0)
Cae_1 = sol.total_element('Ca')*1e3
CO2e_1=sol.total('CO2')*1e3
#4mole-filter-1
sol2 = pp.add_solution_raw({
'temp': ws1['I2'].value.
'units': 'mg/l'.
'pH': ws1['I3'].value.
'Ca': ws1['I4'].value.
'Alkalinity': '7.69 as HCO3'.
'Cl': ws1['I6'].value.
'Na': ws1['I7'].value.
'Fe': ws1['I8'].value.
'Mg': ws1['I9'].value.
'K' : ws1['I10'].value.
'Al': ws1['I11'].value.
'S(6)': ws1['I12'].value
})
CO2_2_0=sol2.total('CO2')*1e3
sol2.saturate('Calcite'.0)
Cae_2 = sol2.total_element('Ca')*1e3
CO2e_2 = sol2.total('CO2')*1e3
#6mole-filter-1
sol3 = pp.add_solution_raw({
'temp': 13.
'units': 'mg/l'.
'pH': ws1['N3'].value.
'Ca': ws1['N4'].value.
'Alkalinity': '6.71 as HCO3'.
'Cl': ws1['N6'].value.
'Na': ws1['N7'].value.
'Fe': ws1['N8'].value.
'Mg': ws1['N9'].value.
'K' : ws1['N10'].value.
'Al': ws1['N11'].value.
'S(6)': ws1['N12'].value
})
CO2_3_0=sol3.total('CO2')*1e3
sol3.saturate('Calcite'.0)
Cae_3=sol3.total_element('Ca')*1e3
CO2e_3 =sol3.total('CO2')*1e3
#8mole-filter-1
sol4 = pp.add_solution_raw({
'temp': 13.
'units': 'mg/l'.
'pH': 4.55. #ws1['S3'].value.
'Ca': ws1['S4'].value.

```

```

'Alkalinity': '5.85 as HCO3'.
'Cl': ws1['S6'].value.
'Na': ws1['S7'].value.
'Fe': ws1['S8'].value.
'Mg': ws1['S9'].value.
'K': ws1['S10'].value.
'Al': ws1['S11'].value.
'S(6)': ws1['S12'].value
})
CO2_4_0=sol4.total('CO2')*1e3
sol4.saturate('Calcite'.0)
Cae_4 = sol4.total_element('Ca')*1e3
CO2e_4 =sol4.total('CO2')*1e3

In [4]: Ca_e = sol.total_element('Ca')*1e3 #saturation ca concentration in mmol/l
Ca_0 = ws1['D4'].value #initial ca concentration in mmol/l
e = ws2['D3'].value #porosity
z= np.arange(0.2000.125) #height in mm
v= ws2['D5'].value #velocity in mm/s
D= 0.81
D_reduction = 0.74
EBCT = z/v # EBCT in s
k = 0.00296* math.sqrt(v) #reaction constant in mm/s using velocity model:
Ca = Ca_e - (exp((-k/D)*(1-e)*EBCT)*(Ca_e - Ca_0)) #end ca concentration in
Ca_reduction = Ca_e - (exp((-k/D_reduction)*(1-e)*EBCT)*(Ca_e - Ca_0)) #end plt.subplot(2.2.1)
plt.plot(EBCT, Ca, label= 'velocity model')
plt.plot(EBCT, Ca_reduction, label= 'velocity model')
plt.xlabel('EBCT(s)',fontsize=15)
plt.ylabel('calcium concentration(mmol/l)',fontsize=15)
plt.xlim(0.2000)
plt.ylim(0.4)
EBCT = []
for column in ws3['B3:B10']:
for cell in column:
EBCT.append(cell.value)
ca = []
for column in ws3['D3:D10']:
for cell in column:
ca.append(cell.value)
plt.subplot(2.2.1)
plt.scatter(EBCT,ca, label= 'measured data')
plt.title('2.9 mmol/l CO2',fontsize=18)
plt.legend(loc='best')
#####
Ca_e1 = sol2.total_element('Ca')*1e3 #saturation ca concentration in mmol/l
Ca_01 = ws1['I4'].value #initial ca concentration in mmol/l
e1 = ws2['I3'].value #prosiy
z1= np.arange(0.2000.125) #height in mm
v1= ws2['I5'].value #velocity in mm/s
D1= 0.81
D1_reduction= 0.74
EBCT1 = z1/v1 # EBCT in s

```

```

k1= 0.00296* math.sqrt(v1) #reaction constant in mm/s using velocity model
Ca1 = Ca_e1 - (exp((-k1/D1)*(1-e1)*EBCT1)*(Ca_e1 - Ca_01)) #end ca concentration Ca1_reduction =
Ca_e1 - (exp((-k1/D1_reduction)*(1-e1)*EBCT1)*(Ca_e1 - Ca_01)) plt.subplot(2.2.2)
plt.plot(EBCT1, Ca1, label= 'velocity model')
plt.plot(EBCT1, Ca1_reduction, label= 'Diameter reduction')
plt.xlabel('EBCT(s)'.fontsize=15)
plt.ylabel('calcium concentration(mmol/l)'.fontsize=15)
plt.xlim(0.2000)
plt.ylim(0.4)
EBCT1 = []
for column in ws3['H3:H10']:
for cell in column:
EBCT1.append(cell.value)
ca1 = []
for column in ws3['J3:J10']:
for cell in column:
ca1.append(cell.value)
plt.subplot(2.2.2)
plt.scatter(EBCT1,ca1, label='measured data')
plt.title('4.5 mmol/l CO2'.fontsize=18)
plt.legend(loc='best')
#####Ca_e2 =
sol3.total_element('Ca')*1e3 #saturation ca concentration in mmol/l
Ca_02 = ws1['N4'].value #initial ca concentration in mmol/l
e2 = ws2['N3'].value #porosity
z2= np.arange(0.2000.125) #height in mm
v2= ws2['N5'].value #velocity in mm/s
D2= 0.81
D2_reduct=0.74
EBCT2 = z2/v2 # EBCT in s
k2 = 0.00296* math.sqrt(v2) #reaction constant in mm/s using velocity model:
Ca2 = Ca_e2 - (exp((-k2/D2)*(1-e2)*EBCT2)*(Ca_e2 - Ca_02)) #end ca concentration

plt.subplot(2.2.3)
plt.plot(EBCT2, Ca2, label='velocity model')
plt.plot(EBCT2, Ca2_max, label='velocity model')
plt.xlabel('EBCT(s)'.fontsize=15)
plt.ylabel('calcium concentration(mmol/l)'.fontsize=15)
plt.xlim(0.2000)
plt.ylim(0.6)
EBCT2 = []
for column in ws3['M3:M9']:
for cell in column:
EBCT2.append(cell.value)
ca2 = []
for column in ws3['O3:O9']:
for cell in column:
ca2.append(cell.value)
plt.subplot(2.2.3)
plt.scatter(EBCT2,ca2, label= 'measured data')
plt.title('7 mmol/l CO2'.fontsize=18)
plt.legend(loc='best')

```

```

#####
Ca_e3 = sol4.total_element('Ca')*1e3 #saturation ca concentration in mmol/l
Ca_03 = ws1['S4'].value #initial ca concentration in mmol/l
e3 = ws2['S3'].value #porosity
z3= np.arange(0.2000.125) #height in mm
v3= ws2['S5'].value #velocity in mm/s
D3= 0.81
D3_reduction = 0.72
EBCT3 = z3/v3 # EBCT in s
k3 = 0.00296* math.sqrt(v3) #reaction constant in mm/s using velocity model:
Ca3 = Ca_e3 - (exp((-k3/D3)*(1-e3)*EBCT3)*(Ca_e3 - Ca_03)) #end ca concentration Ca3_reduction =
Ca_e3 - (exp((-k3/D3_reduction)*(1-e3)*EBCT3)*(Ca_e3 - Ca_03)) plt.subplot(2.2.4)
plt.plot(EBCT3, Ca3, label='velocity model')
plt.plot(EBCT3, Ca3_reduction, label='Diameter reduction')
plt.xlabel('EBCT(s)'.fontsize=15)
plt.ylabel('calcium concentration(mmol/l)'.fontsize=15)
plt.xlim(0.2000)
plt.ylim(0.6)
EBCT3 = []
for column in ws3['R3:R9']:
for cell in column:
EBCT3.append(cell.value)
ca3 = []
for column in ws3['T3:T9']:
for cell in column:
ca3.append(cell.value)
plt.subplot(2.2.4)
plt.scatter(EBCT3,ca3, label='measured data')
plt.title('9.5 mmol/l CO2'.fontsize=18)
plt.legend(loc='best')
plt.subplots_adjust(top=2, left=0.007, right=2,
hspace=0.5, wspace=0.5)

```

Appendix VII –E PhreeqPython code-translate-full-scale

translate-full-scale

January 9, 2018

```
In [2]: import numpy as np
from math import sqrt
import matplotlib.pyplot as plt
%pylab inline
import phreeqpython
pp = phreeqpython.PhreeqPython()
from openpyxl import load_workbook

In [3]: wb = load_workbook('Yamauchi-CO2.xlsx', data_only=True, read_only=True)
ws1 = wb['water-quality']
ws2 = wb['operation']
ws3 = wb['measurement-data']
In [4]: sol = pp.add_solution_raw({
'temp': 12.
'units': 'mg/l'.
'pH': 5.77.
'Ca': ws1['D4'].value.
'Alkalinity': '8.5 as HCO3'.
'Cl': ws1['D6'].value.
'Na': ws1['D7'].value.
'Fe': ws1['D8'].value.
'Mg': ws1['D9'].value.
'K': ws1['D10'].value.
'Al': ws1['D11'].value.
'S(6)': ws1['D12'].value
})
CO2_1_0=sol.total('CO2')*1e3
sol.saturate('Calcite'.0)
Cae_1 = sol.total_element('Ca')*1e3
CO2e_1=sol.total('CO2')*1e3
HCO3_1 = sol.total('HCO3')*1e3
pH = sol.pH
sol2 = pp.add_solution_raw({
'temp': 12.
'units': 'mg/l'.
'pH': 5.42.
'Ca': ws1['D4'].value.
'Alkalinity': '8.5 as HCO3'.
'Cl': ws1['D6'].value.
'Na': ws1['D7'].value.
'Fe': ws1['D8'].value.
'Mg': ws1['D9'].value.
'K': ws1['D10'].value.
'Al': ws1['D11'].value.
'S(6)': ws1['D12'].value
})
CO2_2_0=sol2.total('CO2')*1e3
```

```

sol2.saturate('Calcite'.0)
Cae_2 = sol2.total_element('Ca')*1e3
CO2e_2 = sol2.total('CO2')*1e3
HCO3_2 = sol2.total('HCO3')*1e3
In [8]: Ca_e = sol.total_element('Ca')*1e3 #saturation ca concentration in mmol/l
Ca_0 = ws1['D4'].value #initial ca concentration in mmol/l
e = ws2['D3'].value #prosimy
z= np.arange(0.3300.125) #height in mm
v= 10./3.6 #velocity in mm/s
D= 0.81
D_reduction = 0.74
EBCT = z/v # EBCT in s
k = 0.00296* math.sqrt(v) #reaction constant in mm/s using velocity model:
Ca = Ca_e - (exp((-k/D)*(1-e)*EBCT)*(Ca_e - Ca_0)) #end ca concentration in
Ca_reduction = Ca_e - (exp((-k/D_reduction)*(1-e)*EBCT)*(Ca_e - Ca_0)) #end plt.subplot(2.2.1)
plt.plot(EBCT/60. Ca. label= 'velocity model')
plt.xlabel('EBCT(s)').fontsize=15)
plt.ylabel('calcium concentration(mmol/l)').fontsize=15)
plt.xlim(0.30)
plt.ylim(0.2)
plt.title('0.65 mmol/l CO2'.fontsize=18)
plt.legend(loc='best')

```

```
#####
```

```

Ca_e1 = sol2.total_element('Ca')*1e3 #saturation ca concentration in mmol/l
Ca_01 = ws1['I4'].value #initial ca concentration in mmol/l
e1 = ws2['I3'].value #prosimy
z1= np.arange(0.3300.125) #height in mm
v1= 10./3.6 #velocity in mm/s
D1= 0.81
D1_reduction= 0.74
EBCT1 = z1/v1 # EBCT in s
k1= 0.00296* math.sqrt(v1) #reaction constant in mm/s using velocity model:
Ca1 = Ca_e1 - (exp((-k1/D1)*(1-e1)*EBCT1)*(Ca_e1 - Ca_01)) #end ca concentration
plt.subplot(2.2.2)
plt.plot(EBCT1/60. Ca1. label= 'velocity model')
plt.xlabel('EBCT(s)').fontsize=15)
plt.ylabel('calcium concentration(mmol/l)').fontsize=15)
plt.xlim(0.30)
plt.ylim(0.2)
plt.title('1.5 mmol/l CO2'.fontsize=18)
plt.legend(loc='best')
plt.subplots_adjust(top=2. left=0.007. right=4.
hspace=0.5. wspace=0.5)

```

Appendix VII –F PhreeqPython code-CO₂-species- distribution

Distribution of CO₂ species at different pH level simulated in PhreeqPython

```
In [1]: %pylab inline
from phreeqpython import PhreeqPython
pp = PhreeqPython()
solution = pp.add_solution({'NaHCO3':1.0})
In [2]: phs = []
co2 = []
hco3 = []
co3 = []
In [3]: for pH in arange(0.14.1.0.1):
solution.change_ph(pH)
phs.append(pH)
co2.append(solution.total('CO2')*1000)
co3.append(solution.total('CO3')*1000)
hco3.append(solution.total('HCO3')*1000)
fig = plt.figure(figsize=[14.6])
plt.plot(phs.co2,label='CO2')
plt.plot(phs.hco3,label='HCO3-')
plt.plot(phs.co3,label='CO3-2')
plt.xlabel("pH")
plt.ylabel("Concentration (mmol)")
plt.title("Carbonic Acid. Bicarbonate. Carbonate distribution")
lgnd = plt.legend()
```